

SOUTH WEST AFRICA/NAMIBIA

DEPARTMENT OF ECONOMIC AFFAIRS

GEOLOGICAL SURVEY

**SERPENTINITES IN CENTRAL SOUTH WEST AFRICA/NAMIBIA—
A RECONNAISSANCE STUDY**

by

SARAH-JANE BARNES

MEMOIR 8

SOUTH WEST AFRICA/NAMIBIA

DEPARTMENT OF ECONOMIC AFFAIRS

GEOLOGICAL SURVEY

MEMOIR 8

**SERPENTINITES IN CENTRAL SOUTH WEST
AFRICA/NAMIBIA - A RECONNAISSANCE STUDY**

by

SARAH-JANE BARNES, M.Sc.

Copyright reserved
1982

Printed by the Government Printer, Bosman Street/Private Bag X85, Pretoria. 0001

Obtainable from the Geological Survey, P.O. Box 2168, Windhoek or from the address above

ISBN 0 621 07582 5

GEOLOGICAL SURVEY OF SOUTH WEST AFRICA/NAMIBIA

Director - R. McG. Miller, Ph.D.

Edited by the Publication Section, Geological Survey of South Africa

C. J. van Vuuren, M.Sc.-Assistant Director

D. J. Winterbach, B.Sc., B.A. (Hons)-Chief Geologist

A. de Grys, M.Sc. D.I.C.-Senior Geologist

J. G. Stagman, O.L.M., D.Sc., F.I.M.M.-Geologist

B. E. Hauter. B.A. (Hons)-Professional Officer

S. Troskie-Typist

CONTENTS

	Page
<i>Abstract</i>	1
1. INTRODUCTION	3
2. FIELD RELATIONS	3
2.1 GAUCHAB SERPENTINITE	3
2.1.1 Rock types	3
2.1.2 Structure	5
2.1.3 Synthesis	5
2.2 ELISENHÖHE SERPENTINITE	9
2.2.1 Rock types	9
2.2.2 Structure	9
2.2.3 Synthesis	12
2.3 OMIEVE SERPENTINITE	12
2.3.1 Rock types	12
2.3.2 Structure	12
2.3.3 Synthesis	15
2.4 OTJIHAENENA SERPENTINITE	15
2.4.1 Rock types	15
2.5 OKAHAU SERPENTINITE	15
2.5.1 Rock types	15
2.5.2 Structure	15
2.5.3 Synthesis	15
3. PETROGRAPHY	15
3.1 DATA	15
3.2 INTERPRETATION OF TEXTURES AND DEDUCTIONS OF METAMORPHIC REACTIONS	21
3.2.1 Olivine serpentinite	21
3.2.2 Hobnail serpentinite	21
3.2.3 Talcose serpentinite	23
3.2.4 Carbonate serpentinite	24
3.2.5 Talc schist	24
3.2.6 Talc-amphibole schist	24
3.2.7 Chlorite schist	24
3.2.8 Actinolite fels	25
3.2.9 Epidote-producing reactions	25
3.2.10 Chlorite-producing reactions	25
3.2.11 Hornblendite 'dykes'	26
3.2.12 Pre-Damara quartz-feldspathic gneiss and epidotised gneiss	26
3.2.13 Pre-Damara amphibolite, epidote amphibolite and chlorite amphibolite	26
3.2.14 Pre-Damara mica schist	26
3.2.15 Damara metaconglomerate	26

	<i>Page</i>
3.2.16 Damara amphibolites	26
3.2.17 Damara mica schist	26
3.2.18 Geological history deduced from textures and reactions.....	26
4. METAMORPHIC CONDITIONS	27
4.1 INTRODUCTION	27
4.2 CONDITIONS BEFORE EMPLACEMENT OF THE SERPENTINITES.....	27
4.3 CONDITIONS DURING EMPLACEMENT OF THE SERPENTINITES.....	27
4.4 CONDITIONS AFTER EMPLACEMENT, AT PEAK OF DAMARA METAMORPHISM.....	27
4.4.1 Ultramafic rocks.....	27
4.4.2 Pre-Damara rocks	30
4.4.3 Damara rocks	30
4.4.4 Conclusions.....	30
5. CHEMISTRY	30
5.1 DATA.....	30
5.2 SYNTHESIS.....	30
5.2.1 Relationships between the ultramafic rock types.....	30
5.2.2 Relationships between the four types of ultramafic occurrences.....	47
5.2.3 Classification of the ultramafic rocks and relationship of the Damara Orogeny	61
5.3 CONCLUSIONS	69
6. OVERALL CONCLUSIONS	69
6.1 INTRODUCTION	69
6.1.1 Relationships between the ultramafic rock types.....	69
6.1.2 Relationships between the four types of field occurrences.....	70
6.2 MODELS.....	70
6.2.1 Introduction.....	70
6.2.2 Aulacogen model.....	70
6.2.3 Plate-tectonic model	73
6.2.4 Pre-Damara model	75
6.3 SUMMARY	76
REFERENCES	76
APPENDICES	
I. SUMMARY OF THE CHARACTERISTICS OF THE SERPENTINITE BODIES INVESTIGATED.....	84
II. PETROGRAPHIC DESCRIPTIONS.....	86
III. MICROPROBE ANALYSES	90

LIST OF ILLUSTRATIONS

Page

FIGURES

1.1	Location of area investigated and regional distribution of serpentinites	viii
1.2	Schematic cross-section through the southern margin of the Damara Orogen.....	4
2.1	Geological map of the Gauchab Serpentine	4-5
2.2	Sketch-map of photolineations around Gauchab and Elisenhöhe	6
2.3	Sense of shear on F_3 folds at Gauchab shown in cross-section and in perspective	8
2.4	Geological map of the Elisenhöhe Serpentine.....	10
2.5	The relationship between S_2 and contacts on Elisenhöhe	13
2.6	Geological map of the Omieve Serpentine.....	14
2.7	Sketch map of the serpentinite on Otjihaenena 196 and typical borehole log.....	16
2.8	Structural details of the Okahau Serpentine	17
2.9	Diagrammatic representation of minor folds in country rocks and in the ultramafic body related to a thrust plane, and intrusion of the serpentinite on Okahau	18
4.1	Stability of lizardite and antigorite	28
4.2	Plot of P_{H_2O} versus T during peak of Damara metamorphism	29
4.3	Isobaric T- X_{CO_2} diagram for the system CaO-MgO-SiO ₂ -H ₂ O-CO ₂	31
4.4	X_{CO_2} diagram for invariant point iii in Figure 4.3	31
5.1	Plot of MnO versus SiO ₂ for serpentinites and talc schists	43
5.2	Plots of trace elements versus SiO ₂ for serpentinites and talc schists	44
5.3	Plots of inter-element ratios versus SiO ₂ for serpentinites and talc schists	45
5.4	Histograms indicating that the chlorite schists contain more TiO ₂ , FeO, Al ₂ O ₃ , MnO, V, Sc and Ga than the serpentinites	48
5.5	Histograms indicating that the serpentinites contain more SiO ₂ , MgO, Cr and Ni than chlorite schists	49
5.6	Triangular plot of Ti, Zr and Y to determine origin of amphibolites.....	50
5.7	Plot of Ti against Zr to determine origin of amphibolite.....	50
5.8	Plot of Al ₂ O ₃ Versus MgO for SWA serpentinites	51
5.9	Plot of FeO _t versus MgO for SWA serpentinites	51
5.10	Plot of SiO ₂ versus MgO for SWA serpentinites	52
5.11	Plot of Factor 1 versus Factor 2 for SWA serpentinites.....	52

	<i>Page</i>
5.12	Plot of Factor 1 versus Factor 3 57
5.13	Plot of Factor 2 versus Factor 3 57
5.14	Dendrogram of SWA serpentinites 59
5.15	Factor 1 versus Factor 2 plots for 308 serpentinites 63
5.16	Factor 3 versus Factor 2 plots for 308 serpentinites 63
5.17	Discriminant analysis..... 66
5.18	Representation of the results of the discriminant analysis using 306 serpentinites 68
6.1	Location of the grabens in the aulacogen model 71
6.2	Model for emplacement of serpentinites 74

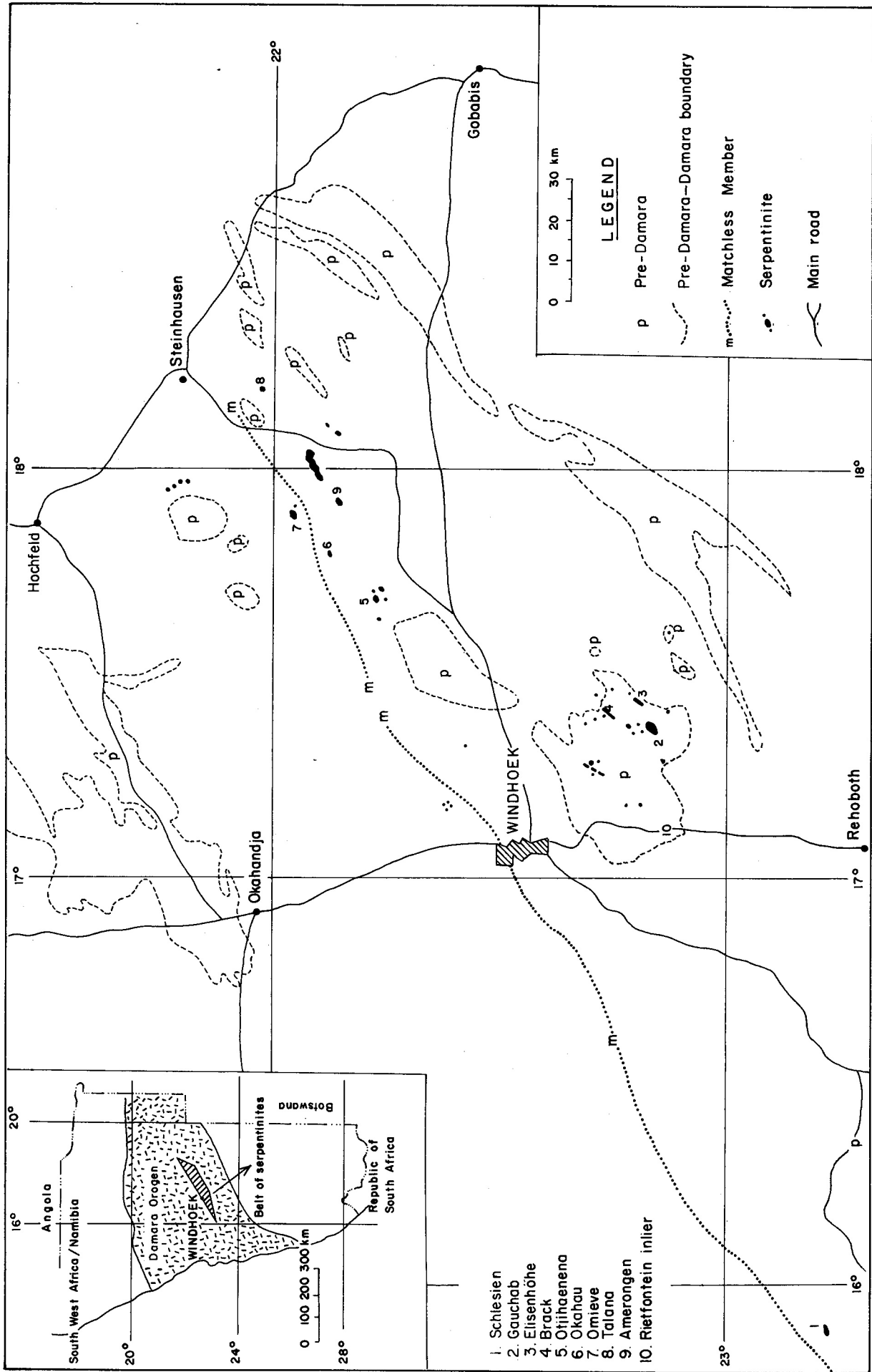
TABLES

1.1	Lithostratigraphic subdivisions of the Damara Sequence along the southern margin of the Damara belt..... 2
2.1	Correlation of structural elements 7
3.1	Abbreviations of mineral names..... 19
3.2	Summary of petrographic information 20
3.3	List of d-spacings used to identify antigorite 22
4.1	Calculated equilibria curves 32
5.1	Location and nature of analysed samples 33
5.2	Chemical analyses of serpentinites, talc and chlorite schists and amphibolites 34
5.3a	Concentrations of minor trace elements in common rock-forming minerals..... 40
5.3b	Concentrations of minor and trace elements in hobnail serpentinite..... 39
5.3c	Concentrations of minor and trace elements in talc schist 46
5.3d	Concentrations of minor and trace elements in chlorite schist..... 46
5.3e	Concentrations of minor and trace elements in actinolite fels..... 47
5.4	Results of BMDP3D t-test 54
5.5	Factor-score coefficients for SW A serpentinites..... 56
5.6	F-values 58
5.7	Summary of serpentinite analyses used 60

	<i>Page</i>
5.8	Factor-score coefficients for 308 serpentinite analyses 61
5.9	Element enrichment or depletion in ultramafic rocks relative to fertile mantle 64
5.10	Results of the discriminant analysis 65
5.11	Trace-element concentrations of mantle-derived material 67

PLATE

2.1	Flattening of pebbles in Nosib metaconglomerate adjacent to serpentinite contact..... 11
-----	--



SERPENTINITES IN CENTRAL SOUTH WEST AFRICA/NAMIBIA

A RECONNAISSANCE STUDY*

by

Sarah-Jane Barnes, M.Sc.

Abstract

In central South West Africa/Namibia approximately 45 bodies of serpentinite are strung out over a zone extending for 400 km along the southern margin of the north-east-trending Damara Orogenic Belt.

The Damara Sequence is of late-Precambrian age. Its stratigraphy and deformation in central South West Africa fit a classic eugeosynclinal model. Along the southern margin of the orogenic belt the Damara rocks have been overthrust on to the pre-Damara basement. Serpentinites occur both in the eugeosynclinal metasediments and in pre-Damara inliers present in the overthrust zone. The long axes of the serpentinite bodies are usually parallel to the dominant north-easterly Damara fabric.

The ultramafic bodies consist of olivine serpentinite, hobnail serpentinite, talcose serpentinite, carbonate-amphibole serpentinite, talc schist, chlorite schist and amphibole fels. Talc schist forms a rim around the bodies and grades into talcose serpentinite which in turn grades into hobnail serpentinite and in some instances into cores of olivine serpentinite. Minor lenses of carbonate serpentinite, amphibole serpentinite and amphibole-carbonate rock may be found in the talcose serpentinite. Lenses of chlorite schist are scattered throughout the bodies. Amphibolite that may represent dykes or xenoliths is also present. Ca-metasomatism has led to the development of epidote in plagioclase-bearing country rocks near the serpentinites. Mg-metasomatism has resulted in the development of chlorite in biotite- and amphibole-bearing country rocks.

Analyses of the serpentinites show that they have low incompatible-element content, low FeO , Al_2O_3 , Na_2O , K_2O and CaO contents relative to SiO_2 and a high Ni/Co ratio. This suggests derivation from chemically depleted material. A principal-component analysis and discriminant analysis of the composition of serpentinite samples of known origin, quoted in the literature, serves to classify the Damara serpentinites as depleted Alpine-type material.

The field relationships, petrography, chemistry and structural setting of the serpentinite bodies have been investigated and it is concluded that: (a) The serpentinite was probably derived from harzburgite, which contained lenses of spinel harzburgite (now chlorite schist) and lenses of lherzolite (now amphibole- and carbonate-bearing rocks). The talc was derived by the reaction of serpentinite with silica-bearing country rocks and possibly by loss of MgO from serpentinite. (b) There are four distinct types of field occurrences but all have a common origin. (c) The serpentinites were emplaced during the Damara deformation and a plate-tectonic model provides both the ultramafic rocks of suitable composition and a mechanism for serpentinite emplacement.

* Based on a thesis submitted in partial fulfilment of the requirements for the degree of Master of Science, in the Faculty of Science, University of Cape Town (1979).

Table 1.1 - LITHOSTRATIGRAPHIC SUBDIVISIONS OF THE DAMARA SEQUENCE ALONG THE SOUTHERN MARGIN OF THE DAMARA BELT (SACS 1980)

Sequence	Group	Subgroup	Formation	Lithology	Maximum thickness (m)	Dated field unit	Method and age in Ma	Remarks			
Damara	Swakop	Khomas	Kuiseb	Biotite-rich quartzo-feldspathic schist, minor graphitic schist, calc-silicate rock Amphibolite, amphibole-chlorite schist, talc schist (Matchless Member)	>10 000	schist	K-Ar biotite 460-481	Tectonic thickness Post-tectonic cooling age			
			Auas	Quartzite, schist, marble, amphibolite, itabirite	2 400						
			Chuos	Pebbly schist, mixtite, conglomerate, schist, quartzite, itabirite, amphibolite, calc-silicate rock	1 650	calc-silicate rock	K-Ar biotite 517+28	Tectonic thickness Post-tectonic cooling age			
	Nosib	Kudis	Hakos	Quartzite		2 000			Only locally developed Stratigraphic position uncertain due to thrusting		
				Corona	Graphitic schist, marble, quartz-mica schist, quartzite, conglomerate, itabirite	1 200			Tectonic thickness		
				Natas	Conglomerate, amphibolite	150			Tectonic thickness		
			UNCONFORMITY	Kamtsas	Duruchaus	Quartzite, arkose		6 200			Transitional contacts and interfingering due to facies changes
						Phyllite, minor quartzite and limestone		500			Tectonic thickness

1. INTRODUCTION

In central South West Africa approximately 45 serpentinite bodies are present in a 400-km zone along the southern margin of the Damara Orogenic Belt, the axis of which trends north-east (Fig. 1.1).

The Damara Sequence is of late-Precambrian age. Its stratigraphy (Table 1.1) and deformation in the central part of the country fit a classic eugeosynclinal model (Martin 1965). To the north, the Damara develops into a miogeosynclinal sequence (Clifford 1967).

Along the southern margin of the belt, the Damara rocks have been overthrust on to the pre-Damara basement (Hälbich 1970, Bickle and Coward 1977) and pre-Damara inliers are present in the overthrust zone (Fig. 1.2). The pre-Damara rocks are gneisses, mica schists and amphibolites.

Serpentinites occur both in the eugeosynclinal sediments and in the pre-Damara inliers.

An unpublished report (Barnes 1977) contains field and petrographic descriptions of 35 of these bodies together with an assessment of their economic potential. It is accompanied by a map, on scale 1:50 000, showing the outlines of the occurrences, and the findings are summarised in Appendix I of this memoir.

The present study deals with the petrographic relationships between the various ultramafic rocks and their relationships with the country rocks. It aims to establish the relevance of the serpentinites to the Damara Orogeny and makes an assessment of the relationships between the following four types of field occurrences:

- (a) Round bodies in the pre-Damara rocks.
- (b) Lensoid bodies in the pre-Damara rocks.
- (c) Round bodies in the Damara metasediments.
- (d) Lensoid bodies in the Damara meta-sediments.

In order to achieve these aims, detailed studies were conducted on selected examples of each of the four types. The serpentinite which forms the mountain known as Gauchab on the farm Binsenheim, a portion of Rietfontein 85, was chosen as an example of type (a). The serpentinite ridge on the farm Elisenhöhe 88 was selected to represent type (b). For chemical and mineralogical studies the serpentinite on the farm Omieve was chosen to represent type (c), but lack of country-rock exposure made a structural interpretation difficult. The occurrence on the farm Otjihaenena adequately represents type (d) for chemical investigation but it is poorly exposed so the serpentinite on farm Okahau was selected for structural investigation of type (d). The samples collected from this latter occurrence proved to be too weathered for satisfactory chemical investigation.

2. FIELD RELATIONS

2.1 GAUCHAB SERPENTINITE

2.1.1 ROCK TYPES

On the farm Binsenheim, at approximately 22°50'S:17°23'E, the Gauchab mountain attains a height of 300 m above the surrounding plain. It is composed of serpentinite and measures 3 km by 2 km (Fig. 2.1). The exposure consists of a large central body surrounded by numerous disconnected satellites of talc and chlorite schists.

The main body has an essentially concentric structure. The core consists of four irregular pods of fine-grained, granular homogeneous olivine serpentinite, with a tendency to negative relief, that occupies the hollows and low ground between ridges of encompassing and more extensively developed hobnail serpentinite.

Fresh olivine serpentinite is dark green and glassy. On weathering it becomes friable, light brown in colour and is traversed by veinlets of black magnetite. The term 'hobnail', used by Keith and Coleman (1971), refers to the irregular light-brown weathered surface of this variety of serpentinite. A cut specimen reveals a light-brown rim containing magnetite and carbonate veinlets. The rim merges into a discoloured area consisting of light-green friable material surrounding dark-green glassy cores. These measure 10 to 20 mm across and may contain irregular blebs of magnetite. Iron-stained veinlets cut the light-green portions. The blotchy discoloured zone grades into uniform dark-green, glassy serpentinite with irregular blebs of magnetite.

On its southern side the hobnail serpentinite grades into talcose serpentinite which contains lenses of talcose actinolite serpentinite. In hand specimen the talcose serpentinite is essentially similar in appearance to hobnail serpentinite but is softer and contains talc flakes 1 to 2 mm in size. The talcose actinolite serpentinite is a deeper green and contains yellow patches of carbonate minerals that measure 0,1 mm across.

Talc schist forms a narrow irregular rim, 1 to 10 m wide, around the main central body. It may also occur as lenses 2 to 3 m long within the main body, up to 300 m from the margin. The talc itself varies from large pale-green flakes to fine-grained pink material.

Lenses of chlorite schist, usually less than 2 m long, are scattered throughout the main body but are generally associated with hornblende 'dykes'. Centrally the fresh surface of the rock is dark green beneath a black weathered crust. It is medium grained and displays crenulation. Towards the margins of the lenses it becomes more strongly schistose and has not developed a weathered crust.

Also present along the edge of the main body are 1-m pods of actinolite fels. The amphibole needles are 50 to 60

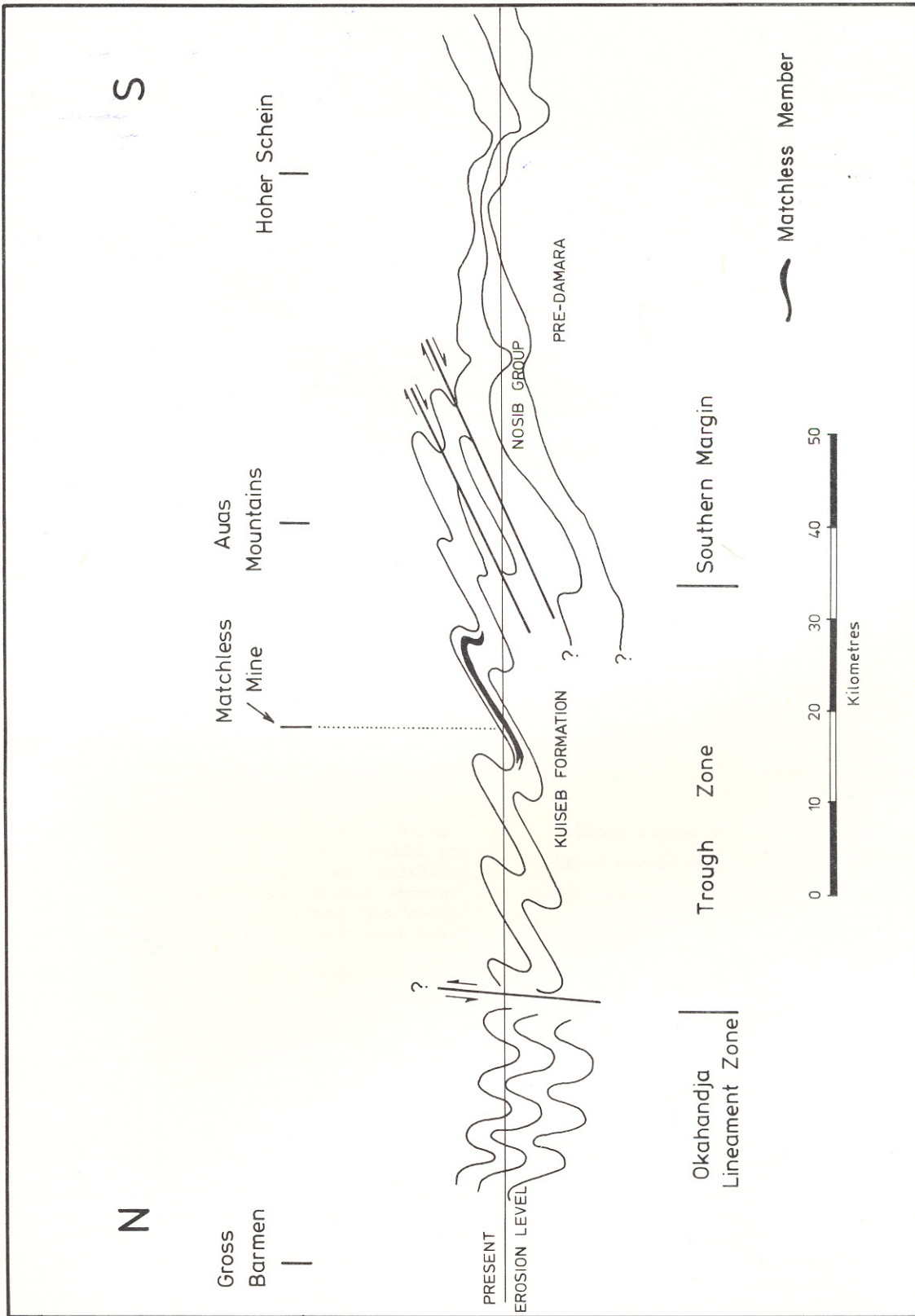


Fig. 1.2 — Schematic cross-section through the southern margin of the Damara Orogen, after Hällbich (1970) and Bickle and Coward (1977)

m long and have radiating habit. They may lie in a base of fine-grained white talc.

The hornblende dykes or tectonic slices, 2 to 3 m wide, transgress the main body striking at 2600 but could not be traced back into the surrounding country rocks. The hornblende is almost black, not foliated and may be porphyritic. Grain size varies greatly, from 0,1 to 20 mm.

The satellite serpentinite bodies contain the same rock types as the main body, but on a smaller scale, and exhibit a similar concentric zoning.

The country rocks belong to the pre-Damara Hohewarte Complex and consist of biotite schist, amphibolite and gneiss. The biotite schist is medium grained, strongly schistose and is mottled black and white. The amphibolite is a medium-grained black and white rock consisting of alternating 3-mm layers of felsic minerals and 5-mm layers of mafic material. The gneiss is a pink quartzofeldspathic rock with a foliation imparted by biotite and flattened feldspar porphyroblasts.

These country rocks have been modified in the vicinity of the Gauchab serpentinite.

Chlorite and epidote have developed in the mica schist, in increasing amount as the contact is approached. The amphibolite has been recrystallised with development of epidote and chlorite, again in increasing amount closer to the contact, so that within 10 m of the contact there are hard, fine-grained epidote amphibolites and chlorite amphibolites. The former are composed of alternating layers of black hornblende and yellow-green epidote each about 20 mm thick. The chlorite amphibolite is also fine grained and yellowish green when fresh but has a black weathered skin. The effect on the gneiss has been the growth of some epidote and accentuation of the foliation.

The talcose serpentinite zone on the southern and eastern sides of the main body consists of alternating slices of talcose serpentinite and country rock. Large quartz veins have developed in the country rock to the north-west, north-east and south-west of Gauchab.

2.1.2 STRUCTURE

The regional structure is featured in Figure 2.2.

The nomenclature adopted for fabric elements is that of Turner and Weiss (1963), in which S_0 denotes a planar penetrative fabric, L denotes a linear penetrative fabric and F denotes a folding of the fabric. The suffixes 1, 2, 3 ... define the generation of a particular element. Bedding is referred to as S . The description of fold profiles also

follows that of Turner and Weiss. For geometrical properties of folded surfaces, such as interlimb angle, attitude of hinge line and dip of axial plane, the terms defined by Fleuty (1964) are used.

A tentative correlation between the numbering of fabric elements used here and that used by other workers is presented in Table 2.1.

The following fabric elements were observed:

- S_1 A weak schistosity in the gneiss marked by micas.
- S_2 A schistosity in the gneiss marked by biotite orientation and elongation of quartz and feldspar pods. It crenulates S_1 in the gneiss. S_2 is marked by a fracture cleavage in the talc and chlorite schists. S_2 is shown on Figure 2.1.
- S_3 Crenulation cleavages post-dating S_1 and S_2 in chlorite-amphibole schists, chlorite schists and talc schists. All crenulations have been called S_3 , even though some crenulations post-date others.
- L_2 A lineation resulting from the intersection of S_1 and S_2 in the gneiss. L_2 is marked by biotite, quartz and feldspar lineation on S_2 planes. It is shown on Figure 2.1.
- F_2 Tight rootless similar folds in the gneiss. S_2 is axial planar to F_2 . The fold axes generally plunge south-eastwards as are indicated on Figure 2.1.
- F_3 Parallel to similar, close to tight mesofolds, in the gneiss and schists. F_3 folds the S_2 schistosity. In the neighbourhood of Gauchab, F_3 folds are asymmetric, but 500 m from the body F_3 folds are weaker and symmetric; they are absent beyond 750 m from the contact. The hinges and axial planes are shown on Figure 2.1.

Quartz veins parallel to S_2 are often boudinaged on the eastern and western flanks of Gauchab but tend to be shortened on the northern and southern margins.

2.1.3 SYNTHESIS

Figure 2.1 displays a synthesis of the field relationships between the various rock types. Structural data have been interpreted as follows:

The country rock was originally deformed, resulting in an S_1 fabric. This fabric is likely to be of pre-Damara age because it is not represented in nearby Damara rocks.

S_2 has a regional trend of 0300 which is similar to the orientation of the fabric in the Nosib Group at Elisenhöhe, 5 km east of Gauchab (Section 2.2.2), and is hence of Damara age. S_2 is thought to be associated with thrusting, since it is axial planar to tight, rootless similar F_2 folds; the intensity of S_2 decreases with increasing dis-

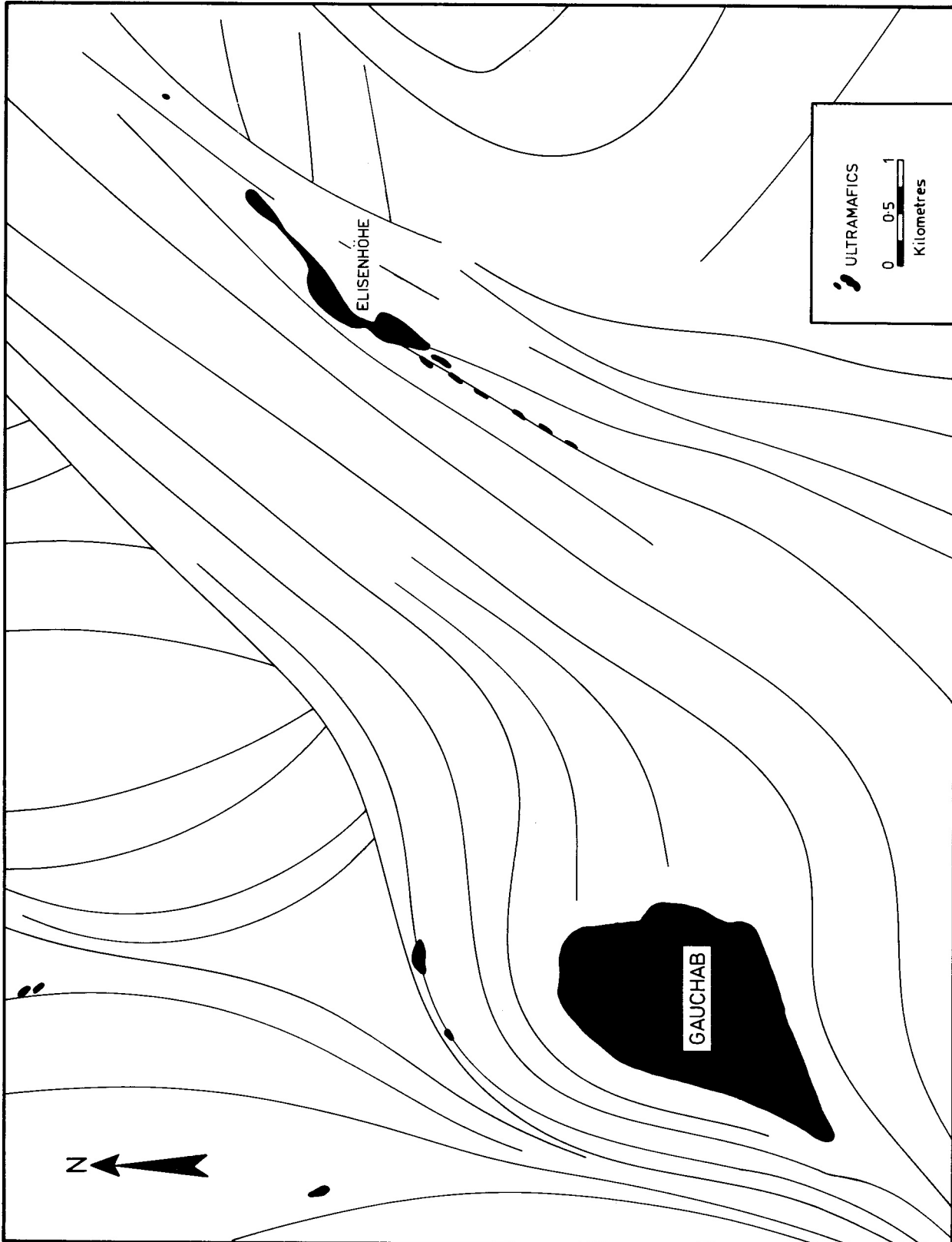


Fig. 2.2 — Sketch-map of photolineations around Gauchab and Eisenhöhe

Table 2.1 - CORRELATION OF STRUCTURAL ELEMENTS USED IN THIS TEXT WITH THOSE USED BY OTHER WORKERS

Body	Fabric element	Remarks	Hálbich (1970)	Porada (1975)	Sawyer (1978)	This work
Gauchab	S ₁	Pre-Damara	N.A.	N.A.	N.A.	N.A.
	S ₂	Damara; strike NE-SW, dip NW	Sf ₂	Sf ₂	TZS ₂	dS ₂
	S ₃	Localised crenulation cleavage	N.A.	N.A.	N.A.	N.A.
Elisenhöhe	S ₀	Nosib bedding	N.A.	N.A.	S ₀	N.A.
	S ₁	Pre-Damara	N.A.	N.A.	N.A.	N.A.
	S ₂	Damara; strike NE-SW, dip NW	Sf ₂	Sf ₂	TZS ₂	dS ₂
	S ₃	Localised crenulation cleavage	N.A.	N.A.	N.A.	N.A.
Omieve	S ₁	Pre-emplacment fabric?	N.A.	N.A.	N.A.	N.A.
	S ₂	Damara; strike NE-SW, dip NW	Sf ₂	Sf ₂	TZS ₂	dS ₂
	S ₃	Localised crenulation cleavage	N.A.	N.A.	N.A.	N.A.
Okahau	S ₁	Damara; strike NE-SW, dip NW	Sf ₂	Sf ₂	TZS ₂	dS ₂
	S ₂	Crenulation cleavage in country rock and ultramafics; strike E-W, dip S	?	?	?	?
	S ₃	Localised crenulation cleavage	N.A.	N.A.	N.A.	N.A.

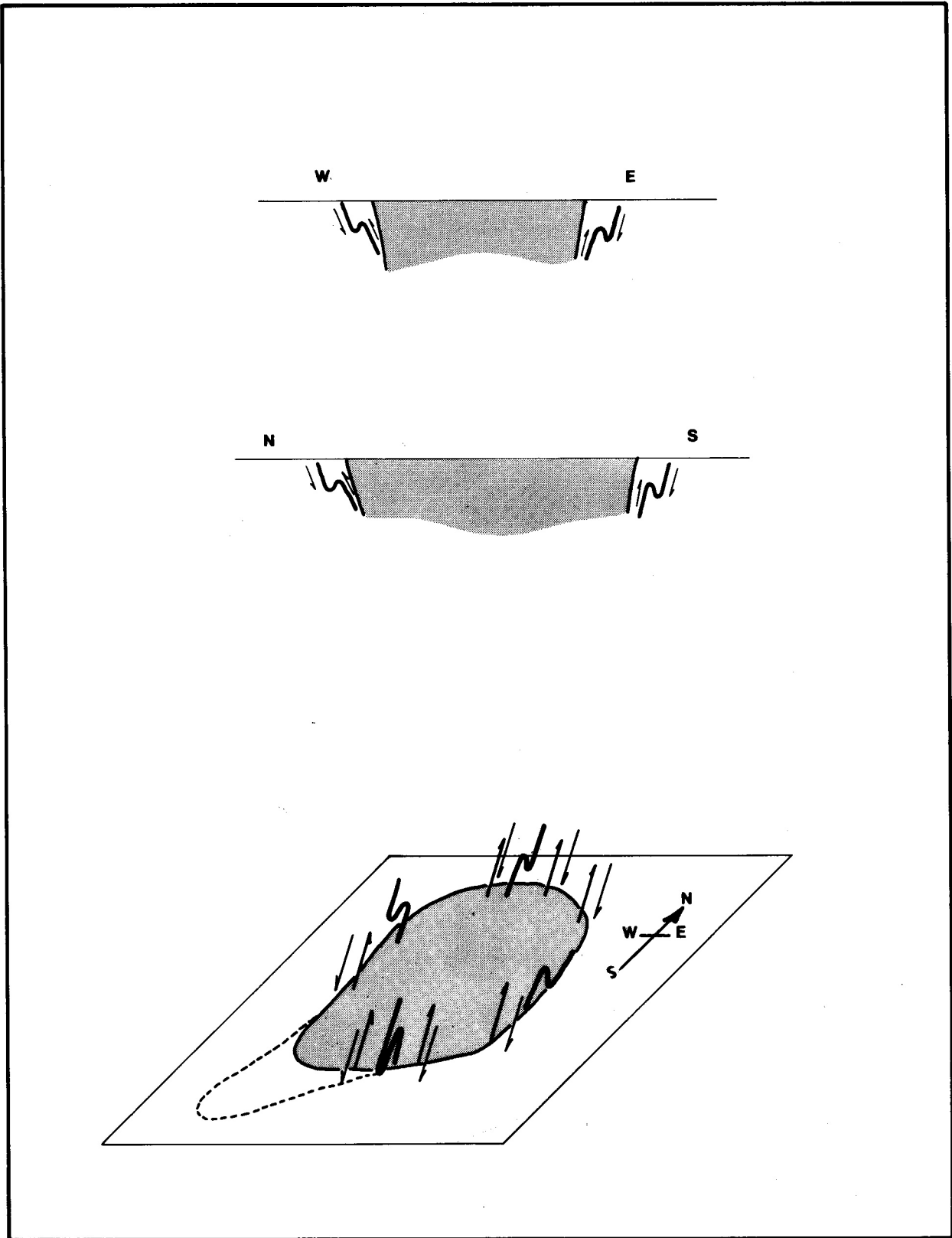


Fig. 2.3 — Sense of shear on F_3 folds at Gauchab shown in cross-section and in perspective

tance from the serpentinite. The schistosity is stronger close to the serpentinites. S_1 biotites are recrystallised in S_2 , thus indicating that S_2 was associated with a metamorphic event.

S_2 planes, F_2 hinges and L_2 lineations are deformed by the serpentinite, hence all these fabric elements pre-date emplacement.

F_3 folds vary in intensity and degree of asymmetry, depending on the distance from Gauchab and they have been interpreted as drag folds which formed during the emplacement of the serpentinite. If this interpretation is correct, the asymmetry of the folds implies that Gauchab rose relative to the country rock (Fig. 2.3).

Since the axes of F_3 folds plunge south-eastwards, Gauchab was emplaced from the north-west. The movement of the serpentinite along the S_2 thrust plane may have been assisted by diapiric action consequent on density contrasts between the serpentinite body (2,2 to 2,5 t/m³ and the country rock (2,65 t/m³).

The F_3 folds and the quartz veins indicate that there has been a post- F_3 shortening in an east-west direction. This may be regional or it may be associated with the emplacement of the body.

The possibility that the distortion in S_2 is a wrap-around structure, formed after emplacement, is discounted on the grounds that:

- (a) The bodies in the pre-Damara rocks are usually orientated with their long axes parallel to the dominant Damara S_2 trend.
- (b) The wrap-around hypothesis provides no mechanism for the formation of F_3 folds and their localisation in the neighbourhood of Gauchab.
- (c) S_2 is much stronger in the vicinity of Gauchab.
- (d) The S_2 fabric is confined to the marginal rocks of the serpentinites despite the fact that rock types capable of adopting a foliation (talcose serpentinite) are present.
- (e) Slices of country rock containing occur within the massive serpentinite.

As the talc and chlorite schists contain S_2 fabric and S_3 crenulations, but no S_1 fabric they must have formed after S_1 and during or before S_2 .

The actinolite is relatively undeformed although occasionally it is crenulated by S_3 and therefore formed after S_2 .

2.2 ELISENHÖHE SERPENTINITE

2.2.1 ROCK TYPES

A ridge of serpentinite is present on the farm Elisenhöhe 88, Windhoek district, at approximately 22°48'8:17°26'8 (Fig. 2.4). The exposures consist of three lensoid bodies

composed of rock types identical to those at Gauchab. The three lenses form an almost continuous strike slightly displaced by faults. Hobnail serpentinite cores are surrounded by talcose serpentinite, carbonate serpentinite and talc and chlorite schists. The serpentinite thins out towards the south so that only chlorite and talc schists are present and farther south, only chlorite schist remains.

The carbonate-bearing serpentinite is purplish, fine grained and homogeneous. It contains pods of ankerite, equidimensional in plan, and measuring 1 m across.

On the western side of the three bodies the country rocks are gneiss, amphibolite and mica schist of pre-Damara age and very similar to the country rocks at Gauchab. They have undergone the same modifications, adjacent to the serpentinite contact, with resultant conversion to chlorite-amphibole schist and epidote amphibolite.

On the eastern side of the body there is a variation. In the central portion a conglomerate of the Nosib Group is developed. At the contact this conglomerate consists of an actinolite-rich matrix containing pebbles of epidote-rich mica schist, actinolitechlorite-schist, and slightly epidotised gneiss. The concentration of epidote and actinolite decreases away from the contact. About 100 m east of the body, a conglomerate free of epidote, chlorite and amphiboles is present.

The degree of flattening of the pebbles increases markedly towards the contact where the length: breadth ratio of the pebbles is 11:1. Some 100 m away this ratio has decreased to 2:1 (Plate 2.1a and c).

To the north and south of the central lens of serpentinite and derivatives, the country rocks are of pre-Damara age.

2.2.2 STRUCTURE

The regional structural setting is illustrated by Figure 2.2. The fabric elements present are:

- S_0 Bedding in the Nosib Group.
- S_1 A weak schistosity in the gneiss marked by micas.
- S_2 The dominant schistosity in the gneiss, amphibolite, talc and chlorite schists. In the gneiss, S_2 is represented by orientated biotite and flattened quartz and feldspar grains. In the schist, S_2 is defined by orientation of talc and chlorite laths. S_2 is visible in the basal Nosib Group but becomes less conspicuous away from the contact.
- S_3 A crenulation cleavage deforming S_2 in the talc and chlorite schists.
- L_{2a} A lineation in the gneiss produced by the intersection of S_1 and S_2 and defined by biotite and flattened quartz and feldspar porphyroblasts.

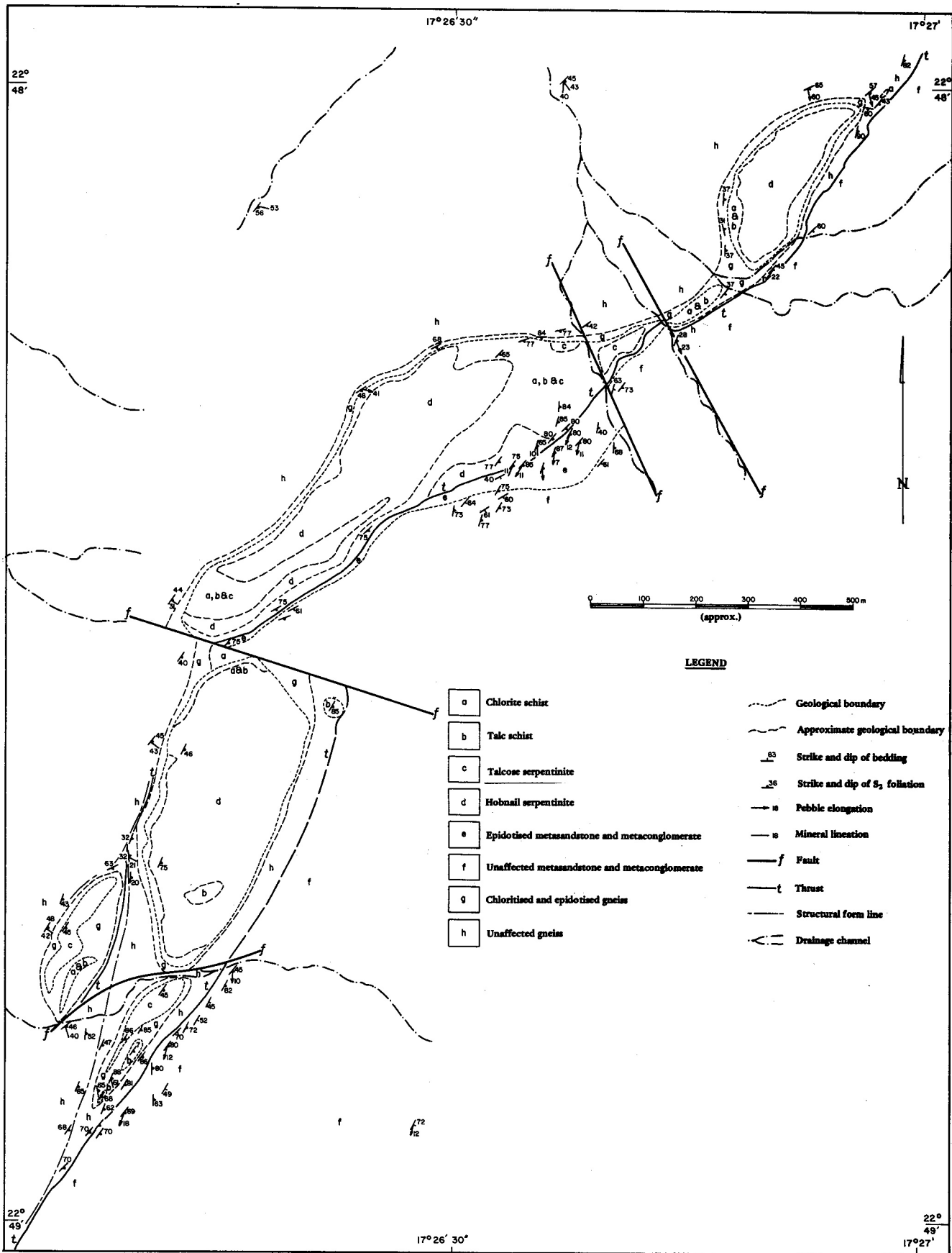
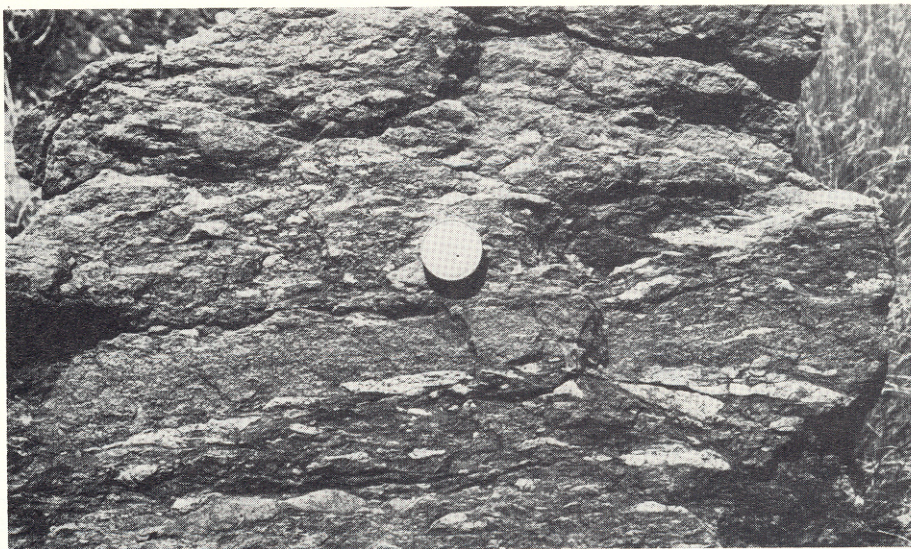


Fig.2.4 – Geological map of the Eisenhöhe Serpentinite, Eisenhöhe 88, Windhoek District

a



b



c



Plate 2.1 — Flattening of pebbles in Nosib metaconglomerate adjacent to serpentinite contact.
a—3 m, b—20 m, c—100 m from contact.

- L_{2b} A lineation defined by the elongation of the pebbles in the metaconglomerate.
- F₂ Rootless, tight similar folds in the gneiss and Nosib Group. S₂ is axial planar to F₂.
- F₃ Parallel to similar, close mesofolds in the chlorite schists, talc schist and chlorite-amphibole schist. S₃ is axial planar to F₃.

2.2.3 SYNTHESIS

Figure 2.4 represents a synthesis of the field relationships of the various rock types.

The following lines of evidence suggest that the contact between the Damara and pre-Damara is a thrust zone:

- (a) The degree of flattening in the pebbles of the conglomerate increases towards the contact between the Nosib Group and the serpentinite (Plate 2.1).
- (b) The relationship between S₂ and the Damara-serpentinite, the pre-Damara-Damara, and the pre-Damara-serpentinite-pre-Damara contacts are shown schematically in Figure 2.5. This relationship suggests that the contact is a shear zone with a sinistral shear couple.
- (c) S₂ is axial planar to tight similar rootless folds suggesting that S₂ was associated with shearing.
- (d) L_{2b} changes in the vicinity of the contact such as L_{2b} is contained in S₂.

The southern end of the exposure consists of a train of small sigmoidal fragments of serpentinites separated from each other by gneiss. In this area, S₂ can be seen to be deformed around the serpentinite. S₂ is associated with thrusting since it shows an imbricate-type relationship towards the shear zone. The serpentinite is therefore believed to have intruded along the thrust zone and deformed S₂ planes. However, talc and chlorite schist contain the S₂ fabric, hence thrusting and serpentinite emplacement may be considered contemporaneous. By this interpretation, the body is of Damara age since S₂ which formed during emplacement is present within the Nosib Group. If S₂ were a wrap-around structure the same problems as outlined in Section 2.1.3 would arise.

Actinolite needles are very rarely deformed and actinolite hence post-dates deformation.

2.3 OMIEVE SERPENTINITE

2.3.1 ROCK TYPES

Rising 200 m out of the plain at 22°03'8":17°54'E, on the farm Omieve 179, is Omieve mountain which is a serpentinite body. The exposure measures 2 km by 3 km (Fig. 2.6).

The central portion consists of brown, sand-polished ser-

pentinite with a siliceous capping. The material 10 to 20 mm below the polished surface is medium brown, fine grained, and contains oval patches of cream-coloured material. Magnetite veinlets cut across both. From 30 to 40 mm below the surface, a zone of blotchy, light- and dark-green material, as described in Section 2.1.1, is developed. This zone grades into fresh hobnail serpentinite in which occasional lenses of talcose serpentinite and carbonate serpentinite may be found.

Around the edge of the body an irregular talc-schist zone is developed. The talc is usually pink, fine grained and may contain 1-mm patches of chlorite and magnetite. The width of the zone varies from 10 to 100 m. Talc lenses up to 2 m in length also occur within the body. They are usually associated with joint zones and may contain amphiboles. The talc is frequently crenulated.

Within the talc schist zone, lenses of chlorite schist 1 to 2 m long are present. The chlorite is dark green with a silvery sheen and contains 10-mm magnetite octahedra. Within the hobnail serpentinite there are lenses of chlorite which are less schistose and darker than those in the talc schist rim. This type acquires a black crust on weathering.

There are no exposures of country rock close to the serpentinite body. A borehole 100 m to the south intersected biotite schist of the Khomas Subgroup and some 45 auger holes, drilled by Johannesburg Consolidated Investments, 300 m south of the body intersected amphibolite which has been tentatively correlated with the Matchless Member.

A lens of rodingite (Coleman 1966) measuring 1 by 2 m was found on the southern side and large quartz veins are developed on the northern side of the body but poor exposure makes it difficult to estimate their size.

Approximately 2 km south of Omieve on Amerongen 181, schist of the Khomas Subgroup is present. It contains biotite, plagioclase, quartz, garnet, kyanite, staurolite, chlorite and muscovite.

2.3.2 STRUCTURE

The following fabric elements were observed:

- S₁ The dominant fabric in the hobnail serpentinite marked by varying degrees of weathering. The fabric has no general trend (Fig. 2.6) and appears to be chaotic.
- S₂ The schistosity in the talc and chlorite schists. S₂ and the long axis of the body are orientated parallel to the dominant dS₂ Damara trend of 030°.
- S₃ A crenulation cleavage that deforms S₂.
- F₃ Asymmetric open mesofolds which fold S₂ and have S₃ axial planar. The body is transected by two fault

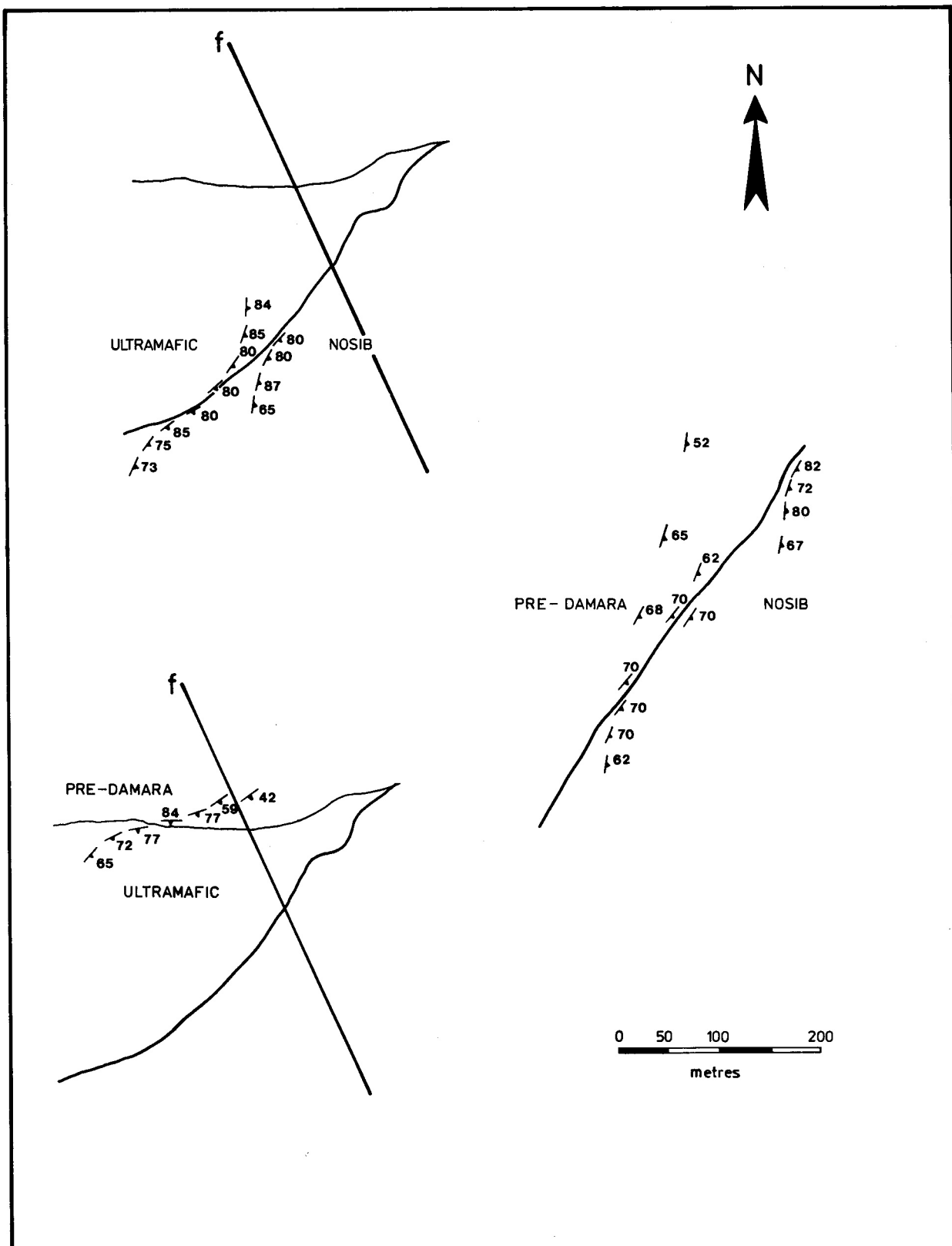


Fig 2.5 – The relationship between S_2 and contacts on Elisenhöhe

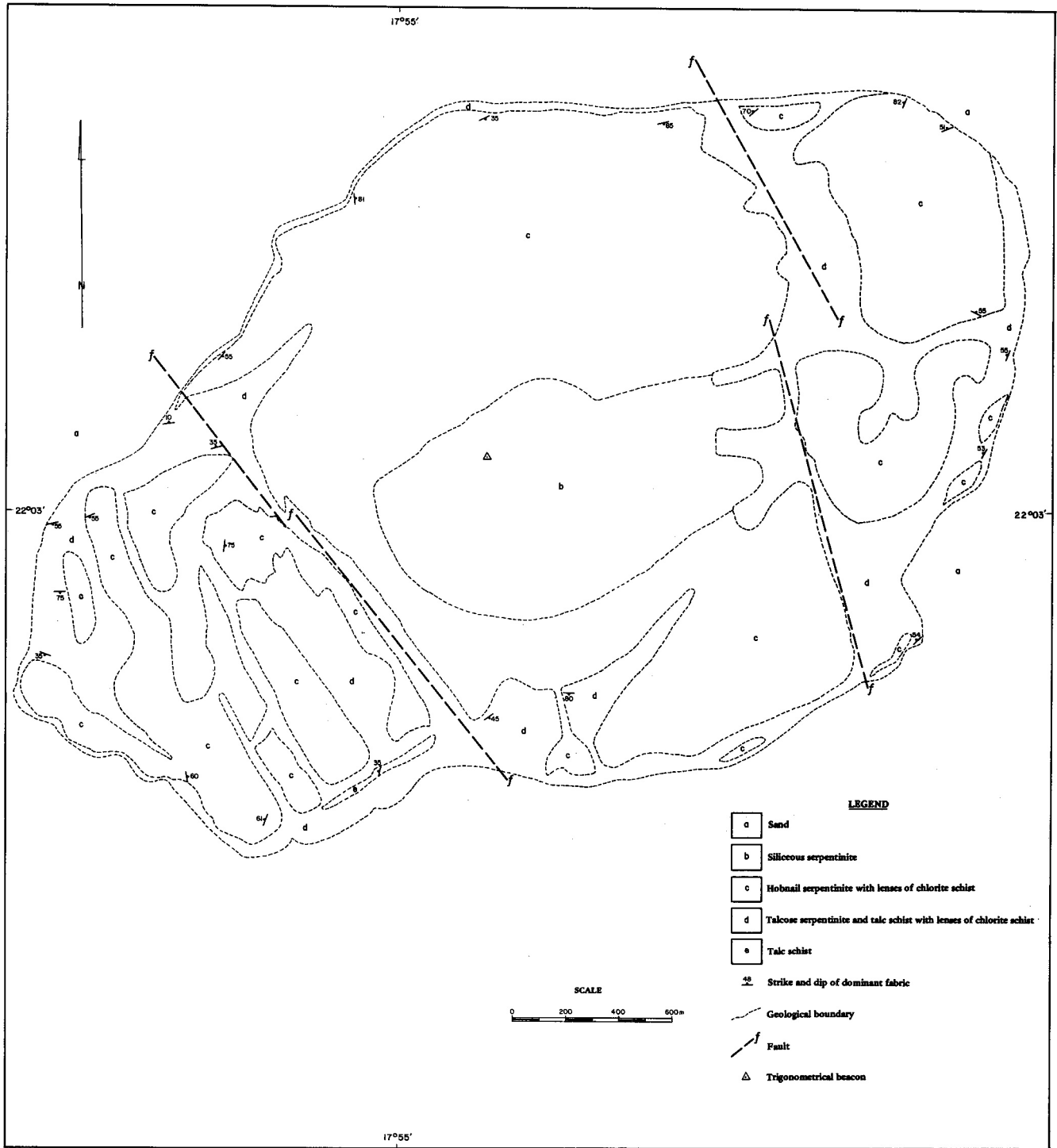


Fig.2.6- Geological map of the Omieve Serpentine, Omieve 179, Windhoek District

zones. The westerly one strikes at 140° and dips 40° west. The other has less topographic expression and strikes at approximately 150°.

2.3.3 SYNTHESIS

Figure 2.6 shows the field relationships of the various rock types.

The lack of country-rock exposure makes structural interpretation difficult. 81 is interpreted as being a pre-emplacment fabric which has been disrupted during solid emplacement of the body. S_2 has the same orientation as the dominant dS_2 Damara fabric. Since the chlorite and talc schist contain S_2 as a fracture cleavage they are assumed to have formed prior to or during the formation of S_2 .

2.4 OTJIHAENENA SERPENTINITE

2.4.1 ROCK TYPES

At 22°13'8:17°45'E, on the farm Otjihaenena 196, is a low hummock consisting of weathered serpentinite. Because outcrop is poor, detailed mapping was not undertaken. Figure 2.7 is a sketch map of the body. The extent of the outcrop is 500 by 750 m but the body probably actually measures 750 by 1 100 m. The long axis is orientated at 040°, which is approximately the strike of the dominant dS_2 fabric in the Damara country rock.

The central portion consists of hobnail serpentinite which grades into talcose and carbonate serpentinites. These are surrounded by a rim of talc schist within which are lenses of chlorite schist 1 to 2 m long. All five lithological varieties correspond to those described in Section 2.1.1.

The surrounding country rock is not exposed but five boreholes drilled through the body intersected amphibolites and mica schist of the Kuiseb Formation.

The typical sequence in a borehole is shown in Figure 2.7.

2.5 OKAHAU SERPENTINITE

2.5.1 ROCK TYPES

Due to the absence of country-rock exposure at the Otjihaenena body the serpentinite on the farm Okahau 185 was selected for making a structural interpretation of lensoid bodies in Damara country rocks. It consists of two lenses located at 22°07'8:17°47'E. The westerly lens is 500 m long and 200 m wide. The easterly lens measures 200 by 150 m (Fig. 2.8). The country rock is staurolite-garnet-biotite schist of the Kuiseb Formation. The ultramafics consist of hobnail serpentinite, talcose serpentinite, chlorite schist and talc schist identical to those described in Section 2.1.1.

2.5.2 STRUCTURE

The fabric elements present are:

S_1 A strong schistosity in the country rock which dips northerly and strikes at 045°. S_1 is tentatively correlated with the S_2 fabric of the Damara Orogeny (Hälbich 1970, Kasch 1978, Hartnady, in press). The talc schist and chlorite schist of the lenses contain the same fabric which may dip to the north or south.

S_2 A crenulation cleavage in the talc schist, the chlorite schist and in the biotite schist. This generally dips steeply to the south and strikes east-west.

S_3 A crenulation cleavage in the chlorite and talc schists axial planar to folds which deform S_1 and S_2 . S_3 dips steeply south.

F_1 Minor tight to isoclinal folds which have S_1 axial planar. F_1 folds a banding which may be due to original layering. The hinge lines of F_1 are often non-cylindrical.

F_3 Minor asymmetric broad open folds in the talc and chlorite schists (F_3) deforming S_1 and S_2 . Along the southern flanks of the serpentinite, F_3 axial planes dip to the south but they dip to the north on the northern flanks. In the central portion, F_3 axial planes are horizontal. F_3 folds are confined to the immediate vicinity of the body.

2.5.3 SYNTHESIS

S_1 is assumed to be a fabric, present in the country rock, along which the serpentinite body was emplaced. Since S_1 is present in the talc and chlorite schists as a fracture cleavage these rock types must have formed before or during S_1 (dS_2 , Table 2.1).

Confined to the neighbourhood of the body, the F_3 folds are assumed to be drag folds resulting from simple shear. The sequence of the folds as shown in Figure 2.8b suggests that the country rock was thrust over the body from the north-north-west. A fold showing overturn of its closure was observed. This may have formed as a result of continued thrusting after the formation of the folds.

The evidence suggests that thrusting outlasted emplacement and that the thrust plane was later folded on a regional scale (Fig. 2.9).

3. PETROGRAPHY

3.1 DATA (cf. Table 3.1 for abbreviations)

The information obtained from the study of approximately 300 thin sections is listed in Table 3.2. Mineral identifications were made on the basis of X-ray diffraction work combined with refractive index determinations. Appendix II contains descriptions of the many lithological varieties present in the areas investigated.

Microscopic examination confirms field observations to the effect that the country rocks have been modified adjacent to

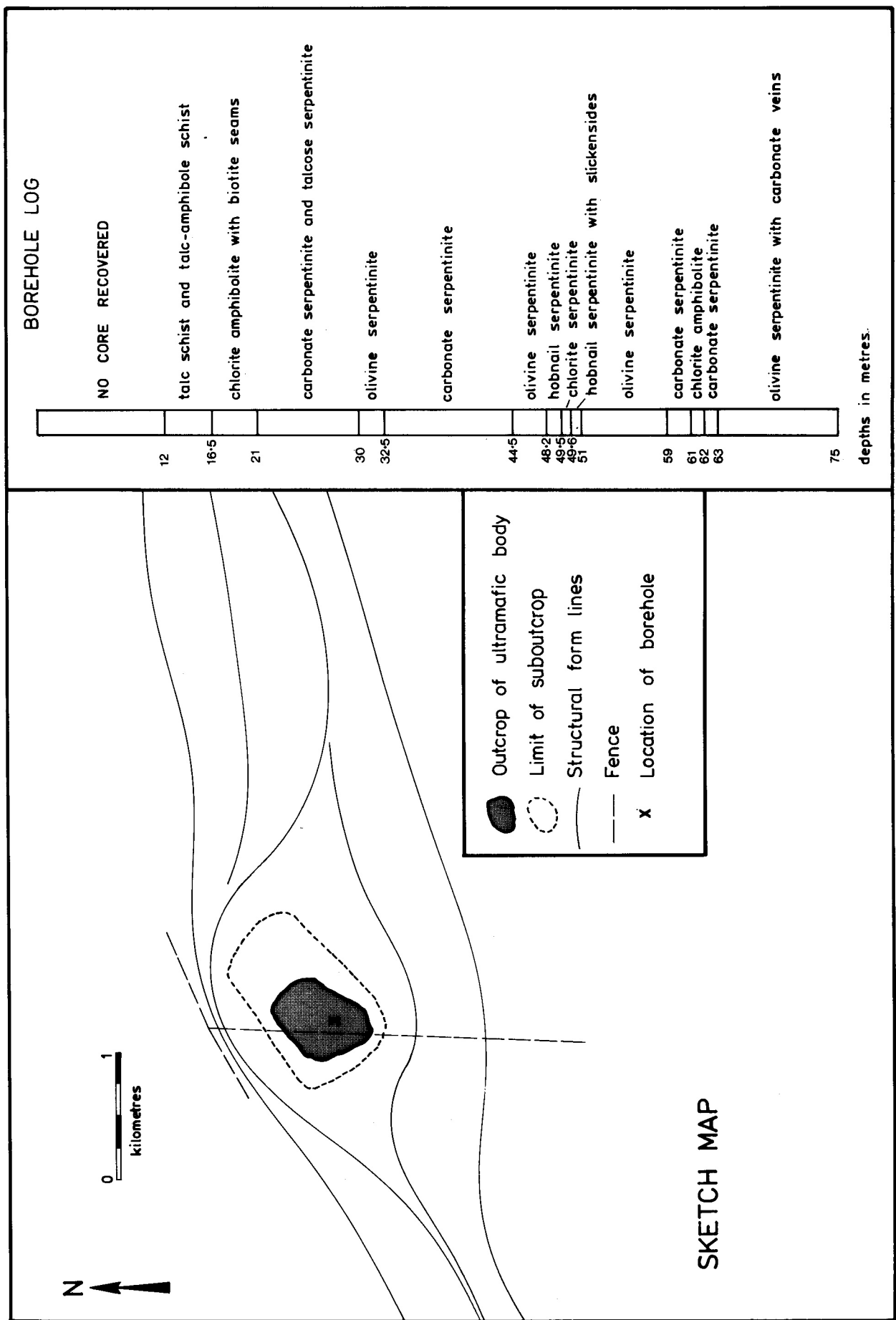


Fig. 2.7 — Sketch map of the serpentinite on Ojijhaenena 196 and typical borehole log

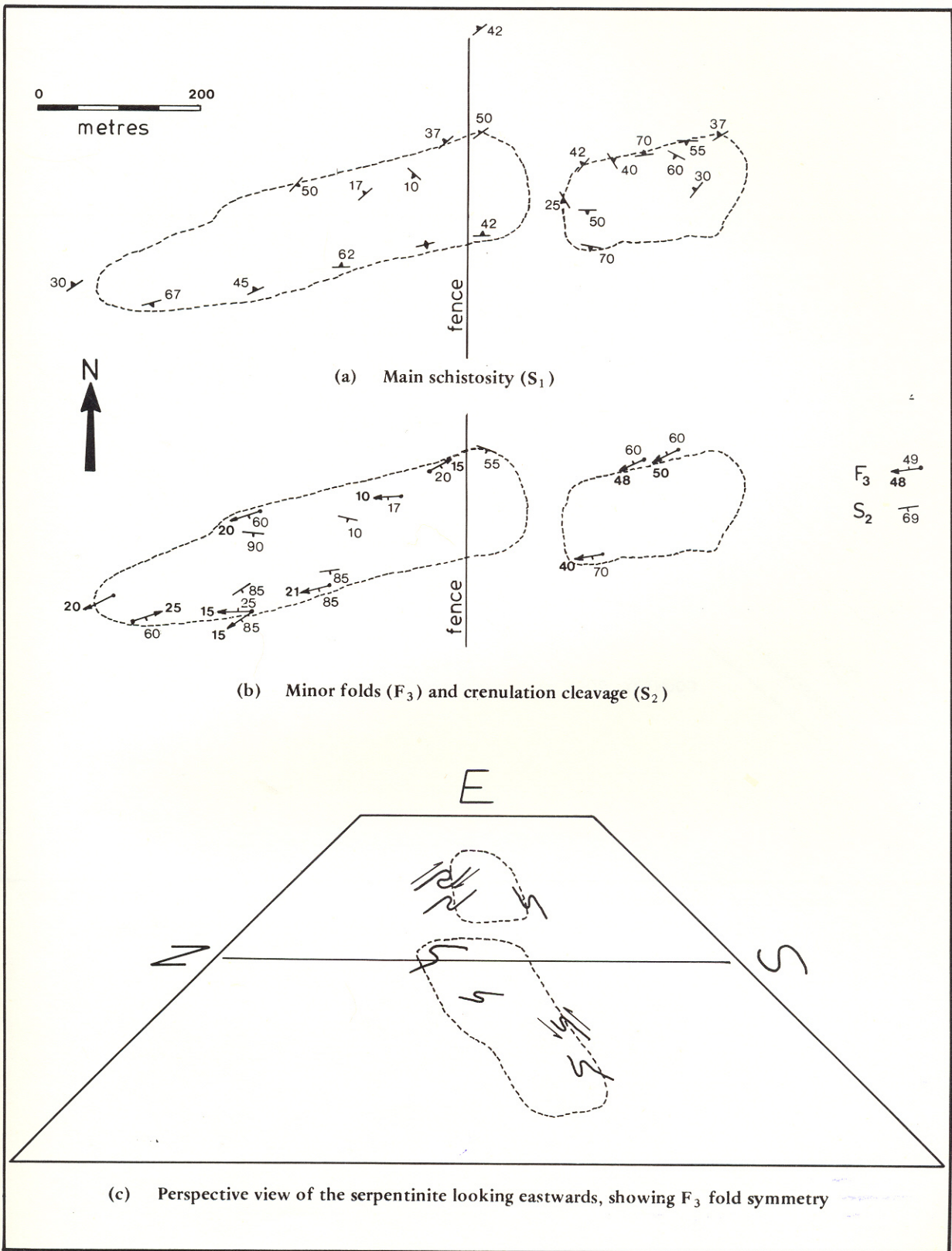


Fig. 2.8 — Structural details of the Okahau Serpentinite

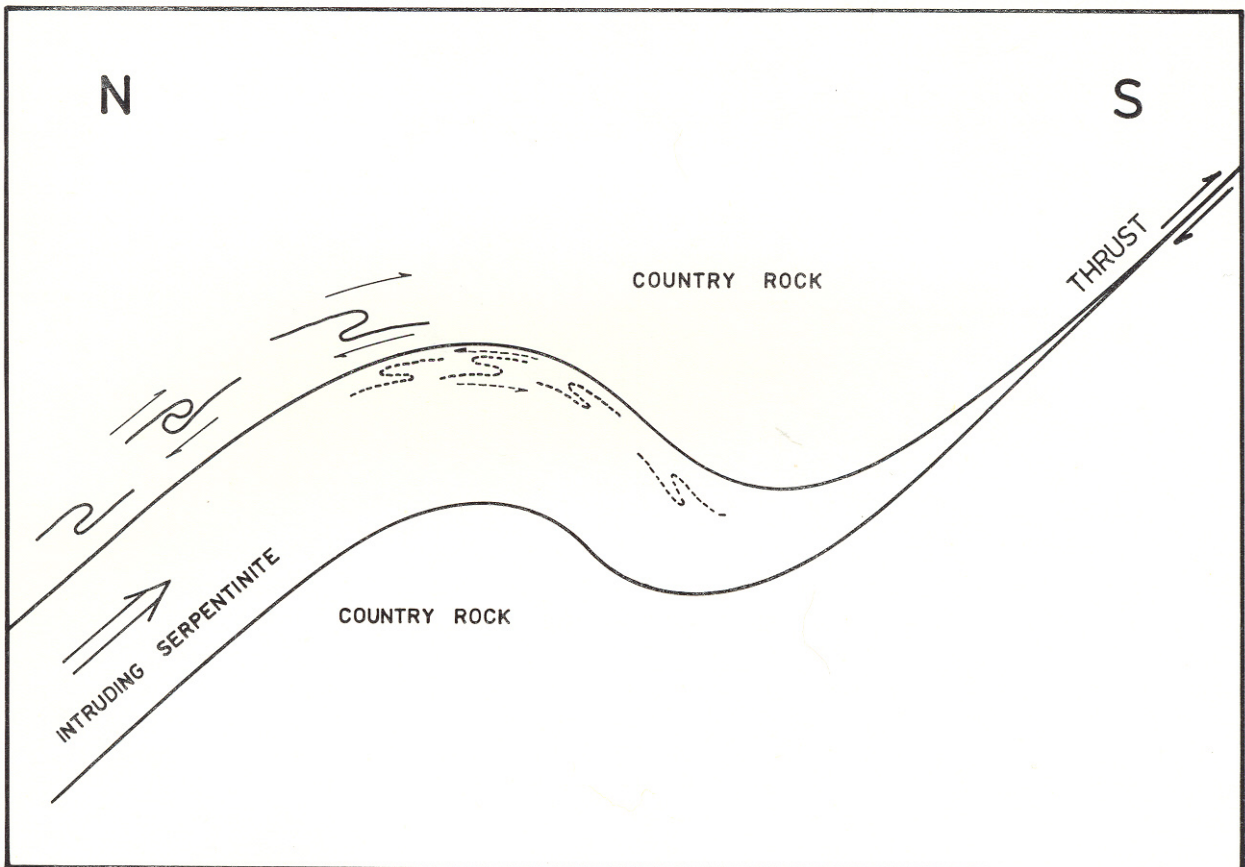


Fig. 2.9 — Diagrammatic representation of minor folds in country rock (solid lines) and in the ultramafic body (broken lines) related to a thrust plane, and intrusion of the serpentinite on Okahau

Table 3.1.1 - ABBREVIATIONS OF MINERAL NAMES

AB	Albite	CHY	Chrysotile	MUS	Muscovite
AC	Actinolite	DI	Diopside	OL	Olivine
AG	Antigorite	DOL	Dolomite	OPX	Orthopyroxene
AK	Ankerite	EN	Enstatite	OR	Orthoclase
AN	Anorthite	EP	Epidote	PLG	Plagioclase
AP	Apatite	FO	Forsterite	QZ	Quartz
AUG	Augite	GA	Garnet	SER	Serpentine
BIO	Biotite	HB	Hornblende	SI	Siderite
BR	Brucite	IO	Idocrase	SN	Spinel
CAR	Carbonate	KY	Kyanite	SP	Sphene
CC	Calcite	LZ	Lizardite	ST	Staurolite
CHL	Chlorite	MA	Magnetite	TC	Talc
COR	Cordierite	MC	Microcline	TR	Tremolite
CPX	Clinopyroxene	MS	Magnetite	ZO	Zoisite

Table 3.2 - A SUMMARY OF PETROGRAPHIC INFORMATION

Rock type	Location	Minerals in decreasing order of abundance	Texture				Grain boundaries		
			1.	G ¹	L ¹	N ¹	S ²	Su ²	C ²
Gneiss, pre-Damara	> 240 m from serpentinite/country-rock contact on Elisenhöhe and Gauchab	QZ, BIO, MUS, AN ₃₅ , SP		X			X		
	> 60 m from serpentinite/country-rock contact on Elisenhöhe and Gauchab	QZ, AN ₃₀ , MC, MUS, BIO, MA, ZO or EP			X		X		
Epidotised gneiss, pre-Damara	< 10 m from serpentinite/country-rock contact on Elisenhöhe and Gauchab	QZ, MC, BIO, EP, CHL, MA, HB			X		X	X	
Amphibolite	> 300 m from serpentinite/country-rock contact on Elisenhöhe and Gauchab	AC, AN ₁₅ , QZ, MA				X	X		
Epidote amphibolite, pre-Damara	< 50 m from country-rock/serpentinite contact on Elisenhöhe and Gauchab	AC, AN, EP, MA, SP, CHL				X	X		
Chlorite amphibolite, pre-Damara	At country-rock/serpentinite contact on Gauchab and Elisenhöhe	CHL, AC, MA, +BIO, +AN ₃₅ , +EP				X	X	X	
Mica schist, pre-Damara	> 100 m from country-rock/serpentinite contact on Gauchab and Elisenhöhe	BIO, MUS, AN ₃₅ , QZ, MA, EP, AP	X					X	
Epidote-mica schist, pre-Damara	< 5 m from country-rock/serpentinite contact on Gauchab and Elisenhöhe	BIO, QZ, MUS, AN ₁₅ , MA			X		X		
	At country-rock/serpentinite contact on Gauchab and Elisenhöhe	CHL, QZ, BIO, MUS, AN ₁₅ , EP, MA			X			X	
Metaconglomerate, Nosib Group	100 m from country-rock/serpentinite contact on Elisenhöhe	QZ, OR, MC, BIO, MA			X		X		
Epidotised metaconglomerate, Nosib Group	At country-rock/serpentinite contact on Elisenhöhe	AC, EP, OR, QZ, MA, SP			X		X	X	X
Biotite-mica schist, Khomas Subgroup	10 m from serpentinite/mica-schist contact at Otjihaenena, Okahau and Omieve	AN ₁₅ , BIO, QZ, OR, GA, MA, +ST, +KY			X		X		
Epidote-mica schist, Khomas Subgroup	1 m from the serpentinite/mica-schist contact at Otjihaenena, Okahau and Omieve	AN ₁₅ , BIO, QZ, OR, GA, MA, EP, CHL, +KY, +ST			X		X		
Amphibolite, Khomas Subgroup	3 m from the serpentinite/amphibolite contact on Talana 199 and Otjihaenena	HB, AN ₃₀ , OR, MA, GA, CHL, 5% EP				X	X		
Epidote amphibolite, Khomas Subgroup	3 m from the serpentinite/amphibolite contact on Talana 199 and Otjihaenena	HB, EP, MA, AN ₃₀ , BIO				X	X		
Hornblende 'dykes', of the ultramafic sequence	Within the serpentinites	HB, EP, SP, MA, +PLG, +CHL, +AUG, +QZ		X			X	X	X
Chlorite schist	Within and at margins of all bodies	CHL, MA, +IO			X		X		
Actinolite fels	Within all bodies towards edge	AC, TC, CHL, +QZ	X				X	X	
Talc-amphibole schist	At margins of Gauchab, Omieve and near faults	TC, OR, AC, +CHL			X		X		
Talc schist	At margins of all bodies and near faults	TC, MA, +CHL, +CAR			X		X		
Carbonate serpentinite	Lenses inside talc-schist rim of many bodies	MS, AK, OR, DOL, AG, MA	2.	P ³	NP ³	IP ³	IL ³	S ³	Su ²
				X	X	X		X	X
Talcosc serpentinite	Within talc-schist rim of many bodies; Gauchab, Elisenhöhe, Omieve and Otjihaenena	TC, AG, +AK, +AC		X	X	X		X	X
Hobnail serpentinite	Central portion of most bodies	AG, MA, +CO, +QZ		X	X	X	X	X	X
Olivine serpentinite	In the core of Gauchab and Otjihaenena	FO ₉₀ , AG, MA		X	X	X	X	X	X

G¹ = Granoblastic
 S² = Straight
 P³ = Pseudomorphic
 NP³ = Non-pseudomorphic

L¹ = Lepidoblastic
 Su² = Sutured
 IL³ = Interlocking

N¹ = Nematoblastic (Harker 1970)
 C² = Cuspate (Spy 1969)
 IP³ = Interpenetrating (Wicks and Whittaker 1977)

the ultramafic bodies and the following observations may be made:

(a) In the quartzo-feldspathic rocks, epidote content is roughly proportional to the distance of the sample from the serpentinite contact. At the contact it is about 20 per cent, falling off to zero at 240-m distance. In the same way texture varies from lepidoblastic to granoblastic.

(b) The proportion of epidote in amphibolites decreases steadily from 40 per cent at the contact to less than 5 per cent 300 m distant. There are two generations of amphibole near the contact but only one 300 m away.

(c) Chlorite is present in all rocks, closer than 5 m from the contact.

(d) The serpentine mineral is antigorite. It may be pseudomorphic, non-pseudomorphic or vein forming. Mesh-structured, hourglass and curtain-textured pseudomorphs of A-antigorite and C-antigorite are present. The non-pseudomorphic material which is both interlocking and interpenetrating is A-antigorite. The veins consist of non-asbestose C-antigorite.

(e) The slides reveal certain structural information, namely (i) in the talc schist dS_2 , as defined in Table 2.1, is a fracture cleavage outlined by magnetite, and the talc is crenulated by F_3 , (ii) the same applies to the chlorite in the chlorite schists and (iii) actinolite fels is not deformed by dS_2 .

3.2 INTERPRETATION OF TEXTURES AND DEDUCTIONS OF METAMORPHIC REACTIONS

Barnes and O'Neil (1969) show that two types of water flow from serpentinites. From partially serpentinitised bodies a water enriched in Ca^{2+} flows, whereas from both partially and completely serpentinitised bodies the water is enriched in Mg^{2+} . They concluded that near-surface serpentinitisation takes place at almost constant composition except for the loss of Ca^{2+} and that waters enriched in that element may cause Ca^{2+} metasomatism at depth. The waters were not enriched in other elements.

Bearing this in mind simple mineral/mineral reactions and metasomatic reactions involving the transport of Ca^{2+} and Mg^{2+} only out of the serpentinites have been used as far as possible in developing a petrogenetic model. This is in direct contrast to the work of Chidester (1962), Coleman (1966, 1967), Jahns (1967), and Williams (1971) who invoke transport of Ca^{2+} , Mg^{2+} , Si^{4+} , Al^+ , Na^+ , K^+ and Fe^{2+} when evolving models for the formation of rock types found at the margins of serpentinites.

3.2.1 OLIVINE SERPENTINITE

The following model explains the textures observed in the serpentinites, i.e. pseudomorphs (mesh, hourglass and curtain textures), non-pseudomorphic texture and veins.

Wicks *et al.* (1977) describe three textures which devel-

op when serpentinite replaces olivine, namely: (a) hourglass textures, (b) mesh textures with olivine centres and (c) mesh textures with isotropic centres.

Only the first two textures were observed in the serpentinite discussed here. Wicks *et al.* (1977) ascribe these textures to the development of serpentine normal to all prism faces or orthogonally fractured olivine at a uniform rate. In (a) development continues until all the olivine is consumed. In (b) the process of serpentinitisation ceases before all the olivine has been altered. Hourglass serpentine is C-serpentine.

Bastite pseudomorphs, with curtain textures, may form after pyroxene, amphiboles, talc, chlorite or phlogopite. Wicks and Whittaker (1977) suggest that A- and C-serpentine bastites form under conditions of falling temperature, absence of shearing and no nucleation of antigorite. However, X-ray diffraction traces of the samples studied indicate that antigorite is the only serpentine present (Table 3.3 contains a list of d-spacings used for identification). Wicks and Whittaker state that bastites usually consist of lizardite. Antigorite bastites are thought to develop when antigorite forms pseudomorphs after lizardite during conditions of rising temperature.

The presence of the non-pseudomorphic interlocking and interpenetrating C-antigorite suggests recrystallisation of lizardite or chrysotile to antigorite while the temperature rose (Wicks and Whittaker 1977).

The serpentine in the veins consists of non-asbestose C-antigorite fibres; it may have a fracture-filling or slip-fibre texture (i.e. fibres respectively perpendicular or parallel to the walls of the vein). The presence of the slip-fibre material implies shearing, whereas the fracture-filling material formed under conditions of low stress. The serpentinite in hand specimen is massive so the slip fibre is thought to have formed by stress being localised in the slip-fibre veins and in the schists developed at the margins of the bodies. The fracture-filling veins may have formed subsequently. Since the veins contain C-antigorite they formed as the temperature rose (Wicks and Whittaker 1977).

The three textures therefore suggest a complex history consisting of:

(a) Low-temperature serpentinitisation, without shearing, resulting in the formation of lizardite bastites, hourglass- and mesh-textured pseudomorphs.

(b) Recrystallisation of the lizardite with rising temperature and pressure to form antigorite, first under conditions where shearing took place and, later under conditions where no shearing was operative.

Page (1968) demonstrates that there is a chemical differ-

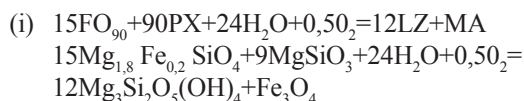
Table 3.3 - LIST OF d-SPACINGS USED TO IDENTIFY ANTIGORITE

	Coleman	SWA	Coleman	SWA
hkl	dÅ	dÅ	I	I
001	7,25	7,20	140	150
20	7,02	7,07	20	20
810	4,67	4,69	4	3
020	4,62	4,62	4	3
910	4,26	4,28	2	2
81	3,96	-	1	-
102	3,60	3,60	70	100
302	3,53	-	6	-
16.0.1	2,52	2,51	30	30
93	2,46	2,45	3	1
003	2,41	2,41	6	4
883	2,169	2,164	10	7
16.0.2	2,15	2,150	9	6
004	1,809	1,815	3	3
933	1,773	1,776	2	2
17.0.3	1,74	1,738	1	1
24.3.0	1,559	1,5618	5	3
24.3.1	1,5359	1,538	2	2
15.0.4	1,523	-	1	-

d-spacings obtained from Coleman (1966) compared with those of South West African serpentines. A Cu tube and Ni filter run at 40 kV and 30 mA were used to obtain the X-ray diffraction traces.

ence between the three serpentines chrysotile, lizardite and antigorite and that the formula $Mg_3Si_2O_5(OH)_4$ is an oversimplification. Nonetheless, this formula has been used in the reactions proposed here, for the sake of simplicity.

The relict olivine has a composition of FO_{90} . Occasionally magnetite can be seen outlining orthopyroxene cleavages in the bastites. On the basis of these observations and points (a) and (b), the following reactions are postulated for the development of the olivine serpentinite:

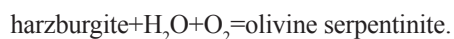


Reaction (i) takes place under low-temperature conditions in the absence of substantial shearing.

Rising temperature and pressure favour the development of antigorite (Iishi and Saito 1973, Evans *et al.* 1976) and the lizardite recrystallises to form antigorite, occasionally under conditions of shearing.



Wicks and Whittaker (1977) suggest that magnetite moves as the degree of serpentinisation increases. In the early stages it forms discrete grains distributed throughout the serpentine. As serpentinisation proceeds the magnetite forms coarser grains and concentrates in mesh centres. In the final stages there is migration out of mesh or hourglass textural units into cross-cutting lenses and veinlets. This migration is due to the lack of a lattice site for Fe in serpentine. All three forms of magnetite were observed in the samples studied. The origin of the olivine serpentinite is therefore:

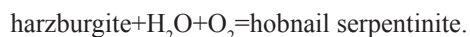


3.2.2 HOBNAIL SERPENTINITE

The hobnail serpentinite contains pseudomorphic, non-pseudomorphic and non-asbestose veins of antigorite. The textures are the same as those present in the olivine serpentinite. It is therefore suggested that the same sequence of events took place as outlined in Section 3.2.1 but in this case reaction (i) went to completion.

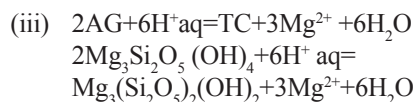
The field relationship between these two rock types is consistent with this statement, as the olivine serpentinite is rimmed by hobnail serpentinite. Presumably insufficient water reached the olivine serpentinite to produce a complete reaction.

Since the quartz veinlets were only found in weathered specimens it is suggested that during weathering, MgO is removed and SiO_2 is not, resulting in the formation of chalcidony veins and the siliceous capping (e.g. Omieva). The origin of the hobnail serpentinite is therefore:

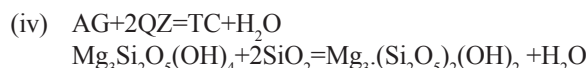


3.2.3 TALCOSE SERPENTINITE

The talcose serpentinite contains the same three textural elements as the hobnail serpentinite, namely pseudomorphs, interlocking and interpenetrating laths, and veins, and hence the same initial reactions are suggested for its formation. Nesbitt and Bricker (1978) outline how serpentinite is dissolved by percolating meteoric waters. Talc is precipitated and a Mg-bearing solution is produced:

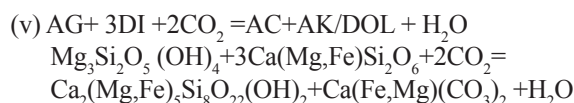


This reaction may account for the development of talcose serpentinite. An alternative possibility is:



Hemley *et al.* (1977) discuss how antigorite becomes unstable with respect to talc as silica activity increases. Evans and Trommsdorff (1970) have described this reaction in serpentinites from the Central Alps. The source of the silica could be the country rock. The talc in the talcose serpentine is not orientated along dS_2 and may therefore have formed after the dS_2 deformation.

In those specimens where dolomite or ankerite, which depends on the locality, and actinolite are present the reaction:

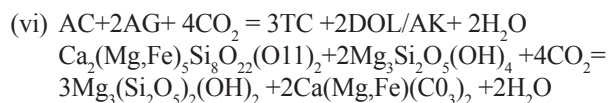


is suggested to account for the presence of a Ca-bearing mineral. Using dolomite and tremolite, Trommsdorff and Evans (1977) have described conditions under which this reaction takes place and have documented its occurrence in the Alps.

The actinolite frequently has a radiating acicular texture and is rarely orientated along the main schistosity, dS_2 . Therefore the reaction took place after the deformation which produced the schistosity. As the bodies were subjected to rising temperatures after the formation of dS_2 , reaction (v) has been chosen in preference to the hydration reaction:



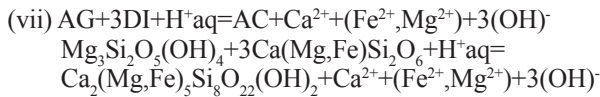
As the X_{CO_2} rises the reaction:



may take place to produce a rock containing AC, AG, TC and either DOL or AK.

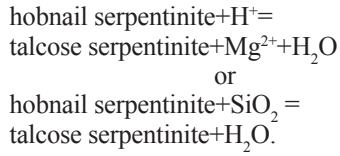
When no CO_2 is present, reactions involving clinopyrox-

ene will produce Ca ions. Reaction (iv) then becomes:

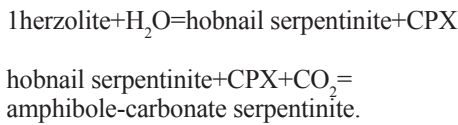


All reactions producing actinolite took place after the deformation which produced dS_2 .

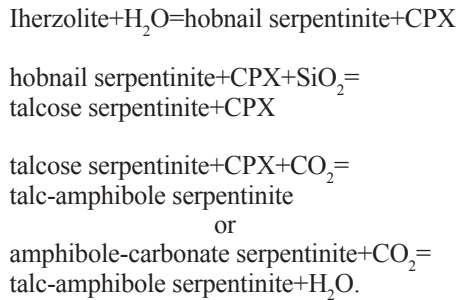
The origin of the talcose serpentinite is either:



The origin of the amphibole and carbonate serpentinite is:



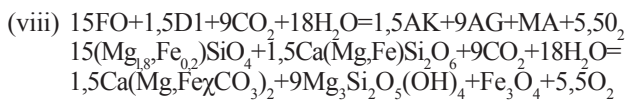
The origin of the talc-amphibole serpentinite might be:



3.2.4 CARBONATE SERPENTINITE

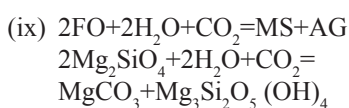
The carbonate serpentinite exhibits essentially the same three textural elements as the olivine serpentinite. In addition, large grains of magnesite, ankerite or dolomite, depending on the locality, are present. The carbonate is filled with minute inclusions of magnetite. The presence of the three forms of antigorite suggests that the same sequence of events took place as in the formation of olivine serpentinite.

However, if some CO_2 and clinopyroxene were present in the initial stages the following reaction might have taken place:



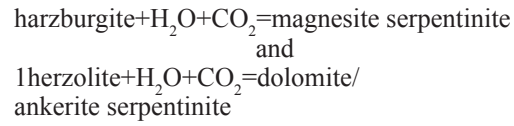
This would account for the development of antigorite needles with hourglass texture which penetrate the carbonate. Trommsdorff and Evans (1977) have outlined the same reaction in which dolomite is the carbonate.

Where the carbonate is magnesite the reaction:



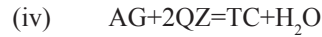
may take place. As both these are hydration reactions, they probably took place at the same time as reaction (i).

The origin of the carbonate serpentinite is then:



3.2.5 TALC SCHIST

The talc schist is usually located at the margins of the bodies. The reaction:



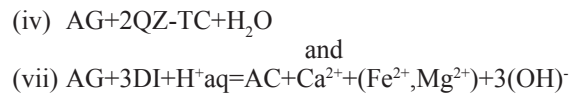
is suggested to account for its formation.

The talc schist is cut by a fracture cleavage, dS_2 but some grains of talc have their long axes aligned parallel to dS_2 . Talc is crenulated by S_3 . The talc therefore formed before and during the deformation which produced dS_2 and is thought to have developed by the reaction:



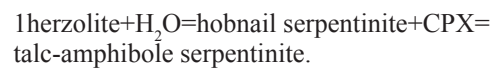
3.2.6 TALC-AMPHIBOLE SCHIST

The talc-amphibole schist may be the end product of reaction (iv) and (vii):



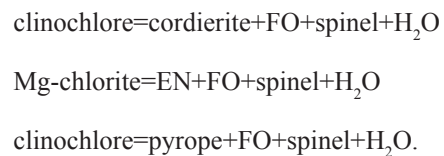
The talc contains a fracture cleavage dS_2 and some talc is orientated along dS_2 . Hence reaction (iv) took place prior to and during the deformation which produced dS_2 . The actinolite has a random orientation and hence formed after dS_2 .

The origin of the talc-amphibole schist is then:



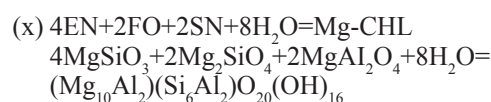
3.2.7 CHLORITE SCHIST

Staudigel and Schreyer (1977) describe three reactions whereby chlorite breaks down:



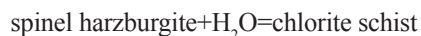
The first reaction takes place at low pressures (less than 3,25 kb), the second is operative at medium and high pressures (less than 20 kb) the third occurs above 20 kb.

The reaction:



is proposed as the most probable for production of chlorite schist within the bodies. The schist is enclosed in rocks that contained olivine and orthopyroxene, hence it represents portions of the bodies in which spinel was present in addition to olivine and orthopyroxene. Since the chlorite schist contains dS_2 as a fracture cleavage, it formed prior to dS_2 . As reaction (x) is a hydration reaction it is thought to have taken place at the same time as reaction (i).

The origin of the chlorite schist is then:



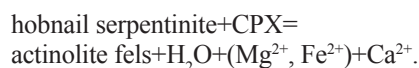
3.2.8 ACTINOLITE FELS

Coleman (1966, 1967) and Jahns (1967) describe the development of actinolite- or tremolite-rich rocks towards the margins of ultramafic bodies. Coleman (1966) outlines the development of tremolite where serpentinite is in contact with greywacke. He suggests that Mg^{2+} and Ca^{2+} are transported out of the serpentinite to produce actinolite fels. If the reaction:



took place this would produce actinolite fels. The ions are carried away in solution, and the solution containing Ca^{2+} , Fe^{2+} and Mg^{2+} may cause metasomatism in the country rock (Section 3.2.9). The trace-element chemistry is consistent with the contention that the protolith of the actinolite fels was ultramafic. The actinolite exhibits no preferred orientation and therefore formed after dS_2 .

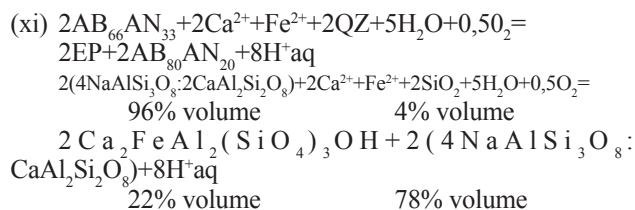
The origin of the actinolite fels is then:



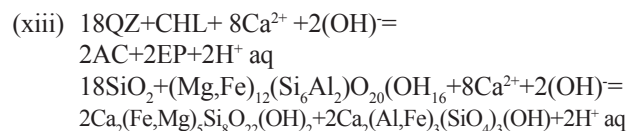
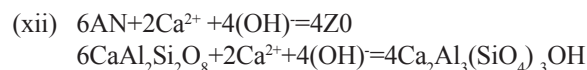
3.2.9 EPIDOTE-PRODUCING REACTIONS

In all the country rocks, 200 m and less from the contact, epidote and/or zoisite are developed. Barnes and O'Neil (1969) have shown that Ca^{2+} is found in high concentrations in waters flowing from partially serpentinitised bodies and Coleman (1967) found exceptionally high Ca^{2+} concentrations in country rocks in immediate contact with serpentinites.

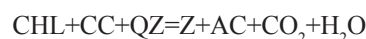
The source of the Ca^{2+} may be clinopyroxene in the ultramafics. The Ca^{2+} would be released during reactions such as (vii). Reactions leading to the formation of epidote and zoisite are:



The plagioclase composition was chosen on the basis of the plagioclase in the country rocks at Gauchab (An_{30-35}).



Coleman (1967) pointed out that with increasing Ca^{2+} activity, reaction (xii) will take place. Reaction (xi) is an adaptation of reaction (xii). Reaction (xiii) is a modification of the reaction:



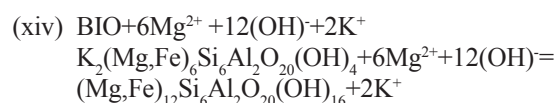
of Deer *et al.* (1974) based on observed mineral compositions.

The reactions would appear to be reasonable in terms of modal percentage of minerals present. Reaction (xi) implies that if a rock containing 30 per cent of plagioclase was metasomatised in this fashion it would produce 6 per cent of epidote. This is similar to the modal proportions determined in the gneiss and epidotised gneiss (Appendix II). Since reaction (vii) which supplies the Ca^{2+} ions took place after dS_2 formation, the epidote-producing reactions must have also taken place after dS_2 .

3.2.10 CHLORITE-PRODUCING REACTIONS

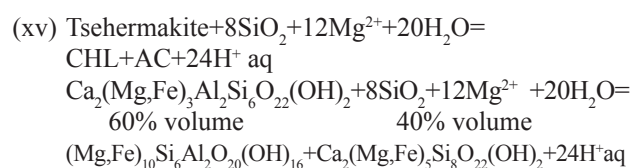
Chlorite is found in all the country rocks within 5 m of the contact with the ultramafic rocks. Chidester (1962), Coleman (1966, 1967), Jahns (1967) and Williams (1971) have described this phenomenon. These authors suggest, on textural grounds, that chlorite has replaced biotite, plagioclase and amphiboles, probably as a result of Mg metasomatism caused by the Mg-rich waters issuing from serpentinites as described by Barnes and O'Neil (1969) and Nesbitt and Bricker (1978).

Chlorite can be seen replacing biotite in some thin sections of South West African samples, suggesting the reaction:



The K^+ may have been removed in solution to form muscovite and K-feldspar porphyroblasts in the quartzo-feldspathic gneiss or schists.

Amphiboles are recrystallised in the vicinity of the ultramafics and in places appear to be replaced by chlorite, suggesting the reaction:



Since Mg-enriched waters flow from all serpentinites

this reaction may take place at any time.

3.2.11 HORNBLENDITE 'DYKES'

The hornblende 'dykes' within the serpentinite bodies show no signs of serpentinisation. The only indications of alteration are the development of zoisite and epidote, which are assumed to have formed by the reactions (xi) and (xii), because in some thin sections zoisite can clearly be seen replacing plagioclase.

3.2.12 PRE-DAMARA QUARTZO-FELDSPATHIC GNEISS AND EPIDOTISED GNEISS

In the vicinity of the serpentinites, epidote is developed in the gneiss and the plagioclase has recrystallised. The epidote is believed to form by reaction (xi).

The chlorite developed in the gneiss within 5 m of the contact may have formed by reaction (xiv).

3.2.13 PRE-DAMARA AMPHIBOLITE, EPIDOTE AMPHIBOLITE AND CHLORITE AMPHIBOLITE

The amphibolite in the vicinity of the ultramafics may contain up to 40 per cent of epidote. This may be a result of Ca metasomatism by reactions (xii) and (xiii).

In amphibolites, less than 10 m from the contact, chlorite is developed and the amphiboles are recrystallised. This could be the product of Mg metasomatism by reaction (xv).

The chlorite and amphibole growth along dS_2 planes is mimetic and these minerals are not deformed. Hence the chlorite and amphibole developed after deformation producing dS_2 .

3.2.14 PRE-DAMARA MICA SCHIST

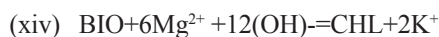
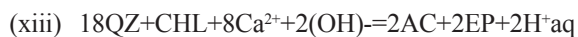
Epidote may have developed in the mica schist by reaction (xi). The chlorite present in samples less than 5 m from the contact may have developed by reaction (xiv).

3.2.15 DAMARA METACONGLOMERATE

Pre-Damara gneiss, amphibolite and mica-schist pebbles are present in the Nosib conglomerates. Towards the serpentinite body the same pattern of mineral changes is seen in these pebbles as in the pre-Damara country rocks, i.e. the formation of a small amount of epidote in the gneiss and mica schist and a large percentage of epidote in the amphibolite. Chlorite is developed in all three types of pebbles. The reactions producing these minerals are assumed to be (xi), (xiii), (xiv) and (xv).

The matrix of the conglomerate away from the body consists largely of quartz and feldspar and a little biotite. At the contact the matrix consists of chlorite, actinolite and epidote.

The reactions:

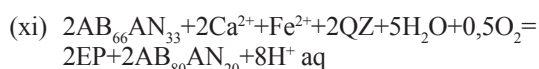


may account for these changes in mineralogy.

Since some actinolite is orientated along dS_2 while some has a radiating acicular growth these reactions occurred during and after the formation of dS_2 .

3.2.16 DAMARA AMPHIBOLITES

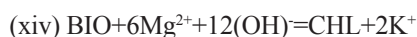
In the Damara amphibolites, epidote has developed after plagioclase presumably by the reaction:



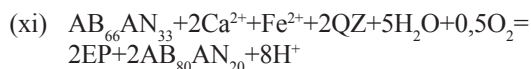
3.2.17 DAMARA MICA SCHIST

In the mica schist of the Damara Sequence, chlorite and epidote may be developed in a narrow zone not more than 150 mm from the contact.

The chlorite appears to have developed from biotite by the reaction:



The epidote is thought to have developed from plagioclase by the reaction:



As the chlorite has not been deformed, reaction (xiii) took place after the formation of dS_2 .

3.2.18 GEOLOGICAL HISTORY DEDUCED FROM TEXTURES AND REACTIONS

On the basis of the evidence presented the following sequence of events is envisaged:

(a) Harzburgite containing lenses of spinel harzburgite and lherzolite was hydrated at low temperatures and low X_{CO_2} without shearing. This resulted in the formation of olivine serpentinite, hobnail serpentinite, carbonate serpentinite and hobnail serpentinite containing clinopyroxene.

(b) The serpentinites were tectonically emplaced, during which process they came into contact with siliceous country rock, resulting in the formation of talc schist and talcose serpentinite. While the rocks were subjected to shearing, slip-fibre serpentine formed in the veins.

(c) During or after emplacement, the bodies were subjected to deformation which resulted in the formation of dS_2 planes. Structural evidence suggests that emplacement took place during the deformation that formed dS_2 (Section 2.1.2).

(d) After deformation the bodies experienced higher temperature. All serpentine recrystallised to antigorite if it had not already done so during emplacement. Under the higher temperature conditions the clinopyroxene reacted with antigorite to form actinolite-bearing serpentinite and actinolite feldspars. Where CO₂ was present, ankerite and talc developed in the serpentinite. The alteration of clinopyroxene resulted in the release of Ca²⁺. These ions metasomatised the country rock resulting in the formation of epidote.

(e) After metamorphism, circulating meteoric waters dissolved magnesium from the ultramafics resulting in the formation of talcose serpentinite and causing Mg metasomatism and the growth of chlorite in the country rock.

4. METAMORPHIC CONDITIONS

4.1 INTRODUCTION

The ultramafic bodies studied consist solely of serpentinite, talc schist and chlorite schist. There is no evidence to suggest that they were part of a differentiated ultramafic to mafic sequence, nor are there any signs of thermal aureoles or partial melting of contained acidic lenses. Consequently they were not derived from olivine or orthopyroxene cumulates by differentiation *in situ*. On structural grounds (Sections 2.1.2, 2.2.2, 2.5.2) it is believed that the serpentinites were emplaced tectonically whilst relatively cold. Three metamorphic regimes must therefore be considered, namely conditions before, during and after emplacement.

4.2 CONDITIONS BEFORE EMPLACEMENT OF THE SERPENTINITES

On the basis of the arguments outlined by Wicks and Whittaker (1977) the presence of serpentinite pseudomorphs suggests that serpentinitisation took place in the absence of substantial shearing and the presence of bastites indicates that the original serpentinite was composed of lizardite.

Lizardite is thought to be the stable serpentine mineral at low temperatures. Coleman (1971), Evans *et al.* (1976), Hemley *et al.* (1977), Moody (1976) and Wenner and Taylor (1971) all believe that lizardite serpentinitisation takes place between 85 and 185°C.

Binns *et al.* (1975) describe how the serpentine mineral changed as metamorphic grade increased in the Australian Yilgarn block. In the prehnite-pumpellyite and lower greenschist facies, lizardite is present. In the mid-greenschist to lower amphibolite facies, antigorite is the stable serpentine. In the mid- to high-amphibolite facies, the minerals are metamorphic forsterite, talc and calcite.

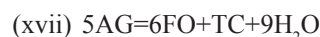
As carbonates are rare and probably only make up one modal per cent of the ultramafics, X_{CO₂} would be less than 0,25 since the reaction serpentine+CO₂=quartz+magnesite+H₂O has not taken place (Johannes 1969).

Direct estimates of pressure are difficult to make. However, if the maximum temperature of serpentinitisation was 185°C then, assuming a geothermal gradient of 20°C/km (world average - Press and Siever 1974), the maximum depth during serpentinitisation would be about 9 km. Pressure may be estimated from the equation $P=gHA\rho$ in which ρ is density, A is area and H is thickness (Means 1976).

Assuming that basaltic terrain has a density of 3 t/m³ and granitic terrain a density of 2,65 t/m³ the respective maximum pressures during serpentinitisation would be 2,6 and 2,3 kb.

4.3 CONDITIONS DURING EMPLACEMENT OF THE SERPENTINITES

Raleigh and Paterson (1965) showed that serpentinite is as strong as granite at low temperatures and pressures, yielding at a stress difference of 12 kb for antigorite and 8 kb for chrysotile/lizardite. However, the ultimate strength falls abruptly to 0,5 kb at 600 to 700°C for antigorite and at 300 to 350°C for lizardite/chrysotile serpentinites. They relate this reduction in strength to the dehydration reactions:



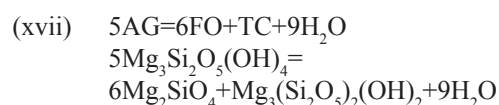
They suggest that these reactions facilitate tectonic emplacement. If so, conditions during emplacement would have accorded with curve (XVI) or (XVII) (Fig. 4.1) depending on which serpentine mineral was present.

4.4 CONDITIONS AFTER EMPLACEMENT, AT PEAK OF DAMARA METAMORPHISM

4.4.1 ULTRAMAFIC ROCKS

At this stage antigorite, the serpentine mineral which is present at high temperatures and pressures, would be present. Wenner and Taylor (1971) suggest that antigorite serpentinitisation takes place between 220 and 460°C. Trommsdorff and Evans (1974) describe chrysotile, in the central Alps, as being the serpentine present below the upper limit of pumpellyite, whereas between this limit and the upper limit of the oligoclase-kyanite-staurolite assemblage, antigorite is present. Forsterite and talc form at higher metamorphic grade.

The upper stability limit for antigorite is determined by the reaction:



A number of authors have investigated this reaction, the two most recent being Evans *et al.* (1976) and Hemley *et al.* (1977). All have produced similar curves (Fig. 4.2). The

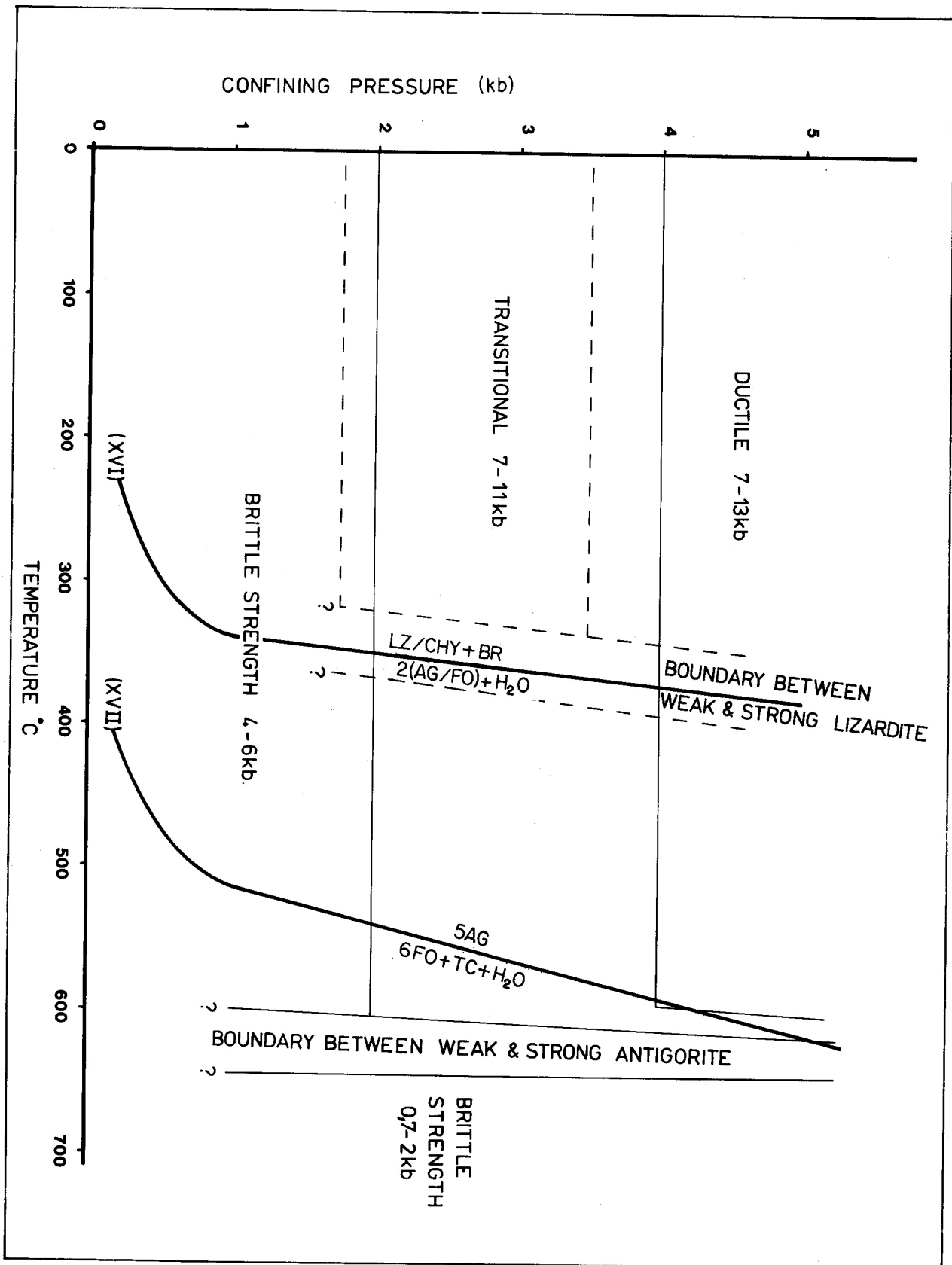


Fig. 4.1 — Stability of lizardite (broken lines) and antigorite (fine lines) after Raleigh and Paterson (1965) and Evans et al. (1976)

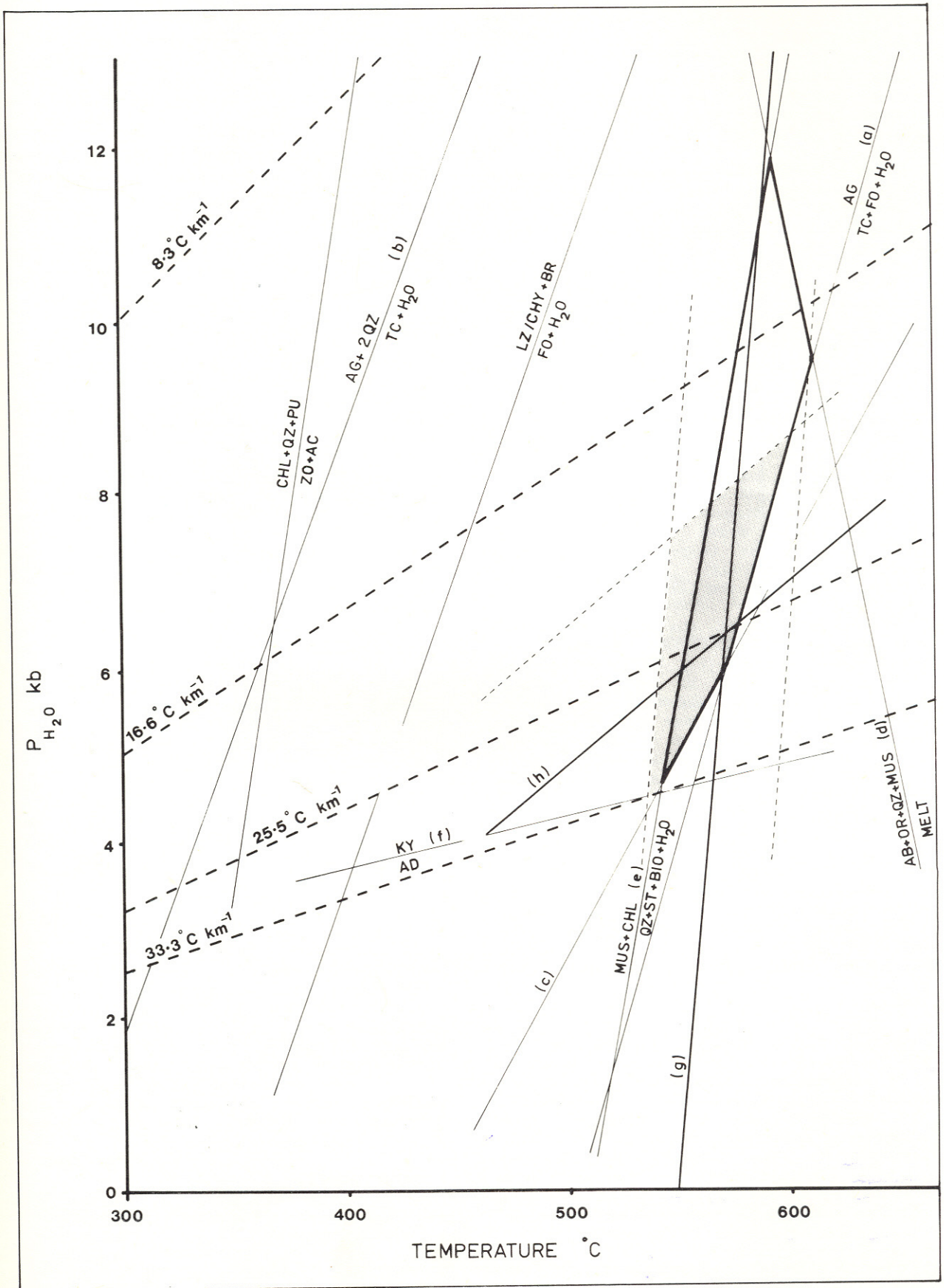


Fig. 4.2 — Plot of P_{H_2O} versus T during peak of Damara metamorphism (shaded)

temperature reliability is $\pm 10^\circ\text{C}$.

Since antigorite is present, conditions must be to the left of curve (a) in the figure, and as reaction (iv) $\text{AG}+2\text{QZ}=\text{TC}+\text{H}_2\text{O}$ has taken place conditions lie to the right of curve (b). The position of curve (b) is determined by the activity of SiO_2 . Since no estimation of this was possible a line between the two extremes given by Hemley *et al.* (1977) was chosen.

The carbonate-bearing serpentinites all contain antigorite and some magnetite. Several contain talc and actinolite in addition and all have magnesite or dolomite/ankerite.

On the basis of these mineral assemblages conditions should lie on the low-temperature side of the invariant points in Figure 4.3, which is adapted from Trommsdorff and Evans 1977.

- (i) FO+TR+AG+DOL+TC
- (ii) FO+TR+AG+DOL+CC and
- (iii) FO+AG+TC+MS

The isobaric invariant point (i) occurs about 10° above (ii) at 2 kb. Trommsdorff and Evans give a PT diagram for (ii). Curve (c) in Figure 4.2 was drawn 10° higher than (ii) to allow for the temperature difference between (i) and (ii). Conditions during metamorphism lay to the left of curve (c).

As pressure rises the X_{CO_2} field over which the mineral assemblage is stable, as outlined by points (i), (ii) and (iii), narrows. Taking 4,5 kb as the minimum pressure during metamorphism and extrapolating (iii), the maximum X_{CO_2} is approximately 0,15 (Fig. 4.4). On the basis of the mineral assemblages in the ultramafics the PT conditions during peak of metamorphism lay between curves (a), (b) and (c) while X_{CO_2} was less than 0,15.

4.4.2 PRE-DAMARA ROCKS

Immediately adjacent to the serpentinites those country rocks which contain quartz, muscovite and K feldspar have not undergone melting. Hence PT conditions must lie below curve (d). Curve (d) was obtained from Winkler (1974) and is based on Merrill *et al.* (1977).

Hoffer (1978) places conditions in the Rietfontein Inlier (Fig. 1.1) in the vicinity of the serpentinites between the staurolite-biotite isograd as defined by (e) $\text{MUS}+\text{CHL}=\text{QZ}+\text{ST}+\text{BIO}+\text{H}_2\text{O}$ and the kyanite-biotite isograd as defined by $\text{ST}+\text{MUS}+\text{QZ}=\text{KY}+\text{BIO}+\text{H}_2\text{O}$. Curve (e) is taken from Hoschek (1969) in which $X_{\text{H}_2\text{O}}=1$. The position of curve (e) is dependent on mineral composition and as these are not known in the area studied, curve (e) only represents a first approximation.

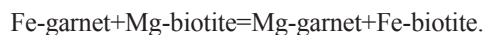
Kyanite related to Damara metamorphism is present at Kyanite Kop along the isograd strike from Gauchab. Therefore PT conditions in the pre-Damara rocks lie above curve (f) (taken from Richardson *et al.* 1969) and to the

right of curve (e).

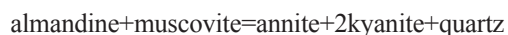
4.4.3 DAMARA ROCKS

Microprobe work was carried out on three samples from the farm Amerongen 181 which contain the assemblage: plagioclase-biotite-garnet-staurolite-kyanite-quartz-muscovite-ilmenite (Table 4.1 - OUI, AM105, AM107).

Temperatures were calculated from analyses of the edges of biotites and garnets which are in contact and using Ferry and Spear's (1977) experimental calibration of the reaction:



Pressure was determined from analyses of minerals in contact using the reaction:



Calibration for this reaction is quoted by Sawyer (1978). The activity model used assumes ideal on-site mixing.

Results of calculated equilibria curves are presented in Table 4.1. Microprobe analyses are contained in Appendix III. The results are shown graphically as curves (g) and (h) respectively on Figure 4.2. The curves intersect at $T^\circ = 575^\circ\text{C}$ and $P=6,3$ kb. The experimental errors are also shown on the figure.

4.4.4 CONCLUSIONS

On the basis of the country-rock reactions and the mineral assemblages in the ultramafics, PT conditions during the Damara metamorphism lay in the area shaded in Figure 4.2.

The X_{CO_2} in the carbonate serpentinites had a maximum value of 0,15 at 4,5 kb and would have decreased slightly with increasing pressure ($0,13X_{\text{CO}_2} \text{ kb}^{-1}$).

5. CHEMISTRY

5.1 DATA

The rock type, mineralogy, locality, country-rock type and shape of the serpentinite body for each sample analysed are listed in Table 5.1. X-ray fluorescence analyses for major, minor and trace elements are presented in Table 5.2. Trace elements and Na were determined on 5 g-whole-rock powder briquettes and major elements were determined the fusion techniques of Norrish and Hutton (1969).

5.2 SYNTHESIS

5.1.1 RELATIONSHIPS BETWEEN THE ULTRAMAFIC ROCK TYPES

The four common rock types and the approximate volume percentages of each are: hobnail serpentinite - 85, talc schist - 10, chlorite schist - 4 and amphibole fels - 1.

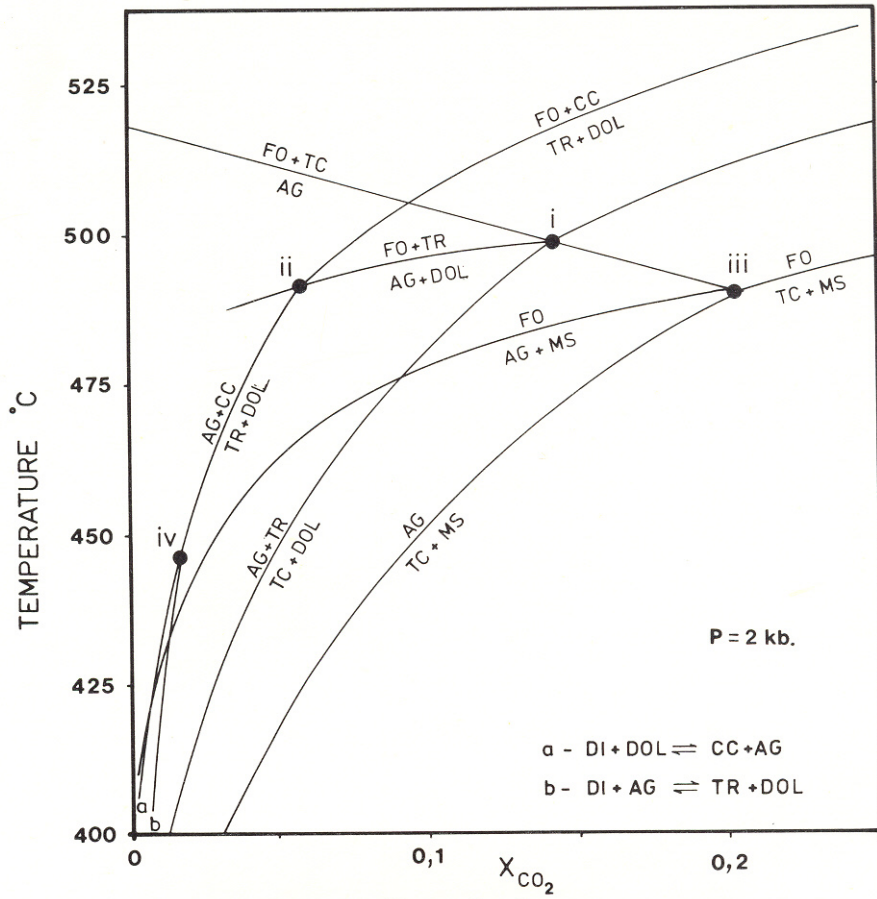


Fig. 4.3 — Isobaric $T-X_{CO_2}$ diagram for the system $CaO-MgO-SiO_2-H_2O-CO_2$

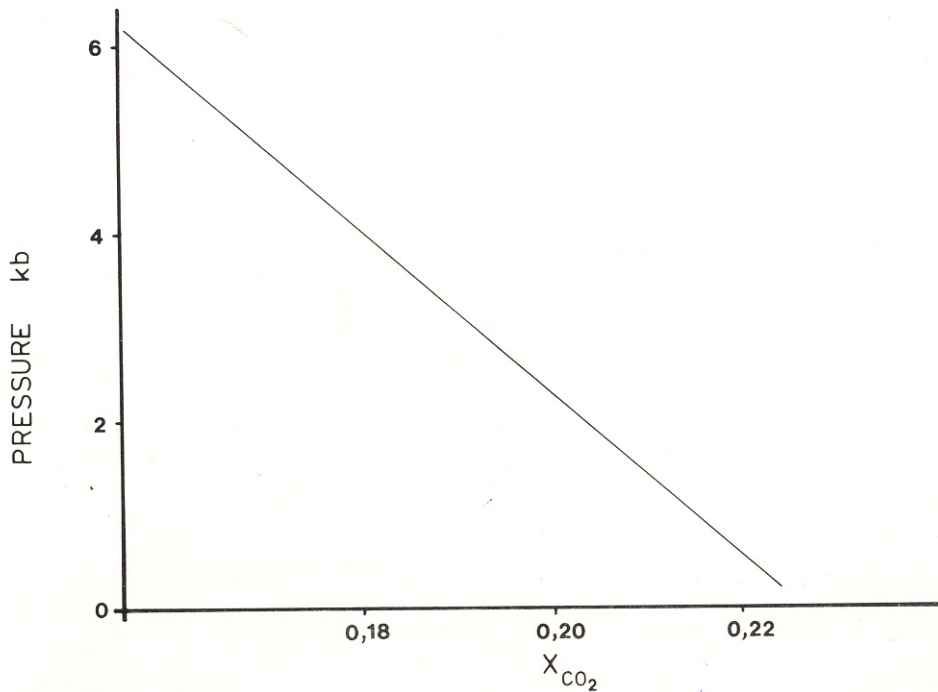


Fig. 4.4 — X_{CO_2} diagram for invariant point iii in Figure 4.3

Table 4.1 - CALCULATED EQUILIBRIA CURVES

Reaction : Fe-garnet + Mg-biotite = Mg-garnet + Fe-biotite							
Rock	garnet	biotite	lnk	4 kb	6 kb	8 kb	
				°C	°C	°C	
AM 105	A	A	-1,8653	536	542	550	
	B	B	-1,8225	548	555	562	
AM 107	A	A	-1,7535	569	576	583	
	B	B	-1,8419	542	549	556	
	C	C	-1,7247	578	585	592	
	D	D	-1,7076	583	591	598	
	E	D	-1,6768	593	601	608	
	F	E	-1,7826	560	567	574	
	G	E	-1,7000	586	593	600	
OU 1	A	A	-1,7455	571	578	586	
	B	B	-1,8402	543	550	557	
	C	C	-1,8353	544	551	558	
	D	D	-1,7510	570	577	584	
	E	E	-1,7856	559	566	573	
Mean AM 105, AM 107 and OU 1			-1,7738	563	570	577	
Reaction : almandine + muscovite = annite + 2 kyanite + quartz							
Rock	garnet	biotite	muscovite	lnk	4 kb	6 kb	8 kb
AM 105	A	A	A	-4,2351	°C 459	°C 553	°C 647

Table 5.1 - LOCATION AND NATURE OF ANALYSED SAMPLES

Number	Rock type	Mineralogy (approx. modes)	Locality	Country-rock type	Shape of body
B 1	Chlorite schist	CHL 90, MA 9, AG 1	Brack 83	Pre-Damara mica schist and gneiss	Lensoid
B 2	Hobnail serpentinite	AG 95, MA 4, CHL 1	Brack 83	Pre-Damara mica schist and gneiss	Lensoid
B 3	Chlorite schist	CHL 90, MA 10	Brack 83	Pre-Damara mica schist and gneiss	Lensoid
B 4	Hobnail serpentinite	AG 90, CHL 9, MA 1	Brack 83	Pre-Damara mica schist and gneiss	Lensoid
B 5	Chlorite schist	CHL 90, MA 7, IO 3	Brack 83	Pre-Damara mica schist and gneiss	Lensoid
B 6	Chlorite schist	CHL 90, MA 7, IO 3	Brack 83	Pre-Damara mica schist and gneiss	Lensoid
B 8	Hobnail serpentinite	AG 90, MA 5, CHL 5	Brack 83	Pre-Damara mica schist and gneiss	Lensoid
E 2a	Talc schist	TC 95, MA 5	Elisenhöhe 88	Pre-Damara mica schist and gneiss	Lensoid
E 2a	Talcose serpentinite	TC 60, AG 30, AK 10	Elisenhöhe 88	Pre-Damara mica schist and gneiss	Lensoid
E 2b	Chlorite schist	CHL 90, MA 10, IO <1	Elisenhöhe 88	Pre-Damara mica schist and gneiss	Lensoid
E 5	Carbonate serpentinite	AG 50, MS 40, MA 10	Elisenhöhe 88	Pre-Damara mica schist and gneiss	Lensoid
G 8/8	Talcose serpentinite	AG 70, TC 20, MA 5, CHL 5	Binsenheim 85	Pre-Damara mica schist and gneiss	Lensoid
GB 24	Hornblendite	HB 70, QZ 5, ZO 25	Binsenheim 85 Gauchab	Pre-Damara mica schist and gneiss	Circular
GB 47	Talc-carbonate serpentinite	AG 70, AK 15, MA 10, TC 5	Binsenheim 85 Gauchab	Pre-Damara mica schist and gneiss	Circular
GB 49	Talcose serpentinite	TC 60, AG 30, MA 10	Binsenheim 85 Gauchab	Pre-Damara mica schist and gneiss	Circular
GB 62	Olivine serpentinite	AG 70, FO 25, MA 5	Binsenheim 85 Gauchab	Pre-Damara mica schist and gneiss	Circular
GB 68	Actinolite fels	AC 90, CHL 5, QZ 5	Binsenheim 85 Gauchab	Pre-Damara mica schist and gneiss	Circular
GB 111	Talc schist	TC 90, CHL 5, MA 5	Binsenheim 85 Gauchab	Pre-Damara mica schist and gneiss	Circular
GB 122	Actinolite fels	AC 90, CHL 10	Binsenheim 85 Gauchab	Pre-Damara mica schist and gneiss	Circular
GB 146	Hobnail serpentinite	AG 90, MA 5, CA 5	Binsenheim 85 Gauchab	Pre-Damara mica schist and gneiss	Circular
GB 189	Amphibole fels	Grunerite 70, MA 15, TC 10, CHL 3, AK 2	Binsenheim 85 Gauchab	Pre-Damara mica schist and gneiss	Circular
GB 193	Hobnail serpentinite	AG 98, MA 2	Binsenheim 85 Gauchab	Pre-Damara mica schist and gneiss	Circular
GB 225	Hobnail serpentinite	AG 90, MA 10	Binsenheim 85 Gauchab	Pre-Damara mica schist and gneiss	Circular
GB 244	Hornblendite	HB 70, ZO 25, SN 5	Binsenheim 85 Gauchab	Pre-Damara mica schist and gneiss	Circular
G 2/1	Talc-carbonate serpentinite	AG 50, TC 30, MA 10, MS 5, CHL 5	Binsenheim 85 Gauchab	Pre-Damara mica schist and gneiss	Circular
OM 1	Hobnail serpentinite	AG 95, MA 5, DOL <1	Omieve 179	Kuiseb Formation biotite schist	Circular
OM 2	Talc schist	TA 95, MA 5	Omieve 179	Kuiseb Formation biotite schist	Circular
OM 3	Chlorite schist	CHL 90, MA 10	Omieve 179	Kuiseb Formation biotite schist	Circular
OM 9	Hobnail serpentinite	AG 80, MA 20	Omieve 179	Kuiseb Formation biotite schist	Circular
OM 11	Chlorite schist	CHL 80, MA 20	Omieve 179	Kuiseb Formation biotite schist	Circular
OM 13	Hobnail serpentinite	AG 95, MA 5	Omieve 179	Kuiseb Formation biotite schist	Circular
OM 37	Hobnail serpentinite	AG 80, MA 15, QZ 5	Omieve 179	Kuiseb Formation biotite schist	Circular
OM 38	Carbonate serpentinite	AG 80, MA 15, MS 5	Omieve 179	Kuiseb Formation biotite schist	Circular
OM 41	Hobnail serpentinite	AG 95, MA 4, MS 1	Omieve 179	Kuiseb Formation biotite schist	Circular
OM 44	Chlorite schist	CHL 90, MA 9, IO 1	Omieve 179	Kuiseb Formation biotite schist	Circular
OM 55	Talc-carbonate serpentinite	AG 50, MS 40, TC 5, MA 5	Omieve 179	Kuiseb Formation biotite schist	Circular
OM 56	Talc schist	TC 90, MA 9, CHL 1	Omieve 179	Kuiseb Formation biotite schist	Circular
OM 67	Chlorite schist	CHL 95, MA 5	Omieve 179	Kuiseb Formation biotite schist	Circular
OM 68	Hobnail serpentinite	AG 95, MA 5	Omieve 179	Kuiseb Formation biotite schist	Circular
OM 73	Hobnail serpentinite	AG 90, MA 5, CHL 5	Omieve 179	Kuiseb Formation biotite schist	Circular
OM 79	Carbonate serpentinite	AG 35, MS 55, MA 10	Omieve 179	Kuiseb Formation biotite schist	Circular
OM 82	Hobnail serpentinite	AG 95, MA 5	Omieve 179	Kuiseb Formation biotite schist	Circular
TL 1	Hobnail serpentinite	AG 95, MA 5	Talana 199	Kuiseb Formation biotite schist	Circular
TL 5	Talc schist	TC 95, MA 4, CHL 1	Talana 199	Kuiseb Formation biotite schist	Circular
OT 1	Chlorite amphibolite	CHL 50, Grunerite 40, MA 10	Otjihaenena 196	Kuiseb Formation biotite schist	Lensoid
OT 6	Carbonate serpentinite	AG 50, MS 45, MA 5	Otjihaenena 196	Kuiseb Formation biotite schist	Lensoid
OT 10	Talcose serpentinite	AG 70, TC 25, MA 5	Otjihaenena 196	Kuiseb Formation biotite schist	Lensoid
OT 11	Talc schist	TC 70, DOL 30	Otjihaenena 196	Kuiseb Formation biotite schist	Lensoid
OT 25	Olivine serpentinite	AG 60, FO 35, MA 5	Otjihaenena 196	Kuiseb Formation biotite schist	Lensoid
SS 1	Talc schist	TC 90, MA 10	Schlesien 493	Kuiseb Formation biotite schist	Lensoid
SS 3	Chlorite schist	CHL 90, MA 9, IO 1	Schlesien 493	Kuiseb Formation biotite schist	Lensoid
SS 10	Hobnail serpentinite	AG 90, MA 9, DOL 1	Schlesien 493	Kuiseb Formation biotite schist	Lensoid
SS 11	Hobnail serpentinite	AG 95, MA 5	Schlesien 493	Kuiseb Formation biotite schist	Lensoid

Table 5.2 - CHEMICAL ANALYSES OF SERPENTINITES, TALC AND CHLORITE SCHISTS AND AMPHIBOLITES

Serpentinites

%	B2	B 4	B 8	E 2A	E 5	GB 47	GB 49	GB 62	GB 146	GB 193
SiO ₂	39,60	41,12	43,32	47,78	31,71	36,56	46,54	36,44	38,92	43,18
TiO ₂	0,04	0,06	0,05	0,01	-	-	0,11	0,03	0,01	0,01
Al ₂ O ₃	2,17	2,37	2,75	1,14	0,10	0,40	2,08	0,32	0,35	0,99
Fe ₂ O ₃	4,63	4,47	3,07	1,16	4,11	1,16	5,82	4,80	9,40	1,27
FeO	4,77	3,62	4,22	0,94	1,06	5,73	4,59	2,26	4,59	2,22
MnO	0,11	0,09	0,13	0,12	0,17	0,15	0,09	0,12	0,09	0,04
MgO	34,09	34,61	33,33	31,66	41,82	36,71	30,16	41,79	33,93	39,42
CaO	0,29	0,01	0,03	3,23	0,08	1,15	0,27	0,07	0,02	0,03
Na ₂ O	0,00	0,01	0,02	0,01	0,02	0,01	0,10	-	-	-
K ₂ O	-	-	-	-	-	0,01	-	0,01	-	-
P ₂ O ₅	-	-	-	0,01	-	-	-	0,08	0,00	0,02
H ₂ O ⁺	12,11	12,34	11,28	7,32	7,12	11,39	8,40	12,39	11,06	12,89
H ₂ O ⁻	0,16	0,15	0,11	4,61	0,08	0,01	0,12	0,60	0,17	0,19
CO ₂	0,58	0,19	0,10	0,04	14,14	5,56	0,39	0,56	0,10	0,10
TOTALS	98,55	99,04	98,41	98,03	100,41	98,84	98,67	99,41	98,64	100,36
ppm										
Zr	-	-	10	-	-	-	-	2	5	2
Nb	-	-	-	-	-	-	-	-	-	-
Y	-	-	-	-	-	-	-	-	2	-
Ba	-	-	-	-	-	5	-	-	5	-
Sr	4	-	-	17	-	11	9	-	6	1
Co	107	122	134	101	130	105	118	100	120	82
Cr	5 640	3 930	5 610	2 440	2 080	2 144	4 240	2 167	5 680	1 670
Ni	1 750	1 245	1 712	2 176	1 420	2 473	2 581	2 206	3 019	1 800
V	84	58	32	19	9	13	17	20	56	16
Zn	76	54	68	141	76	88	89	8	85	44
Cu	32	2	33	44	4	15	12	-	-	-
Sc	13	14	5	5	3	4	3	4	6	4
Ga	4	3	4	2	4	1	1	-	2	1
Ni/Co	16,4	10,2	12,8	21,5	10,9	23,6	21,9	22,1	25,2	22,0
%	GB 225	G 2/1	G 8/8	OM 1	OM 9	OM 13	OM 37	OM 38	OM 41	OM 55
SiO ₂	39,91	40,05	43,51	39,96	40,99	41,45	49,41	39,70	38,09	38,49
TiO ₂	-	0,10	0,05	0,01	-	0,02	0,04	0,01	0,06	0,02
Al ₂ O ₃	0,21	2,31	2,55	0,91	0,91	1,30	0,65	0,81	0,85	0,82
Fe ₂ O ₃	8,34	9,58	3,63	5,41	2,20	5,97	4,78	5,02	5,06	3,37
FeO	1,87	4,09	3,88	1,49	4,91	1,39	2,93	1,41	3,33	3,17
MnO	0,06	0,12	0,13	0,13	0,11	0,08	0,18	0,08	0,08	0,10
MgO	36,48	31,50	33,35	37,52	37,32	37,60	29,85	38,71	36,72	35,60
CaO	0,03	0,02	0,02	0,57	0,03	0,01	0,10	0,02	0,04	0,14
Na ₂ O	-	-	-	-	0,01	-	-	0,01	-	-
K ₂ O	-	-	-	-	-	-	-	-	-	-
P ₂ O ₅	0,03	-	-	-	-	-	0,11	-	-	-
H ₂ O ⁺	11,87	10,56	11,48	12,31	12,47	13,13	10,27	12,26	11,53	7,40
H ₂ O ⁻	0,16	0,30	0,27	0,09	0,07	0,09	0,07	0,09	0,07	0,04
CO ₂	0,25	0,10	0,10	1,03	0,16	0,11	0,12	1,99	3,47	11,45
TOTALS	99,21	98,73	98,97	99,43	99,18	101,15	98,51	100,11	99,30	100,60

Table 5.2 - CONTINUED

Serpentinites

ppm	GB 225	G 2/1	G 8/8	OM 1	OM 9	OM 13	OM 37	OM 38	OM 41	OM 55
Zr	3	2	13	-	-	-	-	-	-	-
Nb	-	-	3	-	-	-	-	-	-	-
Y	2	-	-	-	-	-	-	3	-	-
Ba	-	8	-	6	-	-	37	5	-	-
Sr	2	-	-	-	-	-	4	-	-	-
Co	112	133	126	93	104	83	113	92	118	97
Cr	2 400	5 200	5 550	2 300	3 060	2 570	3 340	2 380	2 880	2 002
Ni	2 500	1 629	1 742	1 800	1 971	2 530	2 850	2 290	2 339	2 106
V	30	85	30	24	27	48	41	23	41	34
Zn	59	67	71	39	49	46	50	18	44	72
Cu	-	-	35	1	7	4	4	-	16	22
Sc	11	8	4	6	7	5	6	6	9	7
Ga	1	3	4	1	2	3	1	1	2	2
Ni/Co	22,3	12,2	13,8	19,4	19,0	30,5	25,2	24,9	19,8	21,7
%	OM 68	OM 73	OM 79	OM 82	OT 6	OT 10	OT 25	SS 10	SS 11	TL 1
SiO ₂	45,84	41,87	36,66	40,24	32,66	46,70	34,60	39,75	40,98	39,16
TiO ₂	0,01	-	0,03	0,06	0,02	0,03	0,05	0,03	0,01	0,05
Al ₂ O ₃	0,70	0,80	0,79	1,56	0,48	0,53	0,10	0,84	0,59	1,09
Fe ₂ O ₃	5,07	1,07	2,67	5,08	2,94	1,47	5,40	5,48	4,31	3,07
FeO	2,52	5,36	3,56	2,44	3,16	7,36	1,94	2,40	1,92	5,44
MnO	0,10	0,09	0,13	0,09	0,08	0,08	0,15	0,07	0,07	0,09
MgO	32,90	38,39	33,45	36,24	33,98	31,98	42,84	37,29	38,32	37,31
CaO	-	0,01	0,10	0,01	1,32	0,05	0,01	0,39	0,09	-
Na ₂ O	0,01	-	0,01	0,01	-	-	0,10	0,01	-	0,01
K ₂ O	-	-	-	-	-	-	0,01	-	-	-
P ₂ O ₅	0,01	0,06	-	-	-	0,02	0,07	-	-	-
H ₂ O ⁺	11,68	11,38	3,56	12,81	4,49	8,76	12,69	12,30	12,74	11,72
H ₂ O ⁻	1,08	1,04	0,03	0,09	0,01	0,04	0,82	0,24	0,25	0,06
CO ₂	0,12	-	17,58	0,11	17,59	0,19	0,88	0,68	0,11	-
TOTALS	100,04	100,07	98,57	98,74	96,73	97,21	99,66	99,48	99,39	98,00
ppm										
Zr	-	-	-	-	-	-	2	-	-	-
Nb	-	-	-	-	-	-	-	-	-	-
Y	-	-	-	-	-	-	-	-	-	-
Ba	11	3	-	-	-	-	-	-	-	3
Sr	-	-	-	-	2	-	-	2	-	-
Co	113	134	102	106	118	98	110	102	86	83
Cr	3 000	1 960	2 500	3 200	8 490	4 160	2 399	3 000	2 500	1 973
Ni	2 471	2 000	2 041	2 383	3 160	2 747	3 339	2 500	2 210	1 929
V	44	19	31	31	10	26	20	21	22	32
Zn	47	43	54	50	43	61	33	34	36	49
Cu	25	20	24	-	35	100	-	12	2	2
Sc	6	6	7	7	5	4	4	4	4	7
Ga	2	1	2	2	1	3	-	1	1	6
Ni/Co	21,9	14,9	20,0	22,5	26,8	28,0	30,5	24,5	25,7	23,2

Table 5.2 - CONTINUED

Talc Schists

%	E 2	GB 111	OM 2	OM 56	OM 57	OT 11	SS 1	TL 5
SiO ₂	54,38	60,29	55,96	57,96	57,10	35,15	55,60	54,18
TiO ₂	0,01	0,01	0,02	0,01	0,03	0,01	0,05	0,03
Al ₂ O ₃	0,88	0,41	0,78	0,07	0,93	0,60	0,56	2,15
Fe ₂ O ₃	5,89	0,83	5,82	5,97	3,64	0,60	7,45	3,43
FeO	1,81	3,13	1,26	2,62	2,38	2,98	0,08	2,74
MnO	0,23	0,06	0,03	0,06	0,02	0,06	0,06	0,03
MgO	27,65	27,61	27,88	26,72	27,86	26,34	26,29	28,10
CaO	0,02	0,01	-	-	-	11,86	0,01	0,01
Na ₂ O	0,02	0,04	-	0,02	0,01	-	0,02	-
K ₂ O	-	-	-	-	-	-	-	-
P ₂ O ₅	-	0,02	-	-	-	-	0,05	0,02
H ₂ O ⁺	5,20	5,70	5,80	5,46	5,80	5,20	7,56	7,80
H ₂ O ⁻	0,29	0,09	0,05	0,06	0,09	0,12	0,05	0,09
CO ₂	0,10	0,09	0,09	0,09	0,03	16,53	-	0,05
TOTALS	96,48	98,29	97,69	99,04	97,89	99,45	97,78	98,63
ppm								
Zr	-	-	-	-	-	-	-	-
Nb	-	-	-	-	-	-	-	-
Y	-	-	-	-	-	-	-	-
Rb	-	-	-	-	-	-	-	-
Ba	32	3	-	-	-	5	-	-
Sr	-	-	-	-	-	-	-	-
Co	136	88	106	70	93	112	66	116
Cr	8 700	2 900	2 600	4 000	2 300	1 697	2 232	1 837
Ni	2 679	1 687	2 015	1 059	1 862	2 094	1 600	1 454
V	48	53	39	105	28	18	29	54
Zn	87	83	43	100	69	26	40	53
Cu	-	-	-	3	-	1	122	21
Sc	-	-	-	-	3	8	12	10
Ga	3	1	2	-	2	1	1	4

Table 5.2 - CONTINUED

Chlorite Schists

%	B 1	B 3	B 5	B 6	E 28	OM 3	OM 11	OM 44	OM 67	SS 3
SiO ₂	25,94	26,66	32,14	31,36	26,11	24,22	17,73	27,21	27,56	30,30
TiO ₂	3,23	0,45	0,11	0,33	1,69	1,99	9,74	0,68	0,10	0,85
Al ₂ O ₃	19,07	19,32	14,04	14,28	18,32	18,89	12,17	14,59	18,21	15,79
Fe ₂ O ₃	3,70	5,31	2,60	3,23	2,42	16,62	20,81	10,61	6,85	2,45
FeO	7,72	5,57	3,06	3,42	12,40	3,50	9,06	4,83	5,92	5,74
MnO	0,27	0,11	0,06	0,08	0,14	0,21	0,54	0,10	0,13	0,07
MgO	26,43	27,71	32,80	32,46	26,12	21,59	17,84	28,75	27,22	29,54
CaO	0,03	0,16	0,52	0,16	0,36	0,39	0,03	0,01	-	0,25
Na ₂ O	0,01	0,00	-	-	-	0,01	-	0,01	0,01	-
K ₂ O	-	0,00	-	-	0,02	0,02	-	-	-	-
P ₂ O ₅	0,01	0,11	0,17	0,11	0,26	0,30	0,02	-	-	0,15
H ₂ O ⁺	12,50	15,10	13,51	13,73	10,72	12,27	10,35	12,47	13,23	13,62
H ₂ O ⁻	0,30	0,10	0,11	0,13	0,11	0,10	0,13	0,10	0,15	0,12
CO ₂	0,10	-	0,10	0,11	-	0,08	0,08	0,08	0,08	0,21
TOTALS	99,31	100,60	99,22	99,40	98,67	100,19	98,50	99,44	99,46	99,09
ppm										
Zr	27	7	3	2	183	-	60	-	-	262
Nb	-	4	8	11	21	-	13	-	-	35
Y	-	-	3	-	6	-	18	-	-	4
Rb	-	-	-	-	-	-	-	-	-	-
Ba	-	-	-	-	-	-	-	-	-	-
Sr	-	-	-	-	2	-	-	-	-	-
Co	112	103	99	101	92	99	120	100	115	66
Cr	160	870	900	900	1 436	854	830	300	1 667	98
Ni	320	300	1 124	700	1 170	530	752	1 000	1 562	352
V	295	72	71	76	135	77	586	435	197	85
Zn	93	79	54	56	291	11	165	73	102	67
Cu	6	5	-	-	-	-	2	-	-	-
Sc	15	29	24	26	30	65	81	55	17	15
U	-	-	-	-	-	-	-	-	-	-
Pb	-	-	-	-	-	-	-	-	-	-
Ga	10	12	11	11	16	14	16	11	14	16
Ni/Co	2,9	2,9	11,4	6,9	12,7	5,4	6,3	10,0	13,6	5,3

Table 5.2 - CONTINUED

Amphibolites

%	GB 24	GB 68	GB 122	GB 189	GB 244	OT 1
SiO ₂	39,77	53,60	53,34	50,25	42,71	19,85
TiO ₂	3,00	0,14	0,11	0,05	1,62	4,95
Al ₂ O ₃	13,13	5,39	4,55	1,96	14,87	13,47
Fe ₂ O ₃	10,83	1,33	1,55	4,77	5,41	14,50
FeO	4,98	6,63	4,15	8,50	6,62	10,00
MnO	0,34	0,18	0,14	0,27	0,32	0,23
MgO	6,00	17,07	18,62	25,76	7,27	19,98
CaO	18,35	11,84	12,79	1,07	17,28	3,05
Na ₂ O	0,29	0,52	0,55	0,05	0,44	0,01
K ₂ O	0,05	0,06	0,06	-	0,11	-
P ₂ O ₅	0,30	-	0,01	0,01	0,17	2,40
H ₂ O ⁺	1,92	2,35	2,80	5,71	1,99	11,37
H ₂ O ⁻	0,11	0,04	0,13	0,14	0,11	0,08
CO ₂	0,08	-	0,12	0,62	0,12	0,13
TOTALS	99,15	99,15	98,92	99,16	99,04	100,02
ppm						
Zr	181	5	6	-	94	1 103
Nb	11	-	-	-	4	70
Y	49	4	-	2	24	76
Rb	-	-	-	-	-	-
Ba	-	4	-	-	11	12
Sr	438	2	4	3	369	61
Co	54	58	72	111	60	73
Cr	72	2 094	2 612	4 120	227	24
Ni	50	247	430	800	200	88
V	408	177	130	113	274	133
Zn	46	72	68	92	71	102
Cu	28	-	18	4	21	-
Sc	49	64	53	36	43	50
Ga	20	5	4	2	16	17

On the basis of field and petrographic relationships (Sections 2 and 3) these four rock types are thought to originate in the following way:

- (i) harzburgite+H₂O=hobnail serpentinite + magnetite
- (iv) hobnail serpentinite+quartz=talc schist+H₂O
- (x) spinel harzburgite+H₂O=chlorite schist
- (vii) Iherzolite+H₂O=CPX-bearing serpentinite= amphibole fels

Reactions (i), (iv) and (ix) are thought to be essentially isochemical, whereas reaction (vii) implies removal of material from the system.

5.2.1.1 Hobnail serpentinite

The basic premise adopted is that if the hobnail serpentinite is derived by reaction (i) then the immobile element concentrations of the serpentinite should reflect that of the parent rock.

Table 5.3a lists maximum and minimum values, found in the literature, for minor and trace elements for various minerals. By taking cognizance of the wide ranges reported and the various rock types involved, the limitations of this approach may be appreciated.

If in reaction (i) forsterite makes up 70 per cent by mass of reactants and enstatite 30 per cent, then the maximum value for an element in olivine is multiplied by 0,7 and the maximum value for an element in enstatite is by 0,3. This gives a maximum value for the anhydrous daughter product, assuming the system to be closed to all constituents except H₂O and CO₂; e.g. the maximum value for TiO₂ in a rock derived from 70 per cent forsterite and 30 per cent enstatite would be:

$$0,7 \times 0,15 + 0,3 \times 0,06 = 0,123 \text{ per cent}$$

Table 5.3b lists the calculated values for hobnail serpentinite derived by reaction (i) and the actual measured values recalculated excluding H₂O and CO₂. The calculated and actual values for most elements are in agreement. The higher limits for Al₂O₃, Zr, Cr, Ni and V in the actual sam-

Table 5.3b - CONCENTRATIONS OF MINOR AND TRACE ELEMENTS IN HOBNAIL SERPENTINITE DERIVED FROM HARZBURGITE BY THE REACTION 15FO₉₀ + 90PX = 12SER + MA

% / ppm	Calculated		Actual (anhydrous)	
	LL	UL	LL	UL
TiO ₂	0,0007	0,123	0	0,12
Al ₂ O ₃	0,3	1,9	0,13	3,16
MnO	0,06	0,19	0,05	0,21
CaO	0,016	0,66	0	0,75
Na ₂ O	0	0,075	0	0,03
K ₂ O	0	0,049	0	0,01
Zr	0	2	0	15
Y	0	4,4	0	4
Rb	0,0003	0,1	0	0
Ba	0,03	11	0	12,6
Sr	0,97	4,3	0	19,8
Co	82	164	94	164
Cr	38,6	1 630	1 850	11 270
Ni	790	3 380	1 442	4 234
V	12,5	51	12	98
Zn	0	177	21	164
Cu	3,9	635	0	113
Sc	2,6	90	3,9	15,2
Ga	0,6	6,5	1,1	7,3

LL = Lower limit
UL = Upper limit

Table 5.3a - CONCENTRATIONS OF MINOR AND TRACE ELEMENTS IN COMMON ROCK-FORMING MINERALS

Element	Forsterite		Orthopyroxene		Mg-spinel		Clinopyroxene		Quartz	
	%/ppm	LL	UL	LL	UL	LL	UL	LL	UL	LL
TiO ₂	0,01	0,15 ⁽³⁾	0,003	0,06 ⁽³⁾	0,03	27 ⁽⁷⁾	0,13	0,8 ⁽³⁾	0,0001	0,00015 ⁽⁴⁾
Al ₂ O ₃	0	0,25 ⁽³⁾	1 ⁽³⁾	6 ⁽¹⁸⁾	19	50 ⁽³⁾	0,68	7 ⁽¹²⁾	0,0001	0,0008 ⁽⁴⁾
MnO	0,09	0,19 ⁽³⁾	0 ⁽⁹⁾	0,18 ⁽¹⁶⁾	0,07	1,8 ⁽³⁾	0,06	0,16 ⁽³⁾	0	0,00005 ⁽⁴⁾
CaO	0	0,20 ⁽³⁾	0,03	1,75 ⁽¹³⁾	0 ⁽¹⁰⁾	0,6 ⁽³⁾	18	24 ⁽¹⁴⁾		
Na ₂ O	0	0,06 ⁽³⁾	0	0,11 ⁽³⁾	0 ⁽¹⁰⁾	0,04 ⁽²⁰⁾	0,52 ⁽¹⁵⁾	1,5 ⁽³⁾	0	0,0011 ⁽⁴⁾
K ₂ O	0	0,04 ⁽³⁾	0	0,07 ⁽³⁾		< 0,001 ⁽²⁰⁾	0,02	0,10 ⁽³⁾	0	0,0002 ⁽⁴⁾
Zr		<2 ⁽³⁾		<2 ⁽³⁾	2	100 ⁽³⁾	10 ⁽¹⁷⁾	1 000 ⁽³⁾		
Y		<2 ⁽³⁾	<2	10 ⁽³⁾		2 ⁽³⁾	1	40 ⁽¹⁾		
Rb		0,1 ⁽²⁾	0,01	0,1 ⁽²⁾		2 ⁽³⁾		2 ⁽³⁾		
Ba	0	10 ⁽¹⁾	0,10	13 ⁽²⁾		2 ⁽³⁾	1	27 ⁽³⁾	7	550 ⁽¹⁾
Sr		4 ⁽²⁾	0,30	5 ⁽²⁾		2 ⁽³⁾	0	100 ⁽³⁾		
Co	100 ⁽⁵⁾	200 ⁽³⁾	40	80 ⁽³⁾	80	200 ⁽³⁾	18	150		
Cr	26 ⁽⁵⁾	400 ⁽³⁾	68 ⁽⁸⁾	4 500 ⁽³⁾	500	59,400 ⁽⁷⁾	1 000 ⁽¹²⁾	15 000 ⁽¹³⁾		
Ni	1 000 ⁽¹¹⁾	4 400 ⁽³⁾	300	1 100 ⁽³⁾	200	2 500	250	400 ⁽³⁾		
V	5 ⁽¹⁾	30 ⁽³⁾	30	100 ⁽³⁾	320	2 000 ⁽²⁾	80	450 ⁽³⁾		
Zn	0	82 ⁽¹⁾	0	400	1 000	1 500 ⁽¹⁾	100	450 ⁽¹⁾	4	11 ⁽¹⁾
Cu	3	900 ⁽³⁾	6	16 ⁽¹⁾	20	500 ⁽¹⁹⁾	7	24 ⁽⁵⁾		2 ⁽¹⁾
Sc		<2 ⁽³⁾	4	300 ⁽¹⁾	6	90 ⁽¹⁹⁾	12	79 ⁽¹⁷⁾		
Ga	0	5 ⁽¹⁾	2	10 ⁽¹⁾	10	100 ⁽³⁾	10	100 ⁽¹⁾	0	6 ⁽¹⁾

Values obtained from:

1. Wedepohl (1970).
2. Asish and Murthy (1977).
3. Ross et al. (1954).
4. Deer et al. (1974).
5. Loney et al. (1971).
6. Fesq et al. (1976).
7. Gogineni et al. (1978).
8. Bloomer and Nixon (1973).
9. Arculus and Smith (1977).
10. Arculus et al. (1977).
11. Gurney et al. (1977).
12. Hatton and Gurney (1977).
13. Lawless et al. (1977).
14. Lewis and Meyer (1977).

Element	Ca amphibole		Biotite		K feldspar		Plagioclase		Garnet		
	%/ppm	LL	UL	LL	UL	LL	UL	LL	UL	LL	UL
TiO ₂	0,10		2,11 ⁽⁴⁾	0,82	4,27 ⁽⁴⁾	0	0,08 ⁽⁶⁾	0	0,0001 ⁽⁴⁾	0,03	55 ⁽⁴⁾
Al ₂ O ₃	3,8		14,6 ⁽⁴⁾	13,1	20,38 ⁽⁴⁾	16	21 ⁽⁴⁾	19	36 ⁽⁴⁾	9	22 ⁽⁴⁾
MnO	0,04		0,95 ⁽⁴⁾	0,01	1,4 ⁽⁴⁾					0,02	1,57 ⁽⁴⁾
CaO	9,7		12,8 ⁽⁴⁾	0	1,64 ⁽⁴⁾	0,05	2,7 ⁽⁴⁾	0	19 ⁽⁴⁾	1,8	37,4 ⁽⁴⁾
Na ₂ O	0,97		2,4 ⁽⁴⁾	0,16	0,96 ⁽⁴⁾	0,49	8,44 ⁽⁴⁾	0,22	11 ⁽⁴⁾	0,01	1,2 ⁽⁴⁾
K ₂ O	0,09		1,9 ⁽⁴⁾	6,5	9,8 ⁽⁴⁾	3,2	16,07 ⁽⁴⁾	0,05	1 ⁽⁴⁾	0	0,01 ⁽⁴⁾
Zr											
Y			73 ⁽¹⁾		226 ⁽¹⁾	4,7	16 ⁽¹⁾	1,1	8,5 ⁽¹⁾	20	27 ⁽¹⁾
Rb	1		780 ⁽¹⁾	200	2 000 ⁽¹⁾	100	1 500 ⁽¹⁾	1	30 ⁽¹⁾		
Ba	2		5 400 ⁽¹⁾	42	8 500 ⁽¹⁾	983	15 000 ⁽¹⁾	10	9 000 ⁽¹⁾	0	150 ⁽¹⁾
Sr								400	2 000 ⁽²⁾		
Co										30	50 ⁽⁶⁾
Cr			1 700 ⁽¹⁹⁾		780 ⁽¹⁴⁾					1 000	3 000 ⁽⁶⁾
Ni			1 100 ⁽¹⁹⁾	0	450 ⁽¹⁹⁾					0	700 ⁽⁶⁾
V	90		300 ⁽¹⁾	50	1 000 ⁽¹⁾	5	10 ⁽¹⁾	5	15 ⁽¹⁾		5 ⁽¹⁾
Zn	34		680 ⁽¹⁾	34	1 700 ⁽¹⁾	2	8 ⁽¹⁾	7	50 ⁽¹⁾	73	5 275 ⁽¹⁾
Cu	1		300 ⁽¹⁾	1	480 ⁽¹⁾	1	20 ⁽¹⁾	10	840 ⁽¹⁾	8	65 ⁽¹⁾
Sc	31,8		95 ⁽¹⁾	31,8	222 ⁽¹⁾					70	1 272 ⁽⁶⁾
Ga	1,5		50 ⁽¹⁾	10	150 ⁽¹⁾	2	88 ⁽¹⁾	10	110 ⁽¹⁾	1	19 ⁽¹⁾

Values obtained from:

15. Merrill et al. (1977).
16. Rawlinson and Dawson (1977).
17. Shimizu and Allegre (1977).
18. Tracy and Robinson (1977).
19. Wass (1977).
20. Levey and Hermes (1977).

LL = Lower limit i.e. the lowest concentration for an element in the mineral. Estimate based on values given in reference.

UL = Upper limit i.e. the highest concentration for an element in the mineral.

Values of minor elements given in per cent.
Values of trace elements given in ppm.

ples is attributed to the presence of spinel in the parent rock (Section 5.2.1.3). Likewise the slightly higher upper limit values for CaO and Sr are ascribed to the presence of carbonates in a few samples. If the serpentinite had been derived from an olivine cumulate, apart from the elements mentioned above, the Ti, Zn, Sc and Ga values would have been lower. If clinopyroxene or a Ca amphibole had been present in the parent rock then the Al₂O₃, CaO, Na₂O, Zr, Y, Ba, Sr, V, Sc and Ga contents of the daughter product would be higher.

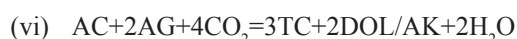
5.2.1.2 Talc schist

If reaction (iv) operated the SiO₂ content would be an index of how far the reaction has proceeded. Therefore plots of the various elements versus SiO₂ were drawn. If only SiO₂ were added to the serpentine the concentration of other elements should be diluted. Plots using anhydrous values of MnO, Co, Ni and Sc versus SiO₂ show a negative correlation between SiO₂ and these elements (Figs 5.1 and 5.2). Regression lines were calculated using the slope formula = σ_y/σ_x and intercept = $y - bx$ for the reduced major axis line (Till 1974).

There is no apparent correlation of Zn, Cu and Ga with SiO₂ but this may be due to great variation in concentration of these elements in the antigorite, which could be a result of the lack of a suitable lattice site for Zn, Cu and Ga in antigorite. No conclusions can be drawn on the basis of these elements.

Since only SiO₂ is presumed to be added by reaction (iv) there should be no correlation between inter-element ratios and SiO₂; this is shown by plots of the ratios of oxides and elements versus silica, given in Figure 5.3.

The concentrations of the incompatible elements Zr, Nb, Y, Rb, Ba and Sr in both the serpentinite and talc schist are below or near the detection limit. A talc-producing reaction involving Ca amphibole, for example:



would be expected to introduce incompatible elements such as Zr, Y, Rb, and Ba.

Using the procedure outlined in Section 5.2.1.1, the trace-element concentrations of a talc schist derived from hobnail serpentinite by reaction (iv) were calculated (Table 5.3c). These were compared with actual values for the talc schist and are found to be in close agreement.

5.2.1.3 Chlorite schist

As outlined in Section 4, the chlorite schist is believed to be derived from a spinel harzburgite. The presence of spinel should result in higher concentrations of TiO₂, FeO, Al₂O₃, MnO, V, Sc, Ga, Zr, Nb and Y in the spinel harzburgite than in the harzburgite. Hence the hydrated product of

spinel harzburgite (chlorite schist) should contain higher concentrations of these elements than the hydrated product of harzburgite (serpentinite). The increase in Zr, Nb and Y values may be observed by reference to Table 5.2. The increase in TiO₂, FeO, Al₂O₃, MnO, V, Sc and Ga values is indicated on histograms in Figure 5.4 on which anhydrous values are plotted.

Similarly the MgO, SiO₂, Cr and Ni contents in the harzburgite would be greater than that in spinel harzburgite and hence greater in the serpentinite than in the chlorite schist (Fig. 5.5).

The presence of spinel would not effect Rb, Ba and Sr concentrations. These are similar in both the serpentinite and chlorite schist, i.e. below or near detection limit. If more than trace amounts of mica or feldspar had been involved in this reaction the Rb, Ba and Sr contents should be greater in the chlorite schists than in the serpentinite.

Making use of the reaction (x) and the method outlined in Section 5.2.1.1, the trace-element concentrations for a chlorite schist derived by this reaction were calculated (Table 5.3d) and the values are in reasonable agreement except for TiO₂, Zr and Y. The values for Zr and Y are appreciably higher in some chlorite schists than expected and this may possibly be due to the presence of clinopyroxene in the parent rock of some samples.

5.2.1.4 Actinolite fels and amphibolites

The actinolite fels samples GB68, GB122 and GB189 have extremely low values for Zr, Nb, Y, Sr, Cu and Ga and extremely high values for Co, Cr and Ni when compared with normal amphibolites or the hornblende 'dykes' GB24 and GB244. This suggests that the source rock was ultramafic. The low Rb and Sr values indicate that feldspars and micas were not involved in the formation of this rock type. The high CaO, V and Na₂O content of the samples is not consistent with orthopyroxene reacting with antigorite to produce amphibole fels.

Clinopyroxene has a trace-element concentration consistent with it being involved in reaction (vii) to produce actinolite fels.



Using the methods outlined in Section 5.2.1.1 the range of trace-element concentrations were calculated for an actinolite fels produced by reaction (vii) from a lherzolite (Table 5.3e). Reasonable agreement was achieved between the actual and calculated values, except for Zr and Ga. This is ascribed to violation of the basic assumption behind the calculation, i.e. reaction (vii) does not take place in a closed system.

On the assumption that GB24 and GB244 are ortho-am-

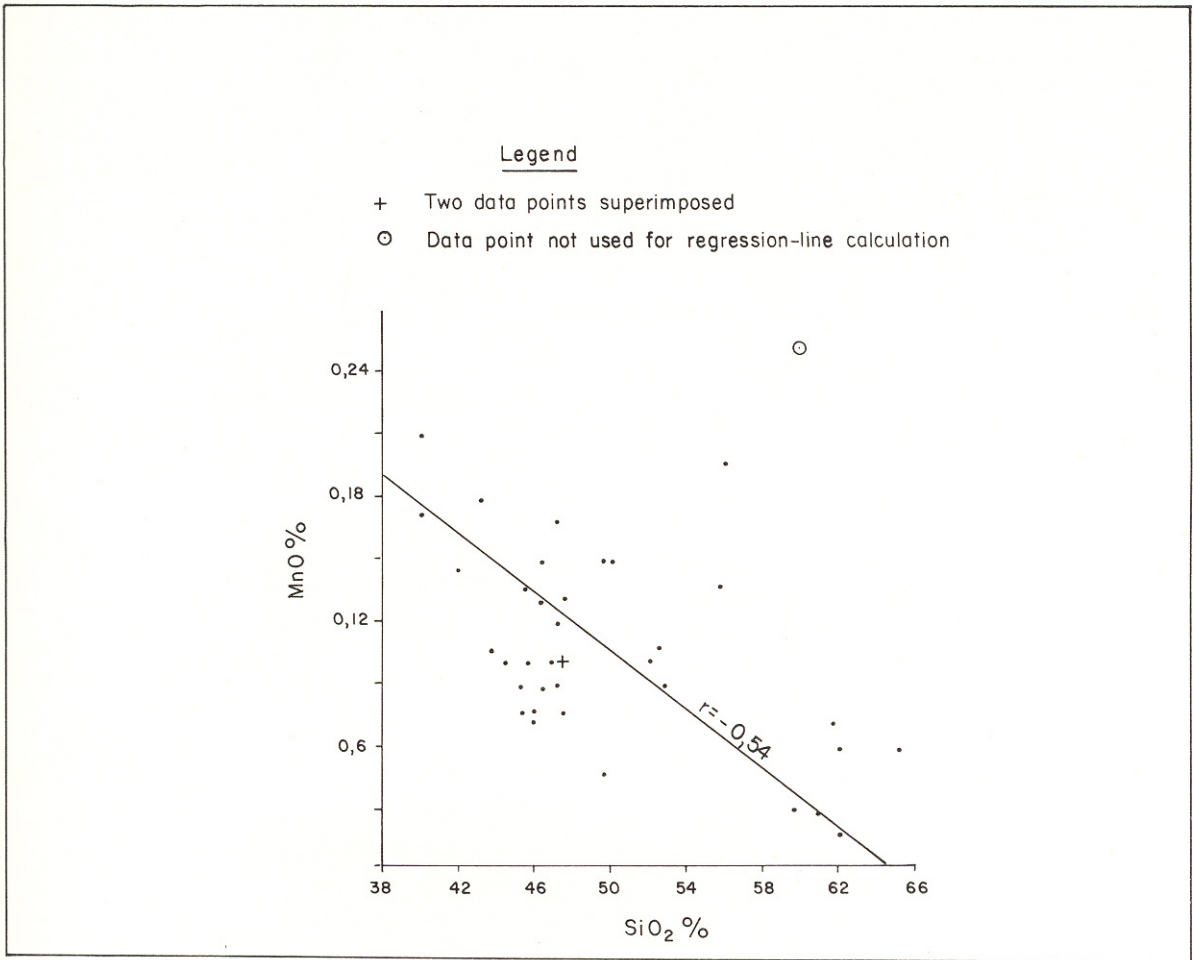


Fig. 5.1 — Plot of MnO versus SiO₂ for serpentinites and talc schists

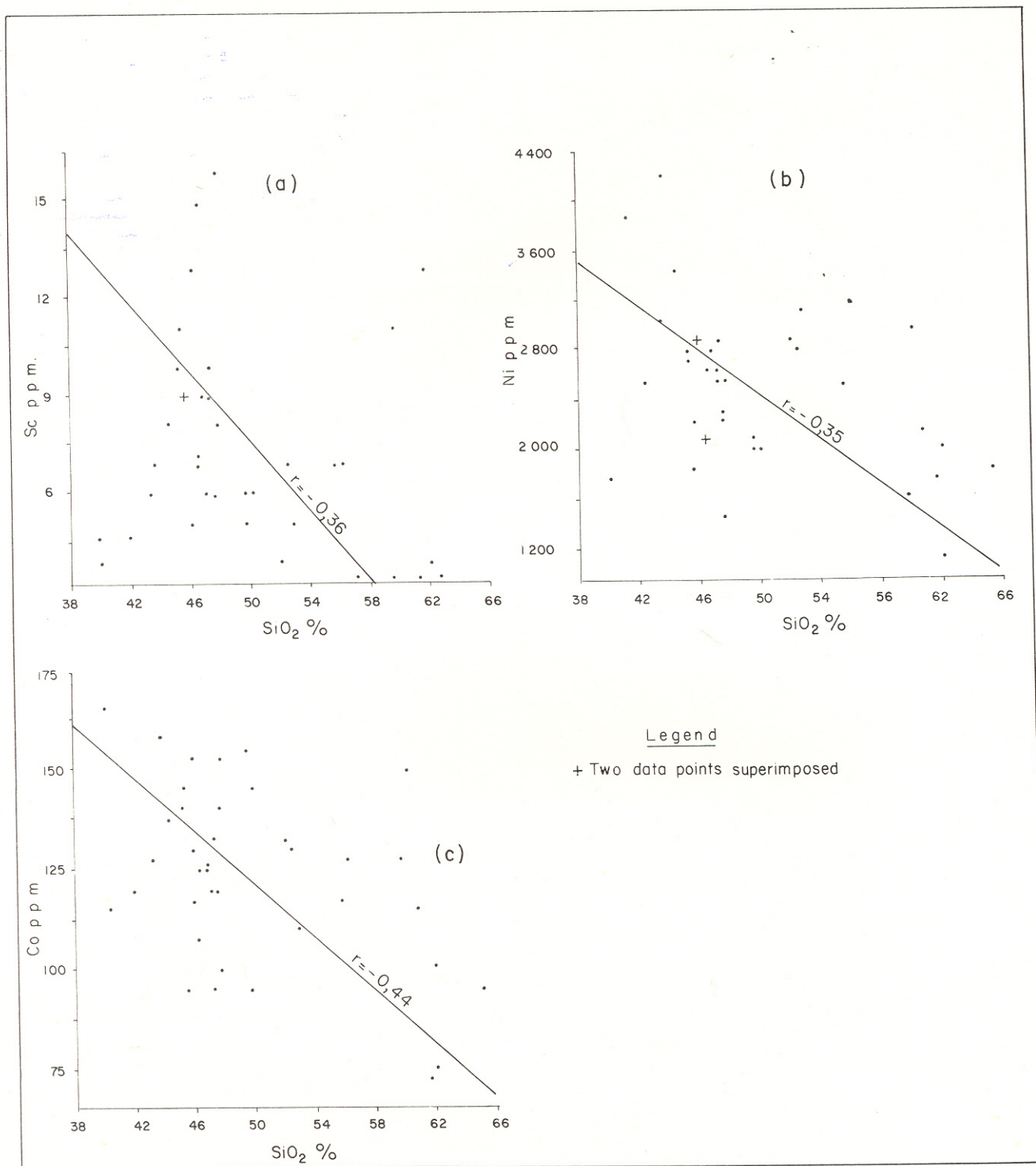


Fig. 5.2 — Plots of trace elements versus SiO₂ for serpentinites and talc schists

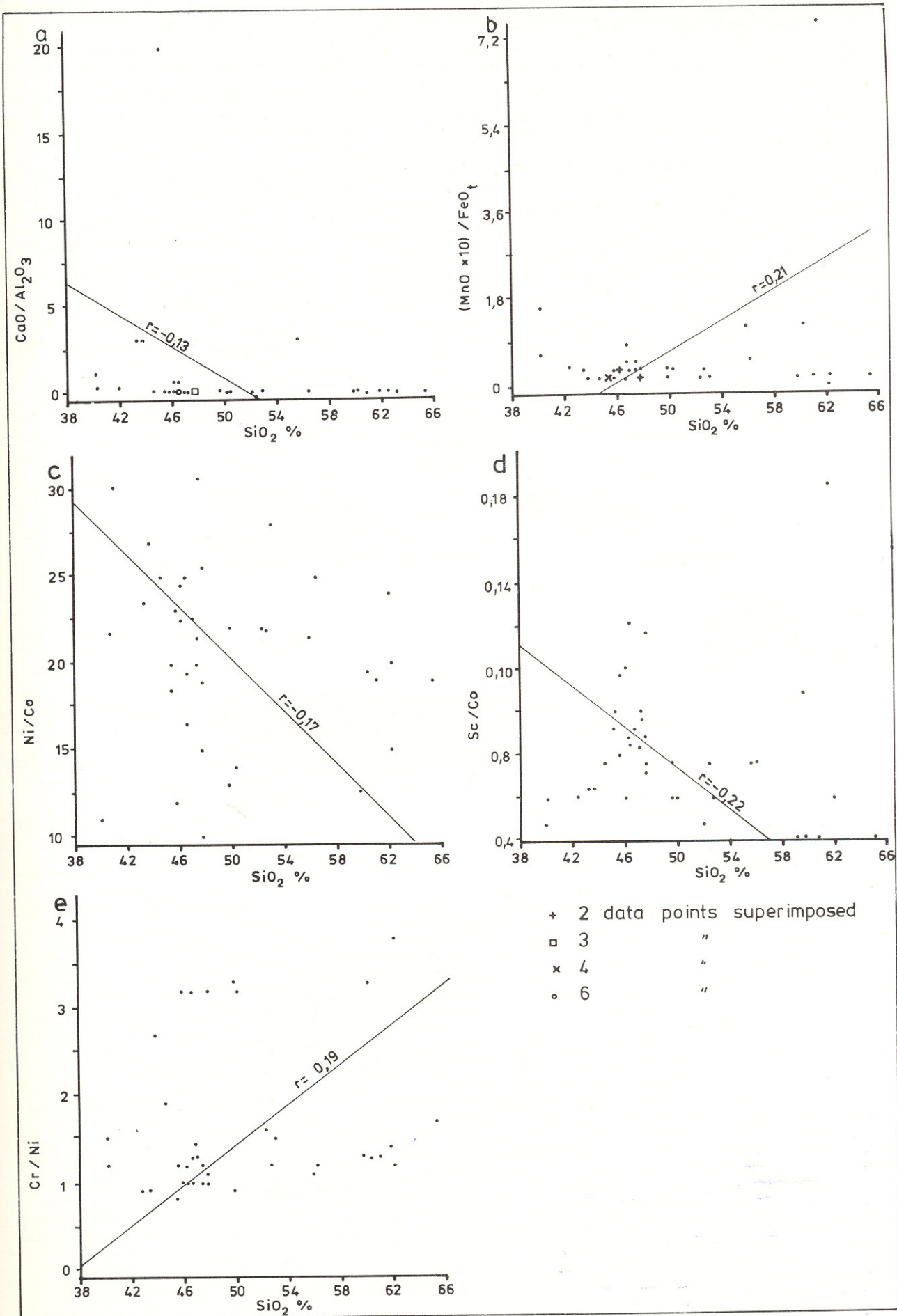


Fig. 5.3 — Plots of inter-element ratios versus SiO₂ for serpentinites and talc schists

Table 5.3c - CONCENTRATIONS OF MINOR AND TRACE ELEMENTS IN TALC SCHIST DERIVED BY THE REACTION
 $AG + 2QZ = TC + H_2O$

% / ppm	Calculated		Actual (anhydrous)	
	LL	UL	LL	UL
TiO ₂	0,0000	0,08	0,01	0,06
Al ₂ O ₃	0,168	2,21	0,07	2,37
MnO	0,035	0,14	0,02	0,25
CaO	0	2,62	0	0,02
Na ₂ O	0	0,014	0	0,04
K ₂ O	0	0,007	0	0,06
Zr	0	10,5	0	0
Y	0	2,8	0	0
Rb	0	0	0	0
Ba	2,1	174	0	35,2
Sr		13	0	0
Co	66	114	73	150
Cr	1 295	7 788	2 026	9 572
Ni	980	2 485	1 133	2 948
V	11,2	68,6	5,7	52
Zn	45,5	130	33	96
Cu	3	79	0	135
Sc	2,8	10,5	0	13
Ga	3	38	0	22

LL = Lower limit
 UL = Upper limit

Table 5.3d - CONCENTRATIONS OF MINOR AND TRACE ELEMENTS IN CHLORITE SCHIST DERIVED FROM SPINEL
 HARZBURGITE BY THE REACTION $4EN + 2FO + 2SN + 8H_2O = Mg-CHL$

% / ppm	Calculated		Actual (anhydrous)	
	LL	UL	LL	UL
TiO ₂	0,013	8,5	0,13	11,08
MnO	0,048	0,669	0,07	0,61
CaO	0,015	0,91	0	0,61
Na ₂ O	0	0,07	0	0,01
K ₂ O	0	0,04	0	0,02
Zr	0	30	0	262
Y	0	4	0	20,5
Rb	0	0,07		2
Ba	0,04	8,8		2
Sr	0,1	3,5		2,3
Co	73	152	76	136
Cr	185	2 373	114	1 953
Ni	470	2 350	351	1 835
V	109	649	83	666
Zn	30	634	12	331
Cu	0	426	0	8
Sc	3,4	147	17	132
Ga	3,7	32	11	19

LL = Lower limit
 UL = Upper limit

Table 5.3e - CONCENTRATION OF MINOR AND TRACE ELEMENTS IN ACTINOLITE FELS DERIVED BY THE REACTION $AG + 3DI + H^+_{aq} = AC + Ca^{2+} + (Fe^{2+}, Mg^{2+}) + 3(OH)^-$

% / ppm	Calculated		Actual	
	LL	UL	LL	UL
TiO ₂	0,09	0,60	0,05	0,14
Al ₂ O ₃	0,52	5,92	2,11	5,57
MnO	0,06	0,13	0,15	0,29
Na ₂ O	0,40	1,18	0,05	0,57
K ₂ O	0,03	0,08	0	0,06
Zr	7,8	784	0	6,5
Y	0,78	30	0	4,3
Rb	0	1,56	0	
Ba	0,78	23	0	5
Sr	0	77	2,8	4,2
Co	39	154	59	120
Cr	1 238	13 955	2 164	4 445
Ni	583	2 345	255	863
V	61	351	122	183
Zn	78	370	70	99
Cu	5	49	0	18
Sc	10	61	30	66
Ga	7,5	74	2,8	5,9

LL = Lower limit
UL = Upper limit

phibolites, Ti, Zr and Y values were plotted on the diagrams used by Pearce and Cann (1973) (see Figs 5.6 and 5.7). The samples fall within the oceanic-basalt field.

Sample OT1 has a trace-element chemistry similar to the amphibolites rather than to the actinolite fels. It resembles country-rock amphibolite which has undergone Mg-metasomatism to produce a chlorite amphibolite by the reaction:



The trace-element chemistry appears to be consistent with this view but as only one analysis of this rock type was carried out the suggestion is purely tentative.

5.2.2 RELATIONSHIPS BETWEEN THE FOUR TYPES OF ULTRAMAFIC OCCURRENCES

The four types of field occurrences are circular and lensoid bodies in both pre-Damara and Damara country rocks. As simple bivariate plots proved unsuccessful in separating them (Figs 5.8 to 5.11) statistical tests were

tried, namely t-tests, principal-component analysis, cluster analysis and multiple-discriminant analysis (Davies 1973).

The t-tests, using computer programme BMDP3D (Dixon 1975), were carried out on the anhydrous analyses, where all iron was treated as FeO, to discriminate between samples from serpentinites within pre-Damara country rock and those from Damara terrain. At the 99-per cent confidence level there is no significant difference between the two groups in the concentrations of 15 of the 16 elements investigated. The exception is zinc (Table 5.4).

In order to justify using chemical analyses to discriminate between serpentinites of different origins, multivariate tests were carried out on analyses of samples, quoted in the literature, where the nature of the rock from which the serpentinite was derived is thought to be known. These tests proved effective in separating serpentinites derived from rocks formed in different environments (Section 5.2.3) and were consequently used on the South West African samples. The effectiveness of the multivariate tests justifies the underlying assumption, in the following dis-

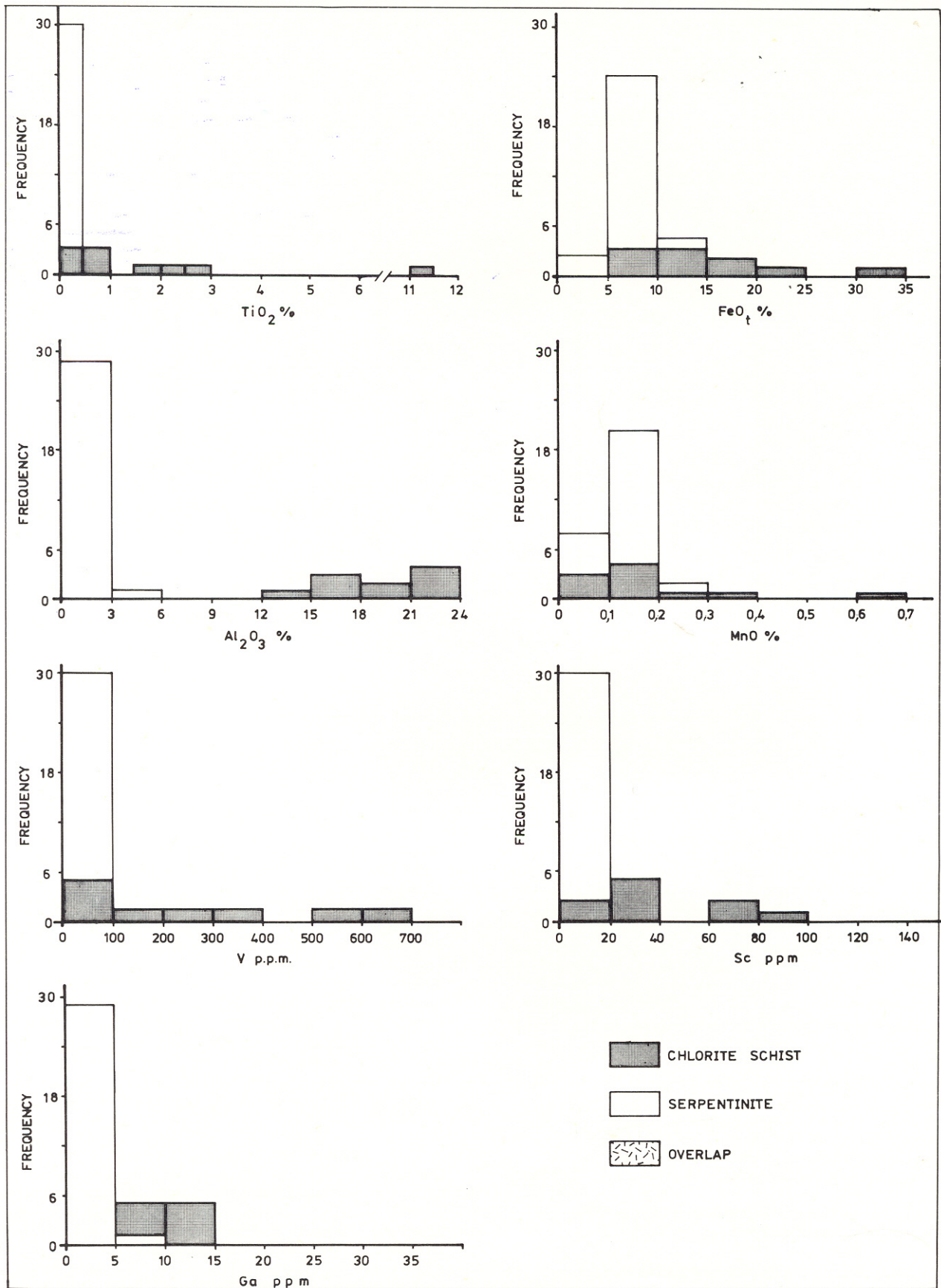


Fig. 5.4 — Histograms indicating that the chlorite schists contain more TiO₂, FeO_t, Al₂O₃, MnO, V, Sc and Ga than the serpentinites

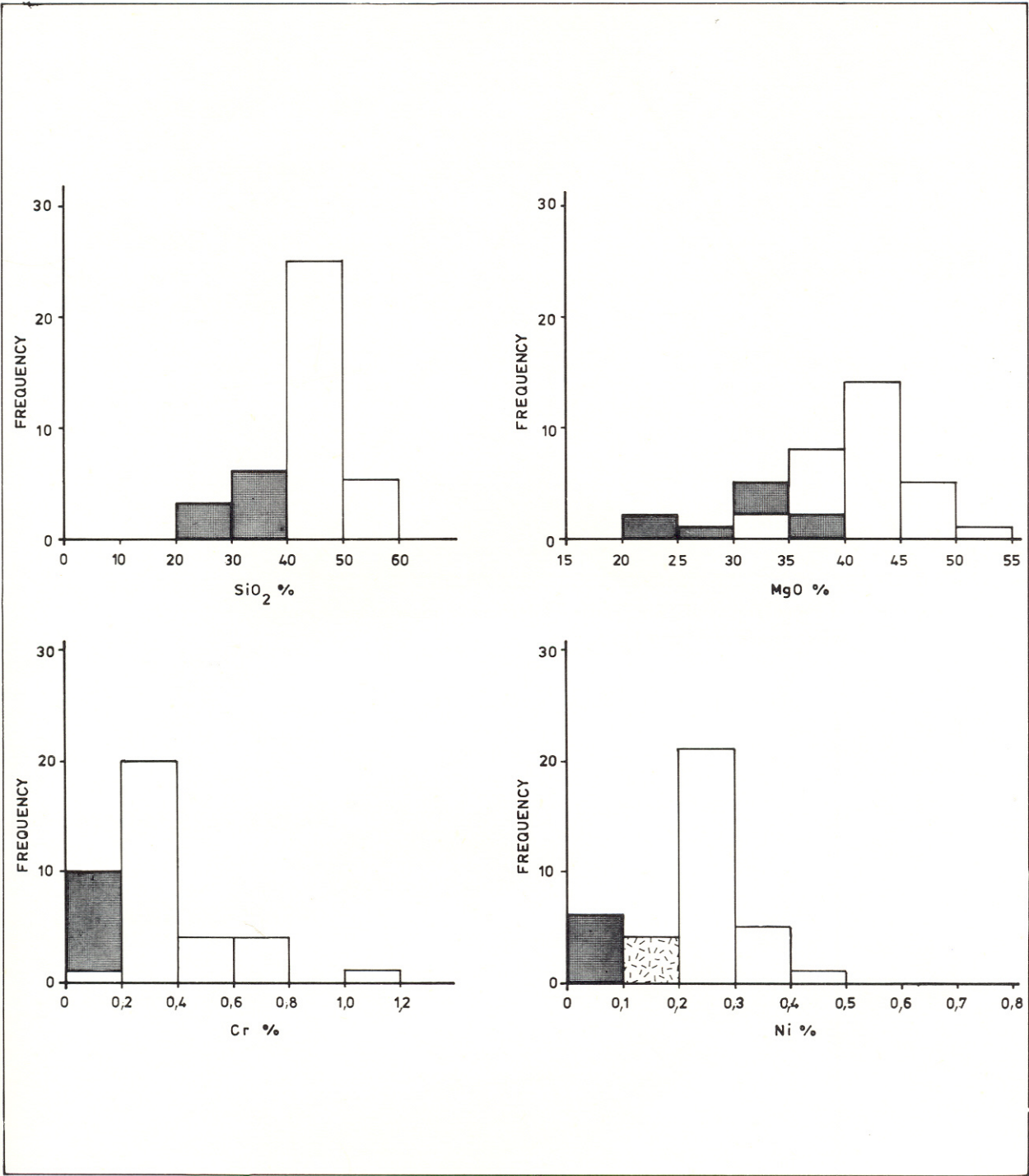


Fig. 5.5 — Histograms indicating that the serpentinites contain more SiO₂, MgO, Cr and Ni than chlorite schists. Legend as for Figure 5.4

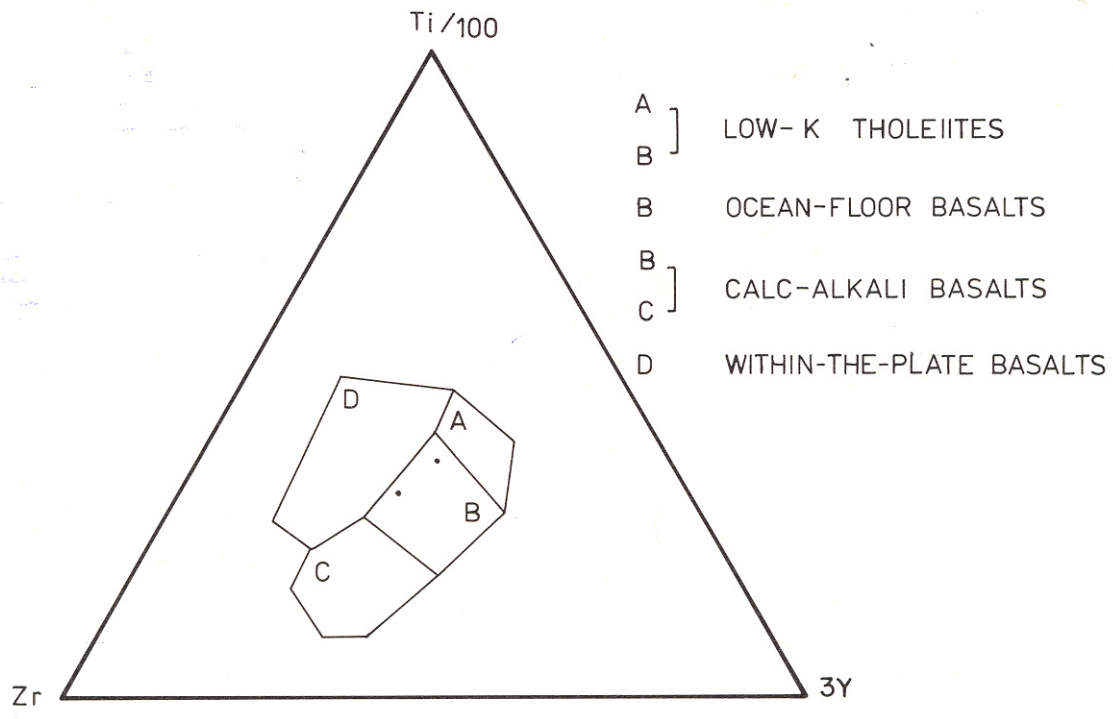


Fig. 5.6 — Triangular plot of Ti, Zr and Y to determine origin of amphibolites, after Pearce and Cann 1973

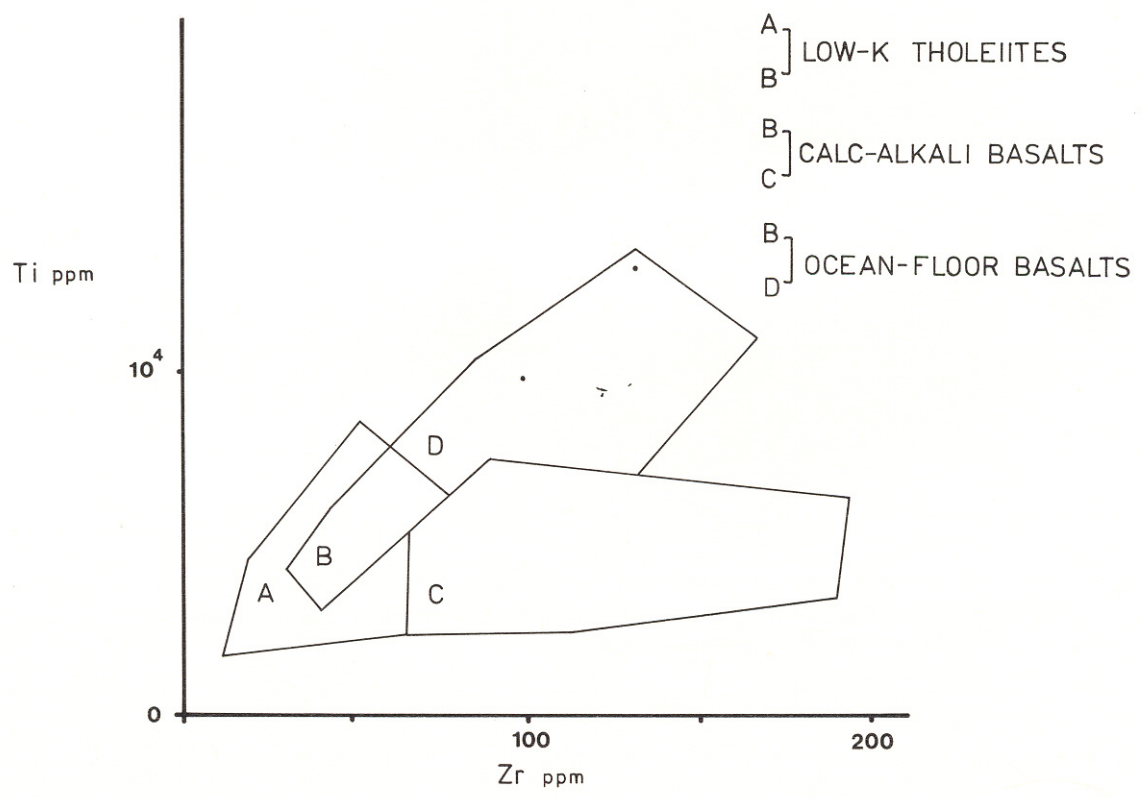


Fig. 5.7 — Plot of Ti against Zr to determine origin of amphibolite, after Pearce and Cann 1973

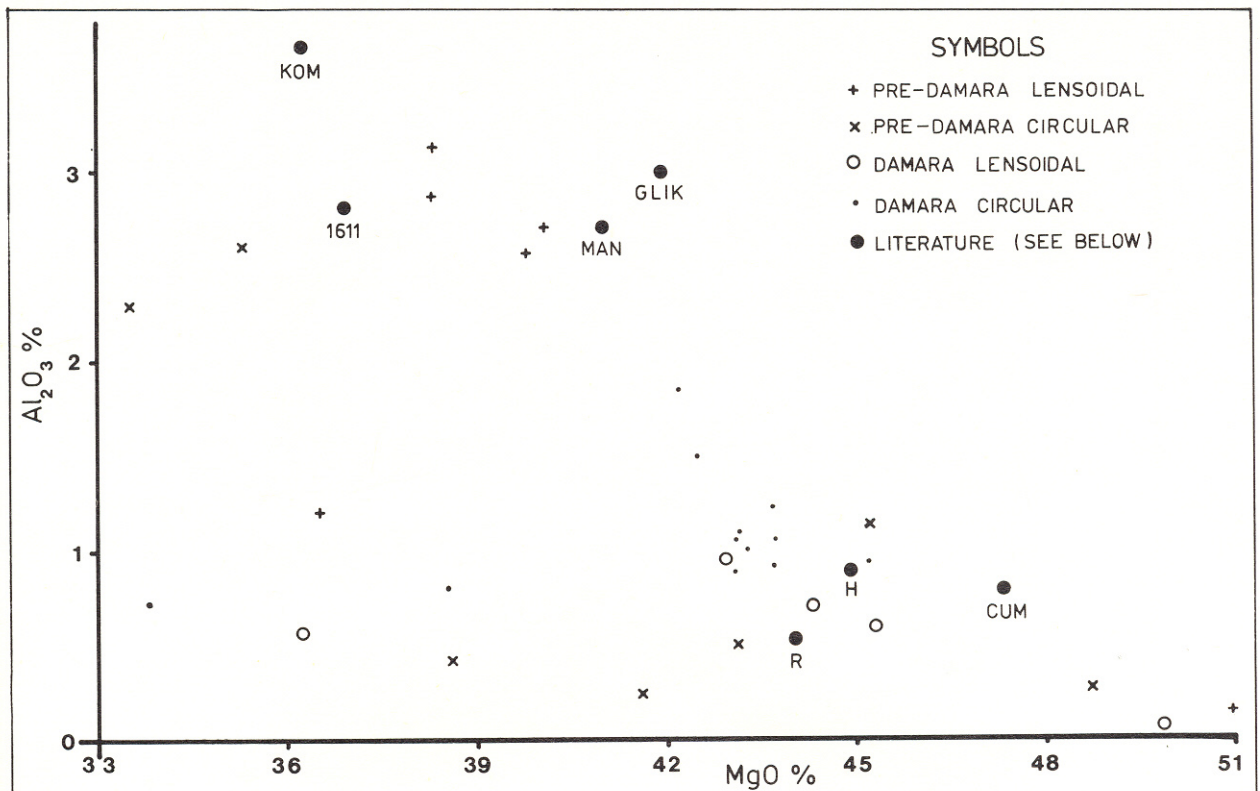


Fig. 5.8 — Plot of Al_2O_3 versus MgO for SWA serpentinites.

GLIK, 1611, MAN: Estimates of fertile mantle (O'Hara et al., Nixon 1975 and this study)

R, H: Estimates of depleted mantle (O'Hara et al. 1975, this study)

KOM: Estimates of primary melt (O'Hara et al. 1975)

CUM: Estimates of mantle cumulates (this study)

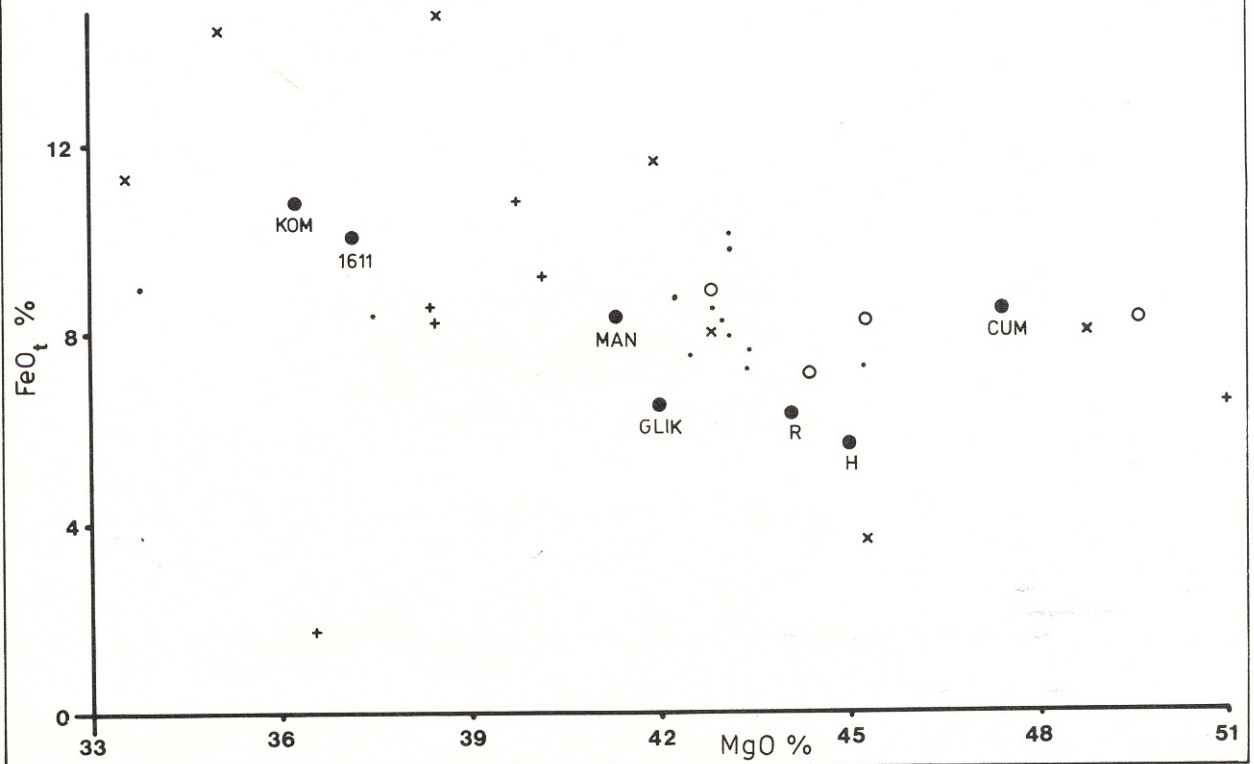


Fig. 5.9 — Plot of FeO_t versus MgO for SWA serpentinites.
Legend as for Figure 5.8

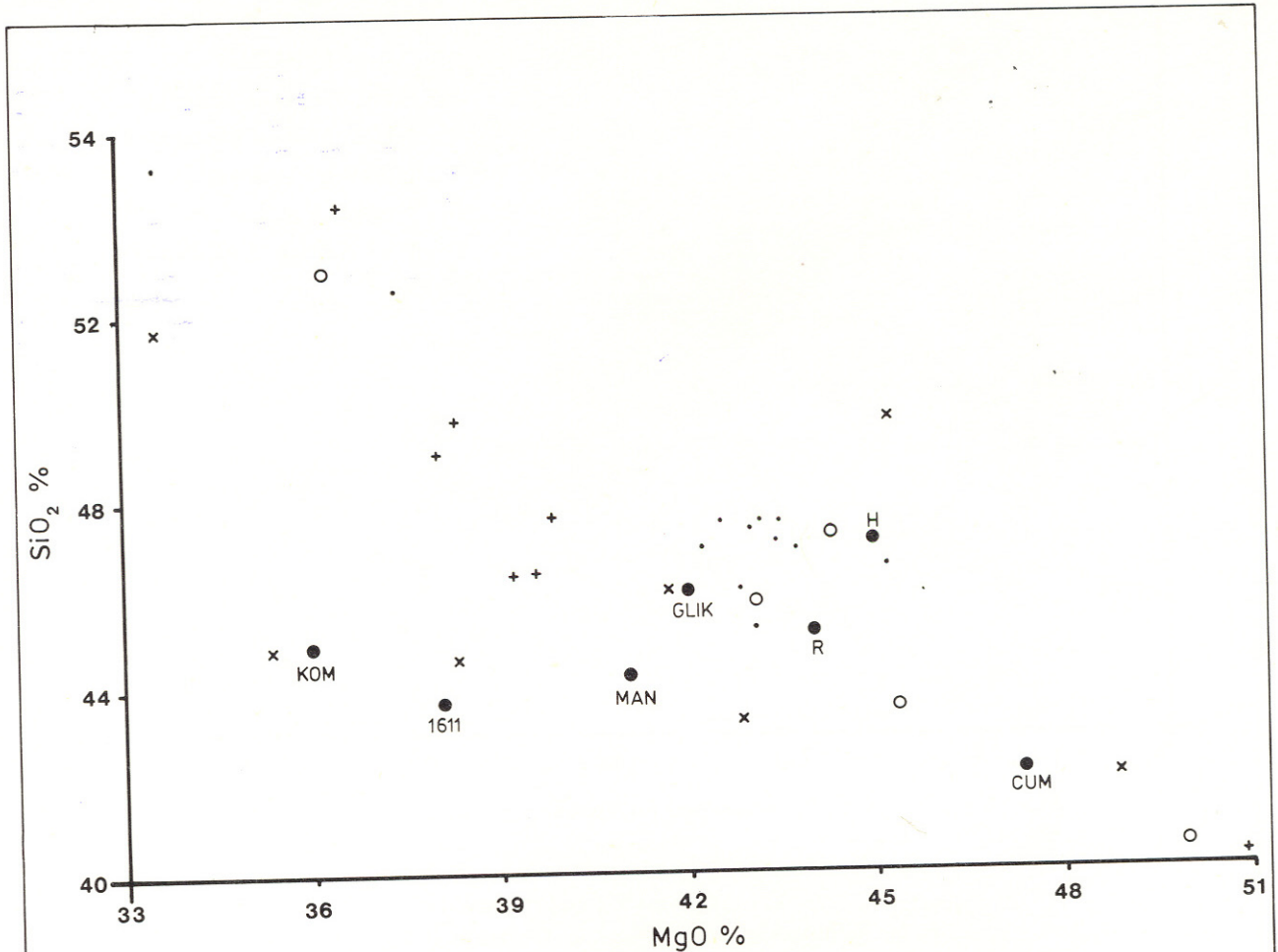


Fig 5.10 – Plot of SiO₂ versus MgO for SWA serpentinites.
Legend as for Figure 5.8

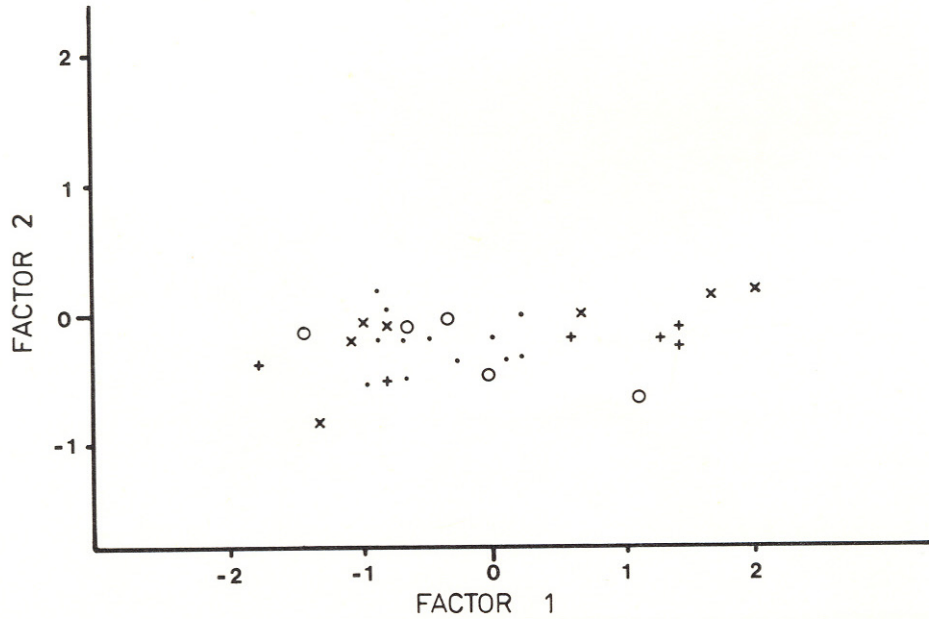


Fig. 5.11 – Plot of Factor 1 versus Factor 2 for SWA serpentinites.
Legend as for Figure 5.8

EXPLANATION OF SYMBOLS USED IN TABLE 5.4:

$$1. \quad T \text{ pooled} = t \text{ value} = \frac{(\bar{x}_1 - \bar{x}_2) - (\mu_1 - \mu_2)}{\sqrt{S^2_p (1/n_1 + 1/n_2)}}$$

\bar{x}_1 = mean of sample of size n_1 from a population with mean μ_1

\bar{x}_2 = mean of sample of size n_2 from a population with mean μ_2

$$S^2_p = \frac{(n_1 - 1)S_1^2 + (n_2 - 1)S_2^2}{n_1 + n_2 - 2}$$

where S_1^2 is the variance of the first group and S_2^2 is the variance of the second sample.

$$2. \quad T \text{ (separated)} = t \text{ value} = t_s = \frac{\bar{x}_1 - \bar{x}_2}{\sqrt{S_1^2/n_1 + S_2^2/n_2}}$$

$$3. \quad F \text{ (for variances)} = S_1^2/S_2^2$$

4. p values = the significance level where $(1-p) \times 100$ = the degrees of certainty (as per cent) with which it can be said that the two are from different populations

5. D.F. = degrees of freedom

6. PREDAM = serpentinite from bodies with pre-Damara country rock

7. DAMAR = serpentinites from bodies with Damara country rock

Table 5.4 - RESULTS OF BMDP3D t-TEST. THE TWO GROUPS USED ARE SERPENTINITES FROM PRE-DAMARA TERRAIN AND FROM DAMARA TERRAIN

For differences on single variables:

VARIABLE NUMBER	1 SiO ₂	GROUP	1 PREDAM	2 DAMAR	1 PREDAM (N = 11)	2 DAMAR (N = 17)
STATISTICS	P VALUE D. F.	MEAN	48,1482	47,0947		X
		STD DEV.	3,6101	5,0610		X
		S.E.M.	1,0885	1,2275		XX
T (SEPARATE)	,64 ,526 25,7	NUMBER	11	17		XXX
T (POOLED)	,60 ,555 26	MAXIMUM	55,5200	56,1200	H H	XXX X
F (FOR VARIANCES)	1,97 ,280 16, 10	MINIMUM	43,0400	31,1800	HHHHHHHH H	XXX X X
					MIN-----MAX MIN-----MAX	
					AN H = 1,0 CASES	AN X = 1,0 CASES
VARIABLE NUMBER	2 TiO ₂	GROUP	1 PREDAM	2 DAMAR	1 PREDAM (N = 9)	2 DAMAR (N = 15)
STATISTICS	P VALUE D. F.	MEAN	,0556	,0313		X
		STD DEV.	,0413	,0220		X
		S.E.M.	,0138	,0057		X X
T (SEPARATE)	1,63 ,132 10,8	NUMBER	9	15	H	X X
T (POOLED)	1,89 ,072 22	MAXIMUM	,1200	,0700	H H	XX X X
F (FOR VARIANCES)	3,52 ,038 8, 14	MINIMUM	,0100	,0100	H H H H H H H H	XX X X X XX
					MIN-----MAX MIN-----MAX	
					AN H = 1,0 CASES	AN X = 1,0 CASES
VARIABLE NUMBER	3 Al ₂ O ₃	GROUP	1 PREDAM	2 DAMAR	1 PREDAM (N = 11)	2 DAMAR (N = 17)
STATISTICS	P VALUE D. F.	MEAN	1,8073	1,1535		X
		STD DEV.	1,1104	,8541		XX
		S.E.M.	,3348	,2072		XXX
T (SEPARATE)	1,66 ,115 17,5	NUMBER	11	17	H H H H H H H H H H	XXXX
T (POOLED)	1,76 ,090 26	MAXIMUM	3,1600	4,2300		XXXX XX
F (FOR VARIANCES)	1,69 ,337 10, 16	MINIMUM	,2400	,4600		X
					MIN-----MAX MIN-----MAX	
					AN H = 1,0 CASES	AN X = 1,0 CASES
VARIABLE NUMBER	4 FeO	GROUP	1 PREDAM	2 DAMAR	1 PREDAM (N = 11)	2 DAMAR (N = 17)
STATISTICS	P VALUE D. F.	MEAN	5,4727	4,2153		X
		STD DEV.	3,6248	2,1108		X
		S.E.M.	1,0929	,5119		XX
T (SEPARATE)	1,04 ,315 14,4	NUMBER	11	17	H H H H H H H H H H	XX
T (POOLED)	1,16 ,255 26	MAXIMUM	10,9100	6,8000		X XXX
F (FOR VARIANCES)	2,95 ,053 10, 16	MINIMUM	1,3500	,7700		XX XXXX XXXX
					MIN-----MAX MIN-----MAX	
					AN H = 1,0 CASES	AN X = 1,0 CASES
VARIABLE NUMBER	5 FeO _t	GROUP	1 PREDAM	2 DAMAR	1 PREDAM (N = 11)	2 DAMAR (N = 17)
STATISTICS	P VALUE D. F.	MEAN	9,1646	7,4002		X
		STD DEV.	3,8485	1,2251		X
		S.E.M.	1,1604	,2971		XX
T (SEPARATE)	1,47 ,168 11,3	NUMBER	11	17	H H H H H H H H H H	XX
T (POOLED)	1,77 ,088 26	MAXIMUM	14,9514	9,8527		X XXX
F (FOR VARIANCES)	9,87 ,000 10, 16	MINIMUM	2,3048	4,5329		XX XXXX XXXX
					MIN-----MAX MIN-----MAX	
					AN H = 1,0 CASES	AN X = 1,0 CASES
VARIABLE NUMBER	6 MnO	GROUP	1 PREDAM	2 DAMAR	1 PREDAM (N = 11)	2 DAMAR (N = 17)
STATISTICS	P VALUE D. F.	MEAN	,1191	,1106		X X
		STD DEV.	,0386	,0347		XXX
		S.E.M.	,0116	,0084		XXX X
T (SEPARATE)	,59 ,561 19,8	NUMBER	11	17	H H H H H H H H H H	XXX X X X X X
T (POOLED)	,61 ,550 26	MAXIMUM	,1800	,2000		XXX X X X X X
F (FOR VARIANCES)	1,23 ,682 10, 16	MINIMUM	,0500	,0800		
					MIN-----MAX MIN-----MAX	
					AN H = 1,0 CASES	AN X = 1,0 CASES
VARIABLE NUMBER	7 MgO	GROUP	1 PREDAM	2 DAMAR	1 PREDAM (N = 11)	2 DAMAR (N = 17)
STATISTICS	P VALUE D. F.	MEAN	39,2718	42,6906		X
		STD DEV.	3,3249	6,0243		X
		S.E.M.	1,0025	1,4611		X
T (SEPARATE)	-1,93 ,065 25,6	NUMBER	11	17	H	XX
T (POOLED)	-1,71 ,099 26	MAXIMUM	45,2200	61,1800	HH H	XXX
F (FOR VARIANCES)	3,28 ,062 16, 10	MINIMUM	33,6400	33,9000	HHHHH H H	XXX XXX
					MIN-----MAX MIN-----MAX	
					AN H = 1,0 CASES	AN X = 1,2 CASES

Table 5.4 - (CONTINUED)

For differences on single variables:									
VARIABLE NUMBER 8 CaO			GROUP	1 PREDAM	2 DAMAR	1 PREDAM (N = 11)		2 DAMAR (N = 15)	
STATISTICS P VALUE D. F.			MEAN	,5364	1,2240	H		X	
			STD DEV.	1,1383	3,9034	H		X	
			S.E.M.	,3432	1,0079	H		X	
T (SEPARATE)	-,65	,527 17,1	NUMBER	11	15	H		X	
T (POOLED)	-,56	,578 24	MAXIMUM	3,7500	15,2800	H		X	
F (FOR VARIANCES)	11,76	,000 14, 10	MINIMUM	,0100	,0100	HH H		XX	X
						MIN-----MAX	MIN-----MAX	MIN-----MAX	MIN-----MAX
						AN H = 1,5 CASES		AN X = 2,2 CASES	
VARIABLE NUMBER 9 Na ₂ O			GROUP	1 PREDAM	2 DAMAR	1 PREDAM (N = 4)		2 DAMAR (N = 7)	
STATISTICS P VALUE D. F.			MEAN	,9700	,0100			X	
			STD DEV.	1,7764	,0000			X	
			S.E.M.	,8882	,0000			X	
T (SEPARATE)	1,08	,359 3,0	NUMBER	4	7			X	
T (POOLED)	1,49	,170 9	MAXIMUM	3,6300	,0100	H		X	
F (FOR VARIANCES)	,00	1,000 3, 6	MINIMUM	,0100	,0100	HH		H	X
						MIN-----MAX	MIN-----MAX	MIN-----MAX	MIN-----MAX
						AN H = 1,0 CASES		AN X = 1,2 CASES	
VARIABLE NUMBER 11 Co			GROUP	1 PREDAM	2 DAMAR	1 PREDAM (N = 11)		2 DAMAR (N = 17)	
STATISTICS P VALUE D. F.			MEAN	132,0909	120,3529				
			STD DEV.	17,0614	17,0732				
			S.E.M.	5,1442	4,1408				
T (SEPARATE)	1,78	,090 21,5	NUMBER	11	17				
T (POOLED)	1,78	,087 26	MAXIMUM	154,0000	153,0000			X X X X X	
F (FOR VARIANCES)	1,00	,967 16, 10	MINIMUM	94,0000	95,0000	H	H H H H H H	XX XXXXXX XX X X	
						MIN-----MAX	MIN-----MAX	MIN-----MAX	MIN-----MAX
						AN H = 1,0 CASES		AN X = 1,0 CASES	
VARIABLE NUMBER 12 Cr			GROUP	1 PREDAM	2 DAMAR	1 PREDAM (N = 11)		2 DAMAR (N = 17)	
STATISTICS P VALUE D. F.			MEAN	3982,5454	2879,5295				
			STD DEV.	1884,1346	1414,9714				
			S.E.M.	568,0880	343,1810				
T (SEPARATE)	1,66	,115 17,10	NUMBER	11	17				
T (POOLED)	1,77	,089 26	MAXIMUM	6505,0000	8106,0000				
F (FOR VARIANCES)	1,77	,296 10, 16	MINIMUM	643,0000	1872,0000	H	H H H H H H H	XX XXX X	X
						MIN-----MAX	MIN-----MAX	MIN-----MAX	MIN-----MAX
						AN H = 1,0 CASES		AN X = 1,2 CASES	
VARIABLE NUMBER 13 Ni			GROUP	1 PREDAM	2 DAMAR	1 PREDAM (N = 11)		2 DAMAR (N = 17)	
STATISTICS P VALUE D. F.			MEAN	2372,4545	2637,7646				
			STD DEV.	626,5334	317,2516				
			S.E.M.	188,9069	76,9448				
T (SEPARATE)	-1,30	,215 13,4	NUMBER	11	17				X
T (POOLED)	-1,49	,149 26	MAXIMUM	3458,0000	3208,0000	H	HH H H H H	X XXX	
F (FOR VARIANCES)	3,90	,015 10, 16	MINIMUM	1442,0000	2144,0000	H	HHH H H H H	XXXXXXXXXXXXXX	
						MIN-----MAX	MIN-----MAX	MIN-----MAX	MIN-----MAX
						AN H = 1,0 CASES		AN X = 1,0 CASES	
VARIABLE NUMBER 14 V			GROUP	1 PREDAM	2 DAMAR	1 PREDAM (N = 11)		2 DAMAR (N = 17)	
STATISTICS P VALUE D. F.			MEAN	46,0909	33,9412				
			STD DEV.	30,6674	12,2294				
			S.E.M.	9,2466	2,9661				
T (SEPARATE)	1,25	,235 12,1	NUMBER	11	17				XX
T (POOLED)	1,47	,152 26	MAXIMUM	98,0000	55,0000	HH H H H H		XXX X X	
F (FOR VARIANCES)	6,29	,001 10, 16	MINIMUM	16,0000	10,0000	HH HH H H		X XXXXXXXXX	
						MIN-----MAX	MIN-----MAX	MIN-----MAX	MIN-----MAX
						AN H = 1,0 CASES		AN X = 1,0 CASES	
VARIABLE NUMBER 15 Zn			GROUP	1 PREDAM	2 DAMAR	1 PREDAM (N = 11)		2 DAMAR (N = 17)	
STATISTICS P VALUE D. F.			MEAN	88,3636	52,3529				
			STD DEV.	30,1671	15,7874				
			S.E.M.	9,0957	3,8290				
T (SEPARATE)	3,65	,003 13,6	NUMBER	11	17				X
T (POOLED)	4,15	,000 26	MAXIMUM	164,0000	91,0000				X XX
F (FOR VARIANCES)	3,65	,021 10, 16	MINIMUM	50,0000	21,0000				XXXXX
						MIN-----MAX	MIN-----MAX	MIN-----MAX	MIN-----MAX
						AN H = 1,0 CASES		AN X = 1,0 CASES	
VARIABLE NUMBER 16 Cu			GROUP	1 PREDAM	2 DAMAR	1 PREDAM (N = 7)		2 DAMAR (N = 16)	
STATISTICS P VALUE D. F.			MEAN	28,5714	23,3750				
			STD DEV.	17,3288	29,0491				
			S.E.M.	6,5497	7,2623				
T (SEPARATE)	,53	,601 18,6	NUMBER	7	16				X X
T (POOLED)	,44	,667 21	MAXIMUM	51,0000	113,0000				X X X
F (FOR VARIANCES)	2,81	,209 15, 6	MINIMUM	3,0000	1,0000	H HH H H H		XXXXXX	X X
						MIN-----MAX	MIN-----MAX	MIN-----MAX	MIN-----MAX
						AN H = 1,0 CASES		AN X = 1,0 CASES	
VARIABLE NUMBER 17 Sc			GROUP	1 PREDAM	2 DAMAR	1 PREDAM (N = 11)		2 DAMAR (N = 17)	
STATISTICS P VALUE D. F.			MEAN	8,7273	7,7059				
			STD DEV.	4,3380	2,0544				
			S.E.M.	1,3080	,4983				
T (SEPARATE)	,73	,479 12,9	NUMBER	11	17				X
T (POOLED)	,84	,408 26	MAXIMUM	17,0000	12,0000				X X X X
F (FOR VARIANCES)	4,46	,008 10, 16	MINIMUM	4,0000	5,0000	HH HH HH	H H H	X XX XX X X	
						MIN-----MAX	MIN-----MAX	MIN-----MAX	MIN-----MAX
						AN H = 1,0 CASES		AN X = 1,0 CASES	

cession, that serpentinisation has not radically altered the chemistry of the rocks. Hence the present composition of the rock is thought to reflect that of the parent rock if allowances is made for the introduction of H₂O by recalculating the composition on an anhydrous basis.

A principal-component analysis considers the position of the samples in n-dimensional space (the number of dimensions depends on the number of variables used). In this case all iron was treated as FeO and the analyses were recalculated excluding H₂O and CO₂, so that 18 variables were used. The vectors along which maximum scatter of samples is achieved are computed and then the vectors or principal components along which most scatter is obtained are plotted against one another (Davies 1973). The computer programme BMDP4M (Dixon 1975) was used to work out the principal components for the South West African serpentinites.

Once the principal components have been calculated, the position of a sample along the factor/principal component j may be calculated from the formula:

$$x_j = \frac{\sum_{i=1}^n \gamma_{ji} (y_i - \bar{y}_i)}{s_i}$$

- x_j is the value of the sample along factor j
- γ_{ji} is the factor score coefficient for the element i, on factor j
- \bar{y}_i is the mean concentration for element i
- y_i is the concentration for element i in sample DC
- s_i is the standard deviation for element i

The factor scores as computed by BMDP4M are listed in Table 5.5. Figures 5.11, 5.12 and 5.13 show factor 2 versus factor 1, factor 3 versus factor 1 and factor 3 versus factor

Table 5.5 - FACTOR-SCORE COEFFICIENTS FOR SWA SERPENTINITES

		Factor 1	Factor 2	Factor 3	Factor 4	Factor 5	Factor 6	Factor 7
SiO ₂	1	,12648	-,06808	,15729	,30455	-,16216	-,13641	-,10561
TiO ₂	2	,21557	,03938	-,09778	,02013	,02846	-,06902	-,04826
Al ₂ O ₃	3	,19331	,03275	,01237	-,03823	-,09557	-,05204	-,29615
FeO _t	5	,18487	,06058	-,17121	-,08965	,07256	,09063	,37030
MnO	6	-,02738	,05059	,02879	,13161	,44293	-,09385	-,14752
MgO	7	-,25499	-,05686	-,10866	-,20661	,12259	,02670	-,08771
CaO	8	-,12548	-,01961	,46516	,00581	-,01762	,21158	,02301
Na ₂ O	9	,07193	,47061	-,03179	,00810	-,07750	-,03651	-,02896
K ₂ O	10	,06670	,47095	-,02714	,01214	-,08506	-,02096	-,02092
P ₂ O ₅	11	-,01144	-,03912	-,08957	,48622	,22157	-,01643	-,01446
Co	21	-,03754	-,12986	-,00288	,00846	,53937	,03880	,13718
Cr	22	,24917	,05225	-,04294	-,04387	,01623	-,07353	,01672
Ni	23	-,00079	-,02516	,04340	-,00086	,02334	-,02689	,56764
V	24	,11079	-,01542	,05923	-,00541	-,03833	,34106	,05167
Zn	25	,00005	,02163	,38348	-,06117	,12163	,13123	,01145
Cu	26	,09055	-,13776	,18634	-,23475	-,03020	-,26196	,25430
Sc	27	-,07641	-,05132	,19308	,04306	-,04982	,61746	-,02331
Ga	30	,07819	-,10391	,02560	-,34965	,14169	-,20516	-,06150

These coefficients are for the standardised variables, mean zero and standard deviation one.

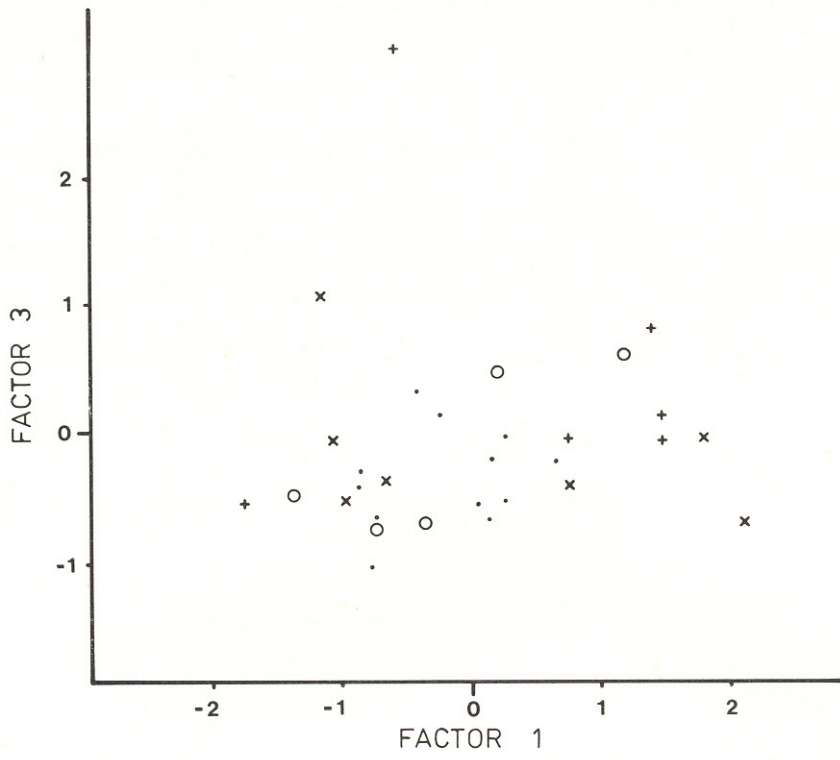
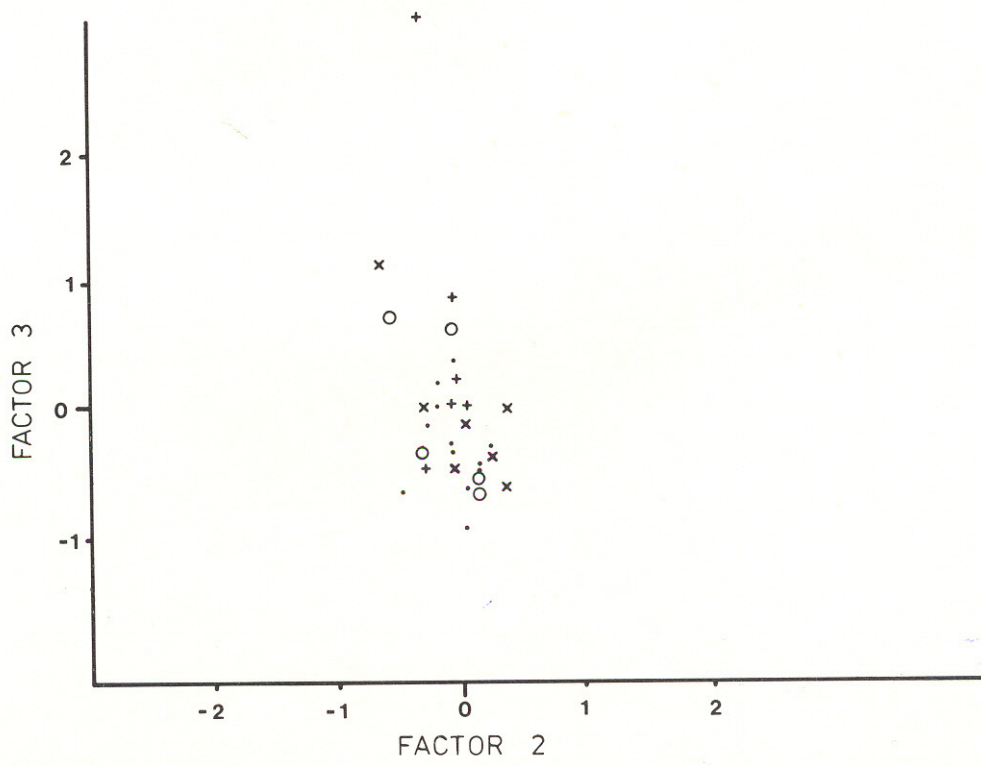


Fig. 5.12 – Plot of Factor 1 versus Factor 3. Legend as for Figure 5.8



2. From these diagrams it is evident that it is not possible to separate the four groups by principal-component analysis.

A cluster analysis using BMDP2M (Dixon 1975) was also carried out. The clusters produced bear no relation to the four types of field occurrences (Fig. 5.14). The essence of the dendrogram is that some samples from the different types of field occurrence are more chemically alike than samples from the same type of field occurrence.

The similarity of samples from different groups is further emphasised by examining the F values for analysis of variance where these are proportional to the ratio between

group variance and within group variance (Till 1974). The larger the F values the greater the difference between groups. The results of the analysis of variance are shown in Table 5.6. Only the F₄ values for Zn reveal a significant difference between serpentinites with pre-Damara and those with Damara country rock.

As the analysis of variance, cluster analysis and principal-component analysis proved unsuccessful in separating the four groups, a discriminant analysis was not justified because the underlying assumption of a discriminant analysis is that definable groups do exist.

On the basis of the t-tests, principal-component analy-

Table 5.6 - F VALUES

Variables	F ₁	F ₂	F ₃	F ₄	Groupings	Degrees of freedom		Significant F at 99%
						V ₁	V ₂	
SiO ₂	10,93	16,66	29,71	5,87	1. Layered complexes	V ₁	V ₂	4,61
TiO ₂	20,79	7,78	9,45	0,79	Archaean complexes	2	306	
Al ₂ O ₃	27,58	17,66	14,02	4,68	Alpine/mantle material			
FeO _t	79,50	40,45	53,04	0,72				
MnO	4,68	2,19	2,87	1,13				
MgO	29,16	26,18	11,21	1,02	2. Horizontal complexes	V ₁	V ₂	3,02
CaO	21,03	32,50	7,80	0,85	Concentric complexes	5	303	
Na ₂ O	10,34	12,53	8,26	0,19	Archaean complexes			
K ₂ O	4,80	2,62	3,84	-	Alpine fertile material			
P ₂ O ₅	0,54	1,47	1,64	7,50	Alpine differentiated material			
Cr	6,75	5,38	4,30	2,11	Alpine depleted material			
Ni	4,27	4,92	5,47	4,51				
Co				3,15	3. Layered complexes	V ₁	V ₂	3,78
V				2,17	Alpine fertile material	3	275	
Zn				17,20	Alpine differentiated material			
Cu				0,12	Alpine depleted material			
Sc				0,70				
					4. Damara/pre-Damara	V ₁	V ₂	7,64
						1	28	

* Discriminant analysis provides a mathematical description of the groups that are defined (Section 5.2.3.4).

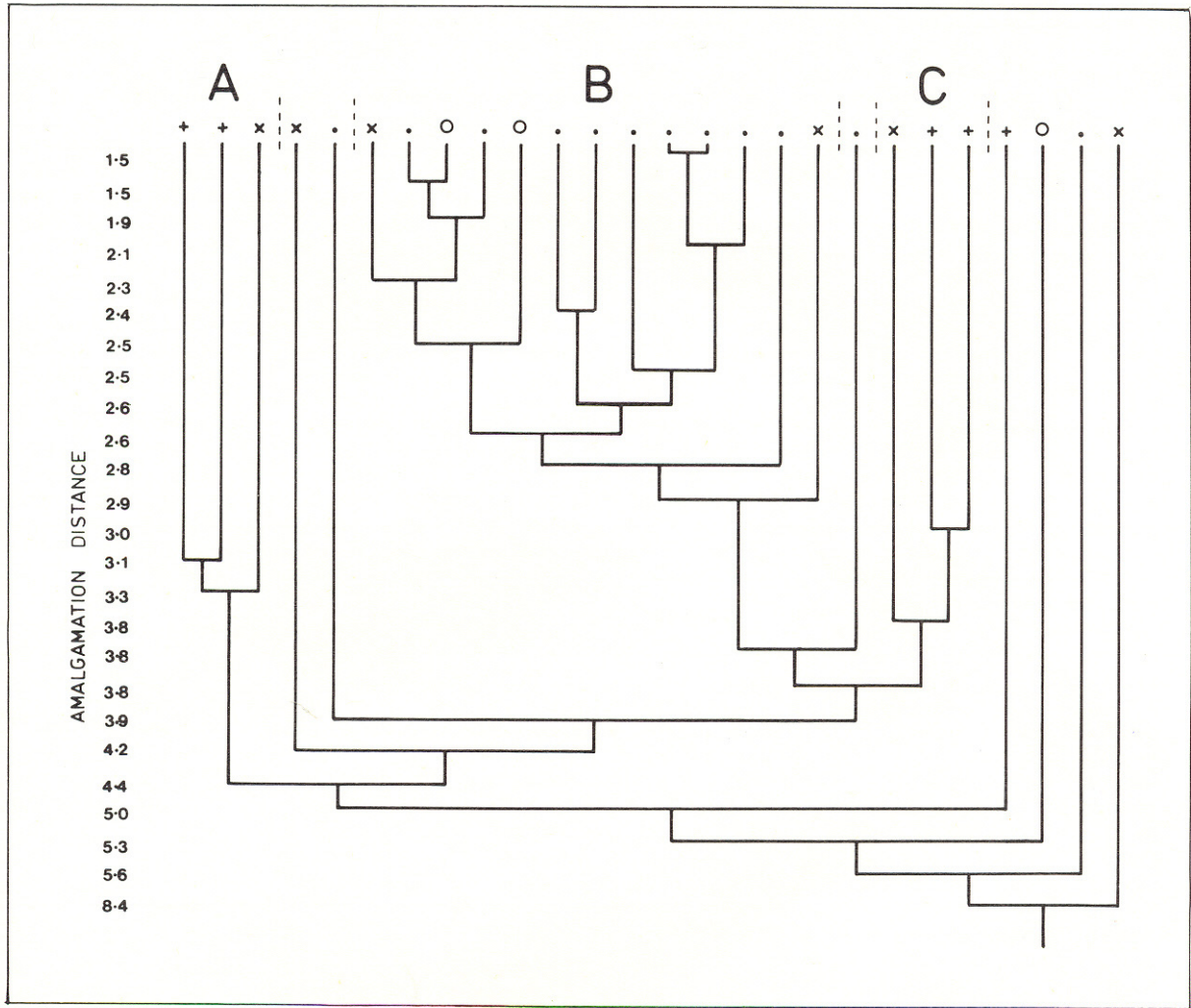


Fig. 5.14 – Dendrogram of SWA serpentinites. Legend as for Figure 5.8

Table 5.7 - SUMMARY OF SERPENTINITE ANALYSES USED

Variable	Horizontal complexes	Zoned complexes	Archaean	Alpine fertile	Alpine differentiated	Alpine depleted	All
Means %							
SiO ₂	42,32	40,04	40,78	44,18	43,55	45,23	44,18
TiO ₂	0,24	0,08	0,22	0,11	0,06	0,06	0,09
Al ₂ O ₃	3,34	0,76	3,80	2,71	1,65	1,51	2,08
FeO _t	12,04	11,18	10,41	8,56	8,42	7,48	8,84
MnO	0,43	0,19	0,16	0,13	0,15	0,13	0,17
MgO	38,82	46,70	36,90	41,43	44,50	44,08	42,54
CaO	1,84	0,31	3,18	2,04	1,09	0,84	1,41
Na ₂ O	0,41	0,20	0,10	0,25	0,15	0,16	0,18
K ₂ O	0,11	0,02	0,04	0,06	0,06	0,05	0,06
P ₂ O ₅	0,05	0,05	0,02	0,07	0,03	0,06	0,04
Cr ppm	6 933	3 334	3 168	2 648	3 226	2 506	3 370
Ni ppm	1 877	1 845	2 357	2 037	2 483	2 173	2 277
Standard deviation							
SiO ₂	2,488	0,872	1,777	1,196	2,2921	2,220	2,225
TiO ₂	0,476	0,028	0,105	0,090	0,0720	0,064	0,162
Al ₂ O ₃	2,141	0,612	1,574	0,885	1,379	1,475	1,316
FeO _t	2,791	3,760	1,899	1,078	1,189	1,732	1,790
MnO	1,485	0,055	0,058	0,074	0,097	0,083	0,465
CaO	1,611	0,352	1,698	0,931	1,275	1,234	1,457
MgO	5,908	3,454	4,374	1,599	4,250	4,0173	3,822
Na ₂ O	0,437	0,285	0,122	0,139	0,123	0,212	0,276
K ₂ O	0,133	0,012	0,041	0,081	0,061	0,068	0,079
P ₂ O ₅	0,150	0,067	0,039	0,111	0,029	0,215	0,116
Cr	16 298	2 682	1 302	1 024	3 226	1 104	5 189
Ni	1 617	1 004	680,6	978,2	2 483	1 001	937,9
n	32	9	30	51	125	61	308
Localities							
Horizontal complexes	Zoned complexes	Archaean	Alpine fertile	Alpine differentiated	Alpine depleted		
Stillwater ¹ Tantalite Valley ² Skaergaard ³ Bushveld ⁴ Great Dyke ⁵ Rhum ⁶ Lebombo ⁷	Tulameen ⁸ Duke Island ⁸	Barberton ¹⁰ Australia ¹¹ Rhodesia ¹² Canada ⁹	St Paul's Rock ¹³ Mediterranean ¹⁴ Puerto Rico ¹⁵ W. U.S.A. ¹⁶ Indian Ocean ¹⁷ Mid-Atlantic Ridge ¹⁸ Nodules ^{19, 24}	Lizard ²⁰ Bay Islands ²¹ Greenland ²² St Paul's Rock ¹³ Mediterranean ¹⁴ Puerto Rico ¹⁵ W. U.S.A. ¹⁶ Mid-Atlantic Ridge ¹⁸	Mid-Atlantic Ridge ¹⁸ New Zealand ²³ W. U.S.A. ¹⁶ Nodules ^{19, 24} Mediterranean ¹⁴		

Sources of analyses presented in Table 5.7:

- Page (1976).
- Kartun (pers. commun.).
- Wager and Brown (1967).
- Liebenberg (1960), De Villiers (1969).
- Worst (1960).
- Wager and Brown (1967).
- Saggerson and Logan (1969).
- Irvine (1974), Findlay (1969).
- Arndt (1977), Villaume and Rose (1977), McCall and Leishman (1971), Nesbitt and Sun (1976).
- Nesbitt and Sun (1976), Viljoen and Viljoen (1969), Villaume and Rose (1977).
- Hancock et al. (1971), McCall and Leishman (1971), Nesbitt and Sun (1976), Golding (1971).
- Nesbitt et al. (1977).
- Melson et al. (1972), Aumento (1970).
- Gulacar and Delaloye (1976), Klemm and Lammerer (1974), Pamic and Majer (1977), Montigny (1973), Moores (1969), Kornprobst (1969), Menzies, (1975; 1976), Menzies et al. (1977), Moores and Vine (1971), Van der Kaaden (1969).
- Burk (1964).
- Coleman (1967); Himmelberg and Coleman (1968), Coleman and Keith (1971).
- Engel and Fisher (1969).
- Cann (1971), Melson and Thompson (1971).
- Rhodes and Dawson (1975), Nixon (1973).
- Green (1964).
- Bowes et al. (1969).
- Mizar (1973).
- Coleman (1966).
- Sobolev (1977), Pinus (1965).

sis and the cluster analysis, samples from the four different types of serpentinite field occurrences cannot be distinguished on chemical grounds, and as will be shown in Section 5.2.3, the nature of the parent rock was probably similar in all four cases.

5.2.3 CLASSIFICATION OF THE ULTRAMAFIC ROCKS AND RELATIONSHIP TO THE DAMARA OROGENY

In order to investigate the nature and origin of the bodies the relationship between the ultramafic rocks and the Damara Orogeny were considered.

5.2.3.1 Principal-component analysis (PCA)

At least 30 samples from a population are needed to establish a parameter which is statistically significant (Davies 1973). Therefore, as insufficient serpentinite analyses with trace-element data for each of the groups were available, the statistical tests were confined to data for the major elements plus Cr and Ni. The analyses were recalculated on an anhydrous basis and all iron was treated as FeO (Table 5.7). In order to ensure that serpentinite analyses only were used, only those containing less than 50 per cent SiO₂, 5 per cent Al₂O₃ and 3 per cent CaO were included.

A principal-component analysis was carried out using computer programme BMDP4M (Dixon 1975). The factor-score coefficients of the first five factors are shown in Table 5.8. The principal-component analysis is completely

objective. A subjective element comes into the calculation when a classification scheme is decided upon and the samples are allocated to various groups. If all the samples group together when the principal-component scores are plotted against each other, then they are chemically homogeneous. If the samples are scattered on a principal-component diagram but the fields, as outlined by representative samples from each group in the classification scheme, overlap erratically the scheme should be reconsidered. In view of the importance of classification, the scheme adopted to distinguish between serpentinites from different tectonic settings is given in detail below.

Moore's (1973) lists five groups of ultramafic rocks based on tectonic considerations:

- (a) Layered complexes, layered-gabbro-norite-peridotite masses, e.g. Bushveld, Skaergaard and Stillwater.
- (b) Concentrically zoned ultramafic complexes such as those in Alaska and Siberia, e.g. Duke Island.
- (c) Ultramafic lavas and associated intrusions of Archaean age, e.g. Barberton, Yilgarn Block and Munro Township.
- (d) Alpine bodies in linear Phanerozoic belts and late-Pre-cambrian deformed belts. Mg/(Mg+Fe) for olivine and orthopyroxene should be greater than 0.9. The body should have a tectonic fabric and be emplaced in the axial regions of mountain systems during initial deformation, e.g. the

Table 5.8 - FACTOR-SCORE COEFFICIENTS FOR 308 SERPENTINITE ANALYSES

		Factor 1	Factor 2	Factor 3	Factor 4	Factor 5
SiO ₂	1	,20959	-,50028	-,14217	,08502	-,07151
TiO ₂	2	,13264	,14577	,09400	,06153	,25561
Al ₂ O ₃	3	,27870	,04497	,01979	-,15056	,00851
FeO _t	5	,12249	,52778	-,09064	,01531	-,09452
MnO	6	,07485	,29109	-,23209	,43521	,09062
MgO	7	-,36848	,05399	,09608	-,07074	,07494
CaO	8	,26954	,00019	,02187	,03195	-,06994
Na O	9	,00761	-,05923	,54001	,04277	-,03881
K O	10	-,07078	-,03357	,59051	,00234	-,05057
P O	11	-,05703	-,02779	-,05873	,00375	,85400
Cr	12	-,01470	,22787	-,11076	-,57700	-,17566
Ni	13	-,04039	,06884	,06731	,53197	-,24348

Coefficients are for the standardised variables, mean zero and standard deviation one.

bodies along the west coast of the U.S.A. or those in the Mediterranean area.

(e) Ultramafic nodules associated with alkaline centres, e.g. kimberlites and alkali basalts.

The concentrically zoned complexes are thought to be layered complexes that have undergone contemporaneous differentiation and deformation (Irvine 1974 and Findley 1969) and are hence a subdivision of layered complexes.

Alpine-type bodies are regarded by Avé Lallemant (1969), Bonatti (1976), Coleman (1971, 1971a), Coleman and Keith (1971), Loubet *et al.* (1975), Menzies (1975, 1976), Menzies *et al.* (1977), Montigny (1973), Moores and McGregor (1972) and Naldrett (1973) as being mantle-derived material brought to the surface either in ocean-ridge systems or as a consequence of plate collision along subduction zones. Ultramafic nodules and fragments in kimberlites are usually thought of as mantle-derived fragments (O'Hara *et al.* 1975). Contemporary views on the mantle suggest that it is heterogeneous and O'Hara *et al.* and Irving (1977) suggest that at least three types of mantle material exist:

(a) Fertile mantle; supposedly garnet lherzolite.

(b) Differentiated mantle formed by partial melting of (a); wherholite, primary partial melt and various cumulates.

(c) Depleted mantle; various harzburgites.

On the basis of this heterogeneity and the hypothesised equivalence of mantle and Alpine material (Menzies *et al.* 1977, Bonatti *et al.* 1971), the Alpine field was further subdivided into fertile, depleted and differentiated mantle. This is an oversimplification since the mantle has a long history. Firstly, differentiation has taken place by dissimilar degrees of partial melting and subsequent crystal fractionation resulting in a gradation between the three fields. Secondly, a single body may contain all three types; a piece of fertile mantle may be brought quickly to the surface and in the process undergo partial melting resulting in the formation of dykes of liquid composition, cumulates and depleted and fertile material. Menzies (1975, 1976) and Menzies *et al.* (1977) suggest that this process has taken place in the case of the Mediterranean peridotites. These considerations led to the following classification scheme being used in this study of serpentinites:

(a) Layered complexes

(i) Horizontal bodies, e.g. Bushveld.

(ii) Concentrically zoned bodies, e.g. Duke Island.

(b) Archaean material, e.g. Barberton, Yilgarn Block.

(c) Mantle-derived material

(i) Fertile mantle, e.g. sheared garnet-lherzolite nod-

ules and Alpine garnet lherzolite.

(ii) Differentiated mantle, e.g. olivine-websterite nodules and differentiated ultramafic-mafic Alpine complexes.

(iii) Depleted mantle, e.g. unshered harzburgite nodules and Alpine harzburgite.

As very few analyses of serpentinised nodules are available the characteristics of mantle-derived material were largely defined by Alpine-type material.

Figures 5.15 and 5.16 indicate the fields outlined by the groups defined in the classification scheme when a PCA was conducted on the 308 serpentinite analyses taken from the literature. The analysis differentiates two primary fields, namely the layered complexes field and the Alpine/mantle field. The layered complexes field contains the Archaean and zoned complexes fields. The Alpine/mantle group is subdivided as outlined in the classification.

The factor scores (Table 5.8 and Figs 5.15 and 5.16) indicate a variation in elements from group to group as shown below in Table 5.9.

The results of the PCA are remarkably consistent with theoretical predictions, namely that presumed primary partial melts (Archaean) are enriched in Al_2O_3 , CaO, FeO, MnO, TiO_2 while the residual material (depleted Alpine) is depleted in these elements and enriched in refractory elements (MgO). This indicates that a PCA approach is valid.

The South West African samples plot in the Alpine field except for G2/l and GB146 (Figs 5.15 and 5.16). Having a high total-iron content, both of these samples plot in the layered complex field. The remaining samples plot in the depleted Alpine field except for B2, GB62, GB225, OT6 and OT25 which lie in the differentiated Alpine field.

The PCA indicates that:

(a) The nature of the parent rock of serpentinite can be determined on the basis of its chemistry.

(b) The South West African samples are largely Alpine (93 per cent) and usually depleted (83 per cent).

(c) The samples from bodies in pre-Damara country rock have a wider spread of values than those occurring in Damara country rock.

5.2.3.2 Analysis of variance

The groups in the classification scheme were subjected to an analysis of variance tests. Using the three groups represented by layered complexes, Archaean complexes and Alpine/mantle material, a significant difference for 10 of the 12 elements investigated became apparent (Ta-

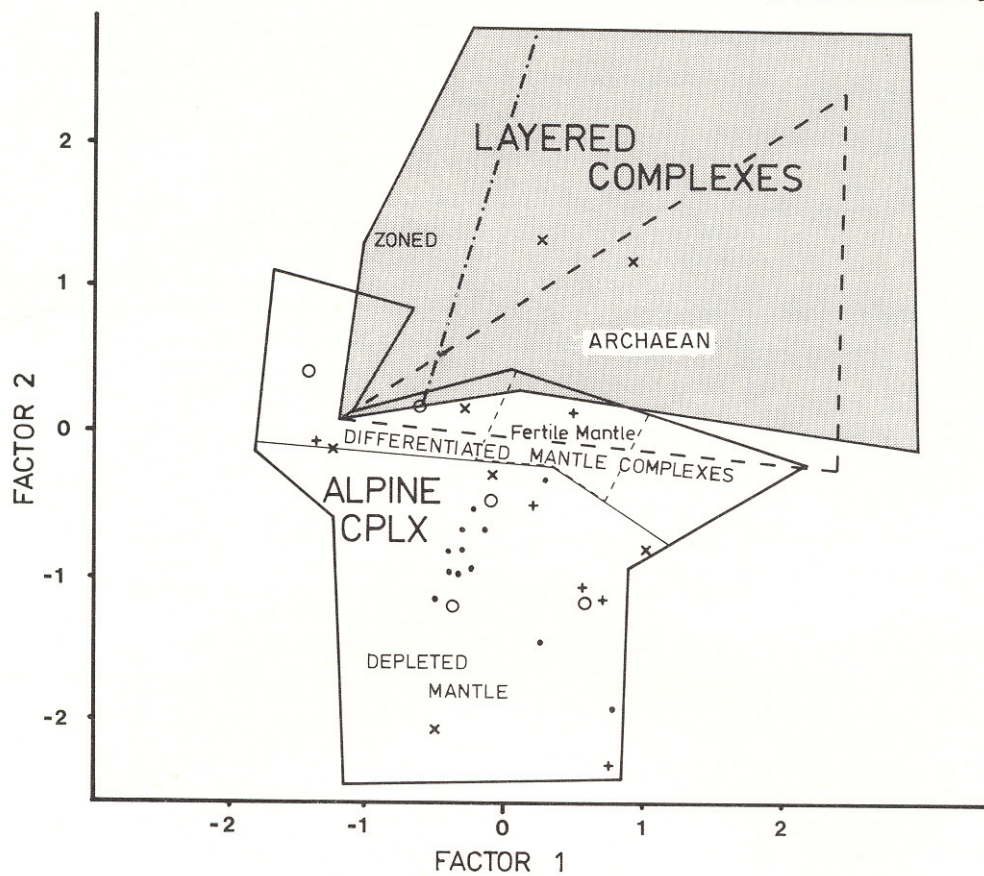


Fig. 5.15 — Factor 1 versus Factor 2 plots for 308 serpentinites.
Legend as for Figure 5.8

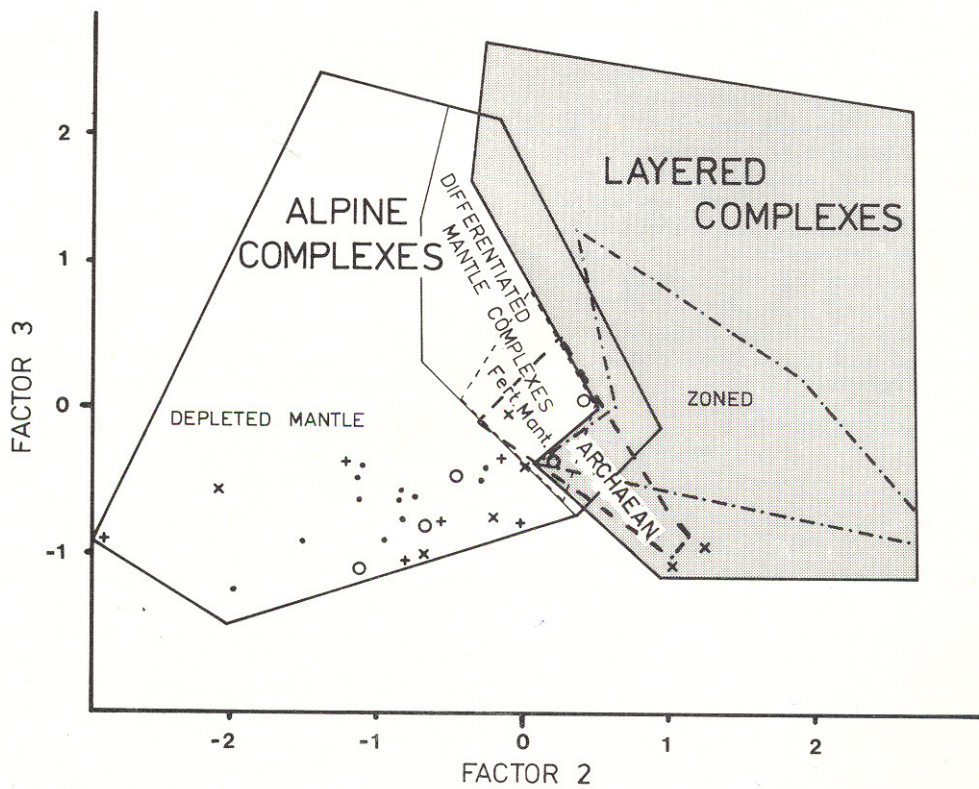


Fig. 5.16 — Factor 3 versus Factor 2 plots for 308 serpentinites.
Legend as for Figure 5.8

ble 5.6). Using the complete scheme there was a significant difference for 9 of the 12 elements.

5.2.3.3 Discriminant analysis

Since the PCA and the F-tests indicated that the groups in the classification scheme can be distinguished on the basis of major-element chemistry, a stepwise discriminant analysis using computer programme BMDP7M (Dixon 1975) was used. In this process a classification scheme is adopted and samples are allocated to each group. Vectors (canonical variables) are then chosen such that there is a maximum dispersion of groups and a minimum dispersion of samples within the group. Only those elements which emphasise differences between groups are considered. The mean position for each group is calculated and the position of each sample compared with it. The sample is classified with the group whose mean is closest. The canonical variable scores for a sample may be calculated by the formula:

$$\text{canonical variable} = \frac{\sum_{i=1}^n \gamma_{ji} (Y_i - \bar{Y}_i)}{s_i}$$

Where γ_{ji} = coefficient of canonical variables for element i on canonical variable j
 y_i = concentration of element i in sample y
 \bar{y}_i = mean concentration of element i
 s_i = standard deviation

To determine the success of the classification reference should be made to the percentage of correctly classified samples. If a number of assumptions are made, the signifi-

cance of the difference between groups may be evaluated using F-tests. The assumptions are:

- (a) The observations from each group are randomly chosen.
- (b) The variables are normally distributed.
- (c) A sample has an equal chance of belonging to anyone group.
- (d) None of the samples used to calculate the means for each group is misclassified.

It is evident that discriminant analysis is an extremely subjective process heavily dependent on the classification scheme used. The PCA indicated that three groups - the layered (horizontal and concentric), Archaean and Alpine (mantle) - are chemically distinct. These groups were used for the first discriminant analysis (Table 5.10). The South West African samples plot in the Alpine field, except GB146 and G2/1. The classification was 81 per cent successful (Fig. 5.17).

The concentrically zoned complexes were treated as a group in their own right. Only nine analyses of serpentinites from these were found. The results are shown in Table 5.10. The discriminant analysis classified olivine cumulates from all groups in the zoned complex field. The analysis was 75 per cent successful. The South West African samples were classified with the Alpine material except GB225, G2/1 and GB146. Sample G2/1 was classified as layered complex material and GB146 and GB225 as zoned complex material.

Because Irvine (1974) suggests that zoned complexes are a type of layered complex and because the F-value was lowest between horizontally layered complexes and zoned

Table 5.10 - RESULTS OF THE DISCRIMINANT ANALYSIS

Classification used	Coefficients of canonical variables (1)	(2)	F-matrix	Degrees of freedom	Serpentinites correctly classified			
1. (a) Layered complexes (b) Archaean material (c) Alpine/mantle material	TiO ₂	1,93080	,16719	(a) (b)	V ₁ V ₂	81%		
	Al ₂ O ₃	,05627	,34773	(b) 11,35	2			
	FeO _t	,45391	-,05809	(c) 28,49	306			
	CaO	,01049	,35749	14,23				
	Na ₂ O	,50775	-2,32461					
	Cr	,00005	-,00004					
	Ni	-,00020	,00039					
	2. (a) Horizontal complexes (b) Concentric complexes (c) Archaean material (d) Alpine/mantle material	TiO ₂	-,194880	,01970	(a) (b) (c)		V ₁ V ₂	75%
		Al ₂ O ₃	-,1278	,41055	(b) 4,61		3	
FeO _t		-,43248	-,12035	(c) 10,05	303			
CaO		-,02333	,33151	(d) 28,44				
Na ₂ O		-,48248	-2,10797	5,56	15,34			
Cr		,00006	,00003					
Ni		,00015	,00045					
3. (a) Layered complexes (b) Alpine/mantle fertile (c) Alpine/mantle differentiated (d) Alpine/mantle depleted		SiO ₂	,37274	,24757	(a) (b) (c)	V ₁ V ₂	60%	
		FeO _t	-,22252	,12935	(b) 22,30	3		
	MgO	,15784	-,05786	(c) 39,00	275			
	Ni	,00023	-,00055	(d) 62,06				

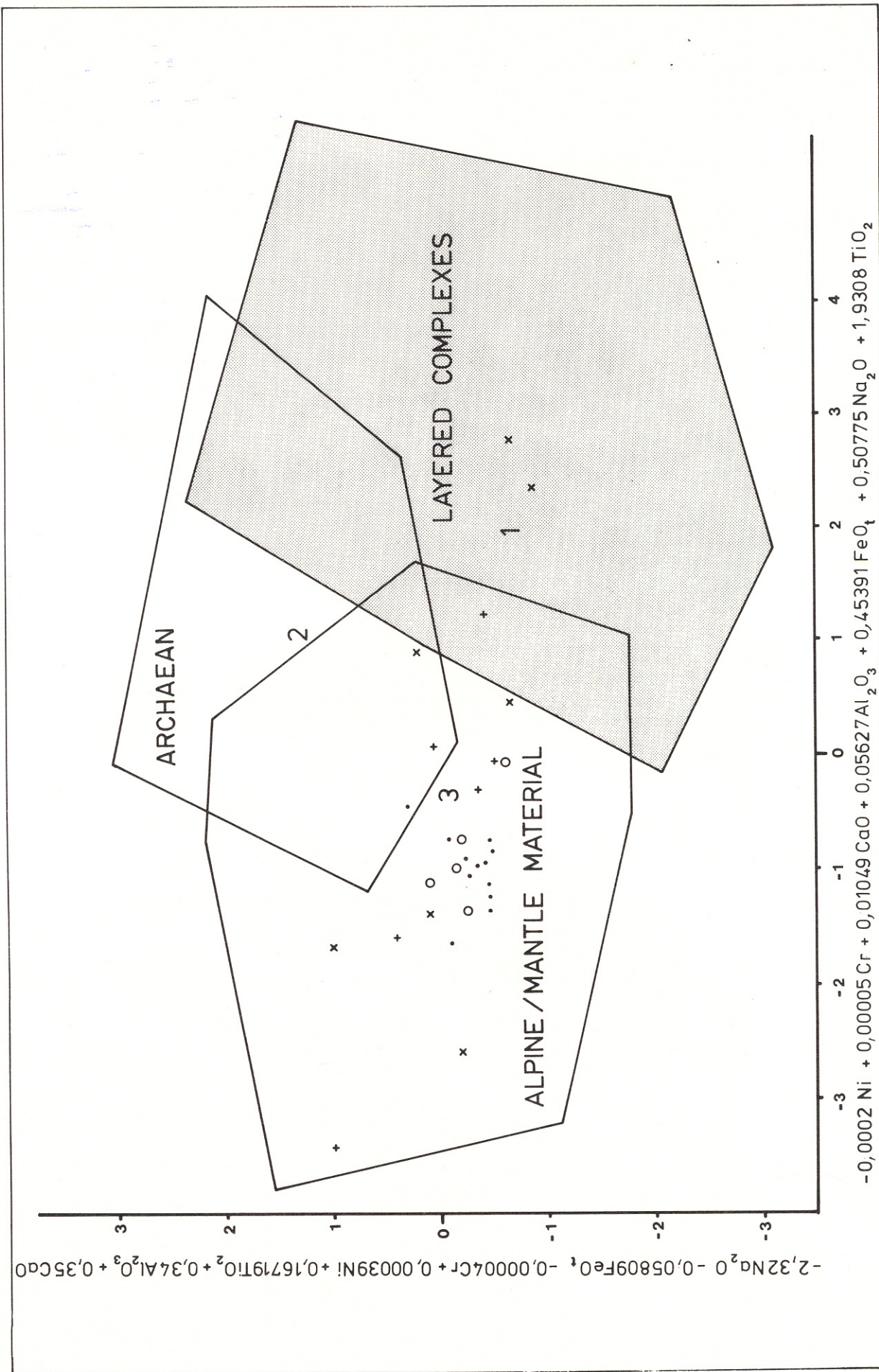


Fig. 5.17 — Discriminant analysis. Symbols as for Figure 5.8

complexes, the zoned complexes were subsequently treated as a subdivision of layered complexes. As stated previously the Alpine or mantle field can be subdivided into fertile mantle, differentiated mantle and depleted mantle. The third classification attempted was: layered complexes (horizontal and layered), fertile mantle, depleted mantle and differentiated mantle. The Archaean group was excluded since the South West African serpentinites occur in Proterozoic rocks. Table 5.10 lists the results. The average percentage of correctly classified samples was 60. The lower percentage of correctly classified samples is attributed to the similarity of the various Alpine types. This is emphasised by the fact that it was only possible to use four variables to distinguish the groups as against seven in the earlier groupings. Furthermore, the posterior probability was smaller. GB146 and G2/1 were classified as layered-complex material. E5, GB62, OT6 and OT25 were classified as differentiated Alpine (mantle) material. The remaining 24 samples were classified as depleted Alpine (mantle) material (Fig. 5.18).

5.2.3.4 Trace elements

The major-element chemistry of the South West Afri-

can serpentinites implies derivation from Alpine material (probably depleted mantle). The Al_2O_3 and FeO_t contents are too low to represent material derived from fertile mantle or a partial melt. The Al_2O_3 , FeO_t , K_2O , Na_2O , MnO and TiO_2 contents are also too low, relative to the silica concentration, for the bodies to represent cumulates. Furthermore, as can be seen from Figures 5.8 to 5.10, the samples exhibit no clear fractionation trends.

If the bodies are depleted mantle material, this should be reflected in the trace-element chemistry. Those elements for which there is no lattice site in the presumed residue of olivine and orthopyroxene, e.g. the incompatible elements Zr, Nb, Y, Ba, Rb, Sr and Ga, should be largely removed in any partial melt whereas elements such as Ni, for which there is a site, should be somewhat enriched in the residue. Table 5.11 lists concentrations of these elements in fertile mantle, depleted mantle, assumed direct partial melt and cumulates. The low concentrations of the incompatible elements and enriched concentrations of compatible elements are consistent with the hypothesis that the South West African serpentinites represent depleted mantle composed of an olivine-orthopyroxene residue.

Table 5.11 - TRACE-ELEMENT CONCENTRATIONS OF MANTLE-DERIVED MATERIAL

	Fertile mantle			Depleted mantle			Differentiated mantle	
	St Pauls ¹ ppm	Gurney ² ppm	Lashaine ³ ppm	Lashaine ³ ppm	Bultfontein ⁴ ppm	w. USA ⁵ ppm	Liquid (komatiite) ppm	Cumulate ⁴ (Bultfontein) ppm
Zr	34	30	4,6	3,8	7	11	21	32
Nb	-	5	1,4	1,2	3	1,1	1	5
Y	-	5	0,9	0,6	3	0,98	7	6
Rb	-	3	3,6	1,7	3	2	1	3
Ba	18	70	-	-	8	5	36	73
Sr	23	25	15	11	34	4,5	7	107
Co	105	120	-	-	116	101	145	116
Cr	3 050	2 830	3 332	1 904	2 300	3 000	4 370	5 100
Ni	2 130	2 000	2 808	3 198	2 250	2 200	1 745	1 530
V	105	-	-	-	26	30	83	68
Zn	35	100	-	-	32	-	80	70
Sc	-	19	-	-	-	0,9	-	31
Cu	19	17	-	-	116	-	36	-
Ga	13	14	2,8	2,2	-	-	-	-

- Sources: 1. Melson et al. (1972), Aumento (1970).
 2. Gurney (pers. commun.).
 3. Rhodes and Dawson (1975).
 4. Gurney et al. (1977a).
 5. Coleman (1967).

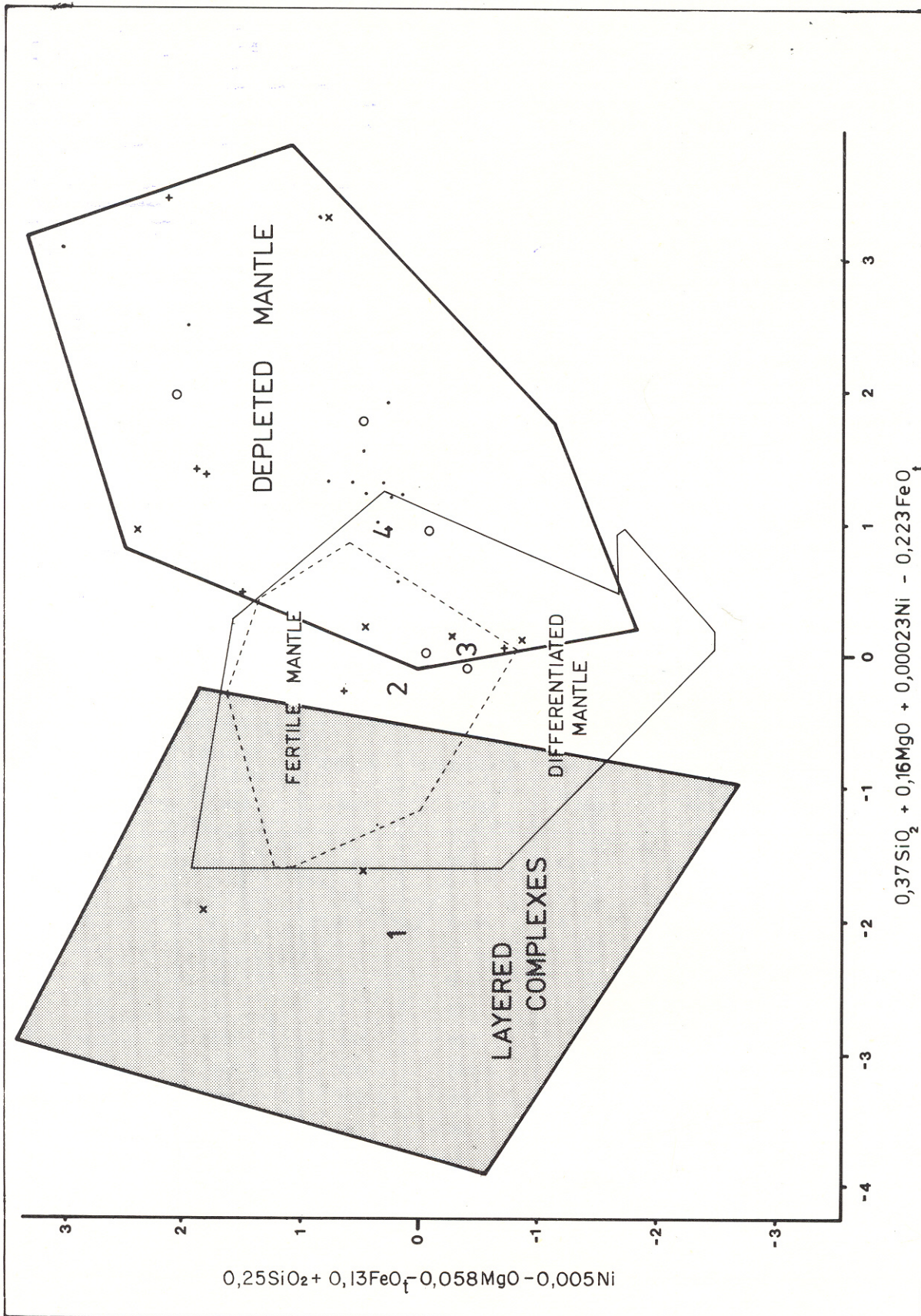


Fig. 5.18 — Representation of the results of the discriminant analysis using 306 serpentinites. Legend as for Fig. 5.8. 1.2.3 and 4 represent the mean for respective groups

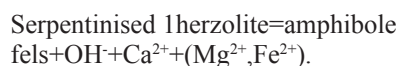
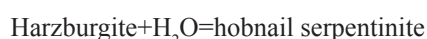
Kogarko (1973) assumed a Ni/Co ratio of 10 to 15 for primary mantle and then calculated Ni/Co for derived magmas. He concluded that all primitive partial melts produced, i.e. those not affected by fractional crystallisation, should have a Ni/Co ratio of 3,4 to 7,6. Inspection of values given by Page (1976) and Yefimov and Ivanova (1963) indicates that the Ni/Co ratio generally remains below 15 for cumulates from layered complexes unless sulphides crystallise. A Ni/Co ratio in the range 15 to 30 appears to relate to depleted material. This is because Co enters the silicate liquid more rapidly than Ni when fertile mantle is melted. The bulk partition coefficient of Co is likely to be smaller (2) than that of Ni (7)*.

However, when a sulphide phase is present during partial melting and fractional crystallisation, Ni sulphides crystallise and the Ni/Co ratio rises dramatically in the fractionated product as outlined by Maclean and Simazaki (1976). The Ni/Co ratios for South West African samples lie in the range 15 to 30 except for samples B4, B8, G2/1 and G8/8 in which the ratio is less than 15.

5.3 CONCLUSIONS

With reference to the three points under investigation it can be stated that:

(a) The four major rock types, that have been studied, may be derived from mantle material by the reactions:



(b) The serpentinite samples from the four different types of field occurrences are chemically indistinguishable. However, as the tests were statistical and the number of samples in each group was less than 30 this conclusion should be treated with caution.

(c) On the basis of PCA and discriminant analysis the serpentinites were found to be of Alpine type. Furthermore, the discriminant analysis indicates that 80 per cent of the samples are of a depleted nature. This classification is confirmed by the low Al_2O_3 , NaO, K_2O and FeO_t contents of the samples relative to SiO. The Ni/Co ratios for 80 per cent of the samples and the low incompatible element concentrations are consistent with depleted Alpine origin. However, the samples from bodies in pre-Damara terrain show a wider scatter of values. Some have concentrations of incompatible elements slightly greater than the detection limit.

The discriminant analysis showed that four of the samples can not be classified as depleted mantle. All these factors indicate that some bodies contain material exhibiting various degrees of depletion. The higher percentage of amphibole and carbonate-bearing rocks and wider epidote rims at Gauchab than at Omieva may point to it being less

depleted.

These considerations suggest that the South West African serpentinites consist of Alpine-type material which has been chemically depleted to varying degrees.

6. OVERALL CONCLUSIONS

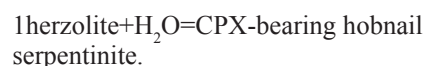
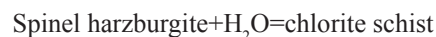
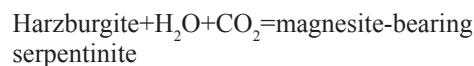
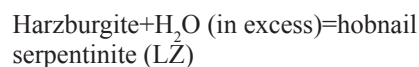
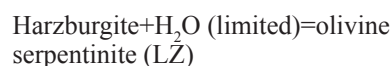
6.1 INTRODUCTION

The investigation set out to establish the relationships between the several different types of ultramafic rocks and to determine whether or not different assemblages of these rocks characterise the four types of field settings in which they occur. Furthermore, these factors have been examined in relationship to the Damara Orogeny.

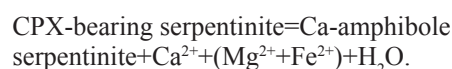
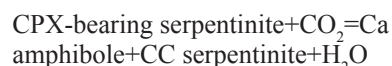
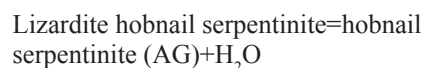
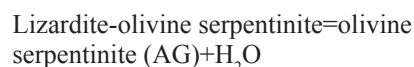
6.1.1 RELATIONSHIPS BETWEEN THE ULTRAMAFIC ROCK TYPES

On the basis of field observations, petrographic work and chemistry, the principal rock types are thought to have formed in the following manner:

(a) Under low-temperature conditions harzburgite containing lenses of spinel harzburgite and lherzolite underwent hydration in accordance with the equations:



(b) Under rising temperature the following hydration reactions are envisaged:



When sufficient clinopyroxene is present all the serpentinite is used in the last reaction.

CPX-bearing serpentinite=amphibole
fels+Ca²⁺+(Mg²⁺+Fe²⁺)+H₂O

Hobnail serpentinite+SiO₂ (limited)=
talcose serpentinite+H₂O

Hobnail serpentinite+(OH)-=TC
serpentinite+Mg²⁺.

Fluids containing Ca²⁺ and Fe²⁺, produced by the hydration of clinopyroxene, react with the country rocks to form epidote and amphiboles. Fluids containing Mg²⁺ react with the country rock to produce chlorite.

6.1.2 RELATIONSHIPS BETWEEN THE FOUR TYPES OF FIELD OCCURRENCES

The similarity in field setting and petrography suggest a similar history and the chemistry suggests a similar origin for bodies from all four types of field occurrences.

In terms of field setting and petrography the same rock types, namely olivine serpentinite, hobnail serpentinite, talcose serpentinite, talc schist, chlorite schist, amphibole fels and epidote-rich rocks occur in bodies within both pre-Damara and Damara country rocks. Secondly, a similar zonation and association of rock types are found in all bodies. Talc schist forms the rims around the bodies and grades into talcose serpentinite which in turn grades into hobnail serpentinite. Minor lenses of amphibole- and carbonate-bearing serpentinites may be found in the talcose serpentinite. Lenses of chlorite schist are sparsely scattered throughout the bodies. In the cores, olivine serpentinite may be developed. There are amphibolite dykes or xenoliths in both Damara and pre-Damara terrain and near the contact with the serpentinites, epidote has developed in plagioclase-bearing rocks, whereas chlorite has grown locally in biotite-bearing rocks and amphibolites.

The chemistry of the samples suggests a common origin. It has proved impossible to distinguish serpentinites from the four types of field occurrence on the basis of simple bivariate element plots, t-tests, cluster analysis or principal-component analysis. Analytical data taken from the literature, pertaining to serpentinites for which the origin of the parent rock is known, were subjected to multivariate tests and these showed that the chemistry of the serpentinites is dependent on their origin.

Using the chemical classification outlined in Section 5.9.3 per cent of the samples were classified by the multivariate tests as being of Alpine type and 83 per cent were chemically depleted. The depleted nature of the samples is confirmed by their low Al₂O₃, Na₂O and K₂O contents relative to SiO₂, the high Ni/Co ratios and the low concentrations of incompatible elements relative to presumed fertile mantle.

6.1.3 RELATIONSHIPS TO THE DAMARA OROGENY

The structural evidence suggests that the bodies were tectonically emplaced along thrust planes parallel to dS₂ or dS₁

during the Damara Orogeny.

Three stages can be outlined in the history of the serpentinite bodies.

- Serpentinisation of the parent rock at low temperatures and without shearing.
- Emplacement under unknown conditions but a low geothermal gradient was probably operative.
- Higher temperature conditions causing dehydration after Damara dS₂ deformation.

6.2 MODELS

6.2.1 INTRODUCTION

Two models are currently in vogue to explain the formation of the Damara Mobile Belt. These are the aulacogen model, as advanced by Martin and Porada (1977), and the plate tectonic model, as advanced by Blaine (1977), Hartnady (in press) and Sawyer (1978).

Three models for the relationship between the serpentinites and the Damara are considered here:

- The bodies are of Damara age and the Damara Mobile Belt is a modified aulacogen.
- The bodies are of Damara age and the Damara Mobile Belt formed in a plate-tectonic environment.
- The bodies originated during the pre-Damara and were emplaced in their present position during the Damara deformation.

6.2.2 AULACOGEN MODEL

6.2.2.1 Aulacogen model applied to the Damara Orogen

Hoffman (1974) describes the development of an aulacogen as having an initial graben stage which occurs when a rising mantle diapir heats the underlying crust enabling it to neck and rift through tensional stresses away from the site of the diapir.

An asthenolithic cushion is then intruded into the transitional zone between the sialic crust and mantle under the rift site. Alkaline magmatism generally, but not always, takes place in the rifted zones along fault lines. Several kilometres of clastic sediments grading upwards into lutites derived from the adjacent area are then deposited into the graben.

In the Damara context Martin and Porada (1977) equate the graben phase with the Nosib Naauwpoort volcanism and clastic sedimentation. They invoke three grabens to explain the present distribution of the Nosib Group (Fig. 6.1). The three rifts which formed during Nosib deposition then subsided and coalesced as the Khomas and Kudis Subgroup were deposited in rifts on adjacent horsts.

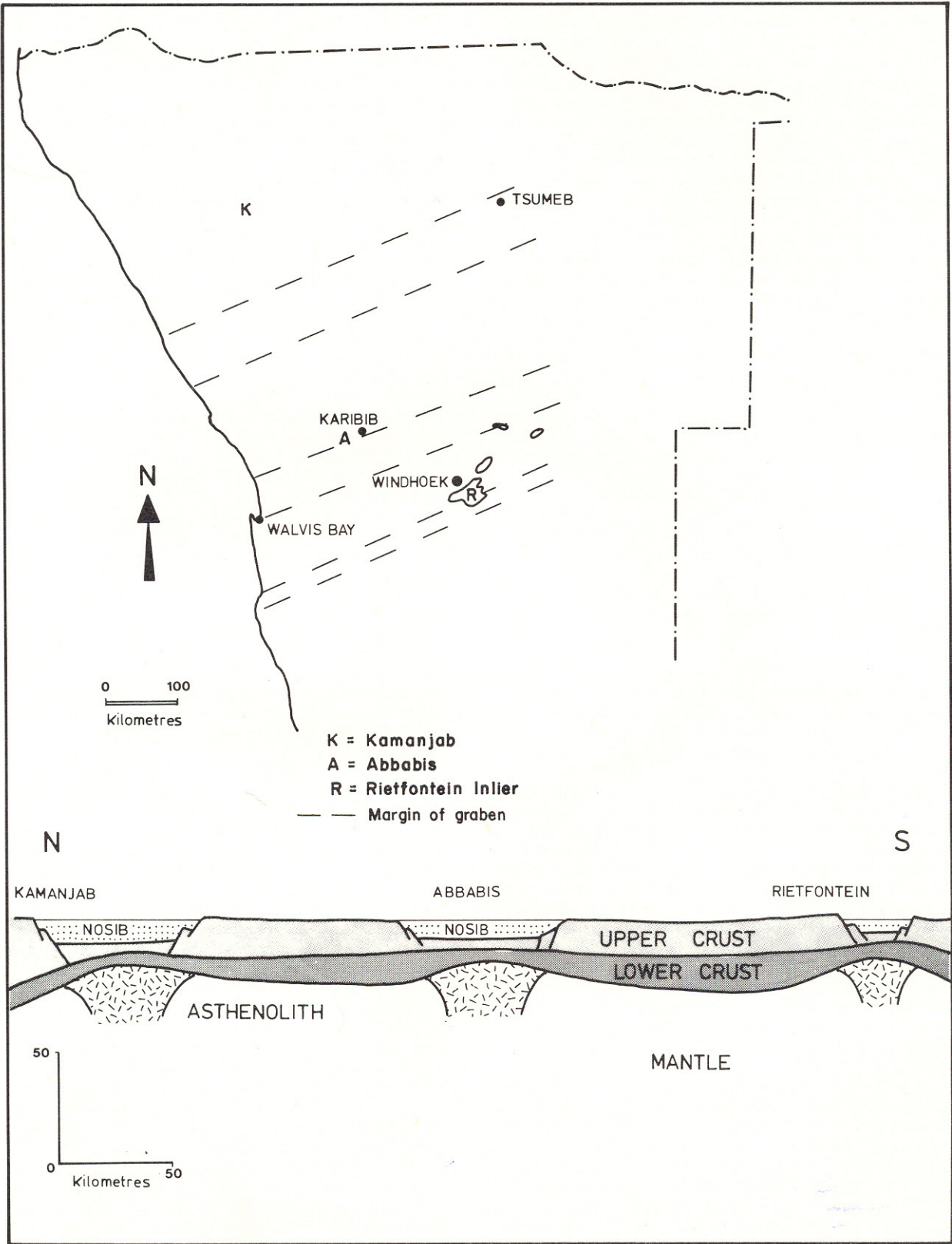


Fig. 6.1 — Location of the grabens in the aulacogen model, after Martin and Porada (1977)

In Hoffman's model (1974) the graben stage is followed by a downwarping phase in which the graben subsides because the whole structure moves away from the heat anomaly in the mantle. The margins of the graben are covered with sediments. The wider basin is filled with quartzites, mudstones and turbidites which pass into stromatolitic carbonate rocks. A molasse phase consisting of mudstones, siltstones and sandstones may develop. The mass is intruded by granodiorite and quartz diorite. The downwarping phase is followed by a lateral compressional stage in which the middle block of the graben subsides. At the same time the crust undergoes partial melting and metamorphism.

Martin and Porada's model differs from Hoffman's aulacogen model from this point onwards. The cushion of asthenolithic material intruded during the graben phase has cooled sufficiently to be denser than the surrounding rock and it sinks. A new batch of asthenolithic material replaces the sinking cold asthenolith. The crust undergoes renewed partial melting, metamorphism and deformation. The major dS_2 fabric of the Damara forms at this stage.

6.2.2.2 Aulacogens and ultramafics

The presence of ultramafic rocks aulacogens has rarely been recorded.

Nwachukwu (1972) argues that the absence of ultramafic rocks in the Benue Trough of Nigeria favours an aulacogen model for the trough.

The Great Slave Lake aulacogen as described by Hoffman (1974) and Olade and Morton (1972) contains alkali basalts and rhyolites but no ultramafics.

Ham and Wilson (1967), in their description of the Oklahoma aulacogen, do not mention the occurrence of ultramafics.

The Dnieper-Donets aulacogen (Chekunov 1967, Lebedinskiy 1967, Dolenko 1970 and Lyashkevich 1974) contains four groups of volcanics and intrusives. These range in composition from olivine basalt to quartz porphyries and from lamprophyres to syenite. The most mafic of these contains 16 per cent of MgO and hence can hardly be equated with the South West African ultramafics which contain 30 to 40 per cent of MgO.

All these examples serve to militate against the aulacogen model, in that it fails to provide a suitable source for the depleted Alpine material.

6.2.2.3 The Martin-and-Porada aulacogen model and the South West African serpentinites

It is conceivable that ultramafic rocks could have been found or emplaced in the graben, downwarping or compressional stage of the aulacogen model.

Igneous rocks produced during the graben phase should

be alkaline (Bailey 1974) and contain more than normal amounts of K_2O and Na_2O . The South West African serpentinites contain on average 0,05 per cent Na_2O and 0,01 per cent K_2O , compared with 0,18 and 0,05 per cent respectively, which are the averages for 308 serpentinite analyses contained in the literature, and are therefore not alkaline.

The location of the rifts as chosen by Martin and Porada (1977) does not coincide with the location of the ultramafics (Figs 1.1 and 6.1). In order to produce the ultramafics in the graben stage they would have to be partial melts of mantle and their chemistry should reflect a liquid composition. As described in Section 5, the low Al_2O_3 , Na_2O and K_2O contents, the high Ni/Co ratio and low incompatible-element content of the South West African samples are inconsistent with them representing frozen liquids or cumulates.

The model predicts that the mantle will be cool during the downwarping stage, so partial melting resulting in the intrusion of ultramafics is unlikely.

The serpentinites could be viewed as cumulates at the base of lavas and sills which may be represented by rocks such as the amphibolites of the Matchless Member. Isolated occurrences of talc and chlorite schists are present at the base of the Matchless Member (Table 1.1). However, these ultramafics do not have the chemistry suitable to continental cumulates, since the FeO , MnO and Cr contents are too low relative to the SiO_2 content. In addition, some liquid would be trapped in a cumulate resulting in some incompatible elements being present.

If the bodies had intruded during the compressional stage then they would originally have been partial melts of mantle material because the mechanical problems of moving a solid peridotite with a density of 3 t/m³ through 20 km of continental material with a density of 2,6 to 2,8 t/m³ in a compressional environment are considerable and furthermore, the model requires the mantle to be hot and undergoing partial melting at this stage.

Additionally the bodies could not have reached their present position as ultramafic melts since they appear to have been tectonically emplaced (Section 2) and they have not induced thermal metamorphism, nor have contained slices of acidic country rock undergone partial melting.

Hence the melts would have had to pause and cool before being emplaced in their present position. The bodies could not have been serpentinitised at such a stage because the original serpentinitisation took place at between 85 and 185°C (Section 4) and the crust is supposed to be undergoing partial melting during the compressional phase (even antigorite serpentinitisation only takes place below 400°C). Furthermore, the present stratigraphic position of the bodies in the aulacogen model implies that there were at least 20 km of sediments above them. An average crust-

tal geothermal gradient of 25°C/km (Miyashiro 1973) results in the temperature at 20 km being 500°C. Therefore, serpentinisation would have had to take place after emplacement and after metamorphism as the temperatures during Damara metamorphism were too high for lizardite or antigorite serpentinisation. This raises three problems:

(a) The solid block of peridotite (3,00 t/m³) would be denser than the country rock (2,6 to 2,8 t/m³), so upward movement of the peridotite seems unlikely.

(b) In this model the formation of talc and chlorite schists should post-date deformation, but the talc and chlorite schists contain the dS₂ fabric.

(c) The serpentinites do not have a suitable chemistry to represent partial-melt material.

On the basis of all these considerations, it seems unlikely that serpentinites were formed in an aulacogen environment, albeit modified as proposed by Martin and Porada.

6.2.3 PLATE-TECTONIC MODEL

The plate tectonic model visualises an ocean trending north-east in the area now occupied by the Khomas Subgroup (Khomas Trough), (Blaine 1977, Hartnady in press; Sawyer 1978). The width of the ocean depends on how the palaeomagnetic data are interpreted. The sediments known as the Nosib Group are thought to have been deposited in the continental areas during rifting or during the early stage of ocean spreading.

After a period of spreading, closure of the basin may have begun with the initiation of a north-westerly-dipping subduction zone beneath the central zone (Sawyer 1978). The thick sediments of the Kudis and Khomas Subgroups were deposited on the margins of the ocean basin before and possibly during closure. The Damara S surfaces (Table 2.1) may reflect the deformation resulting from ocean closure with considerable thrusting along the southern margin (Bickle and Coward 1977). After closure, metamorphism took place in the orogen.

In contrast to an aulacogen environment, ultramafic rocks are common in orogenic belts which are believed to have formed by plate-tectonic processes (Dewey and Bird 1971). This is because in the oceanic phase of the plate-tectonic model, mantle material is exposed.

Bonatti *et al.* (1971) outline two types of ultramafics observed along the equatorial Mid-Atlantic Ridge. In one type, the ultramafics formed as cumulates in ultramafic complexes in the lower oceanic crust and in the other, serpentinites formed as isolated bodies on the basaltic sea floor.

Some ophiolite sequences which contain these two types

of ultramafic rocks (Rod 1974) are interpreted as slices of oceanic crust abducted onto continental margins.

A second source of ultramafic material, during continent collisions, is slivers of continental mantle which may be thrust into suture zones, resulting in transport of fertile mantle material to near the surface (Dewey 1977). If this rise is rapid, fertile mantle may undergo melting, and when the body reaches surface it consists of fertile material containing dykes of primary partial melt and perhaps cumulates and lenses of residual composition.

Assuming the serpentinites to be of Damara age, the following sequence of events may have taken place:

Stage 1 - Serpentinisation (De Wit *et al.* 1977)

Transverse zones of tectonic weakness dominate the basement morphology of large areas of oceanic crust. Water percolates along the fractures and hydrates the mantle peridotite (Fig. 6.2). In this case the reactions would be:



At this stage, hourglass pseudomorphs and bastites develop under low-temperature serpentinisation. The upper mantle in the oceanic areas is thought to consist of depleted material (Ringwood 1977). The depleted nature of 80 per cent of serpentinites is consistent with their derivation from oceanic upper mantle.

Stage 2 - First emplacement (Bonatti 1976)

The process of serpentinisation of a peridotite involves a volume increase of about 30 per cent. As serpentinisation proceeds the density of peridotite decreases dramatically from 3 t/m³ to 2,2 to 2,5 t/m³. Raleigh and Paterson (1965) show that the strength of crysotile-lizardite serpentinite decreases markedly at pressures greater than 1 kb (Fig. 4.1).

The combination of volume increases, density contrast and decrease in strength may enable the serpentinised peridotites to rise diapirically into the ocean crust. If the South West African serpentinites originated in this way, the hornblendite 'dykes' (which plot in the ocean-floor basalt field, Figs 5.6 and 5.7) may have been intruded while the serpentinites formed part of the ocean floor or they may be tectonically included fragments.

Stage 3 - Second emplacement

During ocean closure the serpentinites would be subducted and subjected to increased stress. Owing to the weakness of serpentine minerals under stress and the density contrast between them and ocean-floor basalt, the serpentinites would tend to "migrate into the lower stress

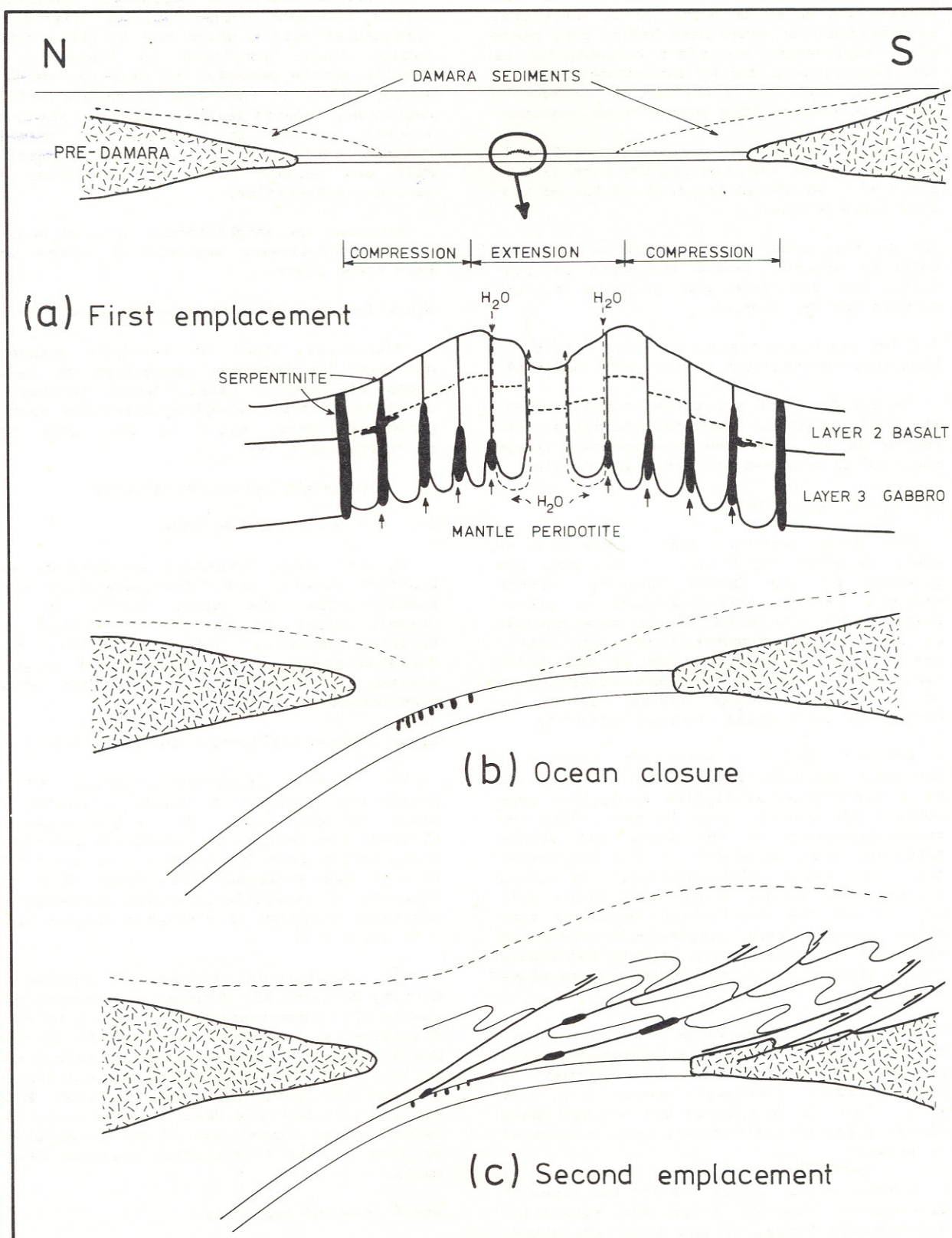


Fig. 6.2 — Model for emplacement of serpentinites.

environment of the overlying trench sediments. Vetter and Meissner (1977) show that stress rises in the subduction zone by a factor greater than ten relative to the surrounding rocks.

Two deformational events are thought to have occurred in the Damara Trough during the final stages of ocean-floor closure, while thrusting took place along the southern margin of the Khomas Trough. The deformation may have provided the impetus for emplacement of serpentinites into the overlying Damara sediments and on to the pre-Damara inlier (Fig. 6.2c) along planes parallel to the present dS_2 planes.

As the bodies were emplaced, the serpentine at the margins would come into contact with quartz-bearing rocks and the reaction:



could proceed. During emplacement, the lizardite may have recrystallised partially to antigorite since this is the stable serpentine mineral at higher pressures and temperatures (Evans *et al.* 1976). The lizardite would then recrystallise to produce largely non-pseudomorphic textures with only a few pseudomorphs remaining.

Stage 4 - Metamorphism

After emplacement and deformation the bodies were subjected to amphibolite-facies metamorphism as described in Section 4. If any serpentine remained as lizardite it would have recrystallised to antigorite under the ruling PT conditions.

During metamorphism relict clinopyroxene in the peridotite may have reacted with antigorite to form amphibole and carbonate-bearing rocks. The solutions containing Ca, Fe and Mg ions, produced by the clinopyroxene reaction, may have interacted with the country rock to form epidote and chlorite. The metamorphism is later than the deformation which produced dS_2 since the amphiboles are not orientated in this foliation.

Dewey (1977) states that as plates containing continents, island arcs, etc. are subducted, collisional strain occurs because they are not subducted smoothly on account of their buoyancy or topography. The result of the collisional strain is welding or suturing of the masses against the subduction zone with which they collide. Sutures therefore mark the zones along which oceanic lithosphere has been totally subducted. Martin and Porada (1977) point to the lack of a suture zone in the Damara Orogen as a major deficiency in the plate-tectonic model. This apparent absence may be understood when the full complexities of subduction are taken into account. As pointed out by Dewey there may be a great variety of high-strain zones associated with wide zones of basement reactivation. This makes it difficult, particularly at a deep structural level in eroded older orogenic systems, to recognise a line along which suturing

took place.

The simplest kind of suture is a high-strain zone containing disrupted ophiolite remnants and occasionally a blueschist melange. The zone should separate two areas with dissimilar pre-collisional strain histories. Porada and Wittig (1975) have identified ten zones of different structural history along the southern margin of the Damara, but only five are laterally continuous. Hartnady (in press) recognises four different laterally continuous structural zones in this area.

In the models of Dewey (1977) and Moores and McGregor (1972), suture-zone fragments of oceanic crust are thrust/abducted on to continental plates resulting in ophiolitic nappes. Ophiolites have been described by Moores and Vine (1971) and early European workers as a gross sequence passing from variably serpentinised dunite and peridotite through gabbros into pillow lavas capped by sediments.

There is no suggestion that the serpentinites in central South West Africa represent an ophiolite suite, as serpentinites alone are present. However, as has been shown, serpentinites may move more readily than the other ocean-floor material and become detached from the rest of the suite. The apparent lack of a complete ophiolite suite could be related to the spreading rate of the oceanic ridge. Barrett and Spooner (1977) suggest that ophiolites that form at smooth, non-rifted, fast-spreading ridges will be less intensively fractured than those that form at rifted slow-moving ridges. The greater cohesion and lateral continuity of a smooth, ridge-generated crust during later tectonic emplacement results in preferential preservation of this type as opposed to the rifted ridge-type crust. Only occasionally would rifted ophiolite suites be emplaced on the continent and then only as disconnected fragments.

The ultramafic bodies usually lie close to the boundary between Hartnady's zones II and III which are the Red Band in the west and Auas quartzite in the east.

Following on these lines of argument it is suggested that the ultramafics in central South West Africa mark the suture zone or zones in a plate-tectonic model of the Damara Mobile Belt. They meet two of the requirements outlined, namely they separate zones of different structural history and they possibly represent the dismembered ultramafic portions of an ophiolitic sequence. The absence of a blueschist melange may be due to its subsequent metamorphism or slow rate of uplift.

The approximate linear distribution of the ultramafic bodies also suggests that they may lie along a suture zone.

6.2.4 PRE-DAMARA MODEL

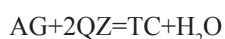
This model examines the possibility of the serpentinites having formed during the pre-Damara and being subsequently re-emplaced during Damara deformation.

It has been shown that the chemically depleted nature of the serpentinites and the low temperature of original serpentinitisation are best explained by a plate-tectonic model. Therefore, evidence of a set of events similar to those outlined, namely hydration of depleted mantle near a spreading ridge, emplacement of serpentinites into oceanic crust and subduction of sea floor resulting in emplacement of serpentinites along a pre-Damara suture zone, warrants examination.

In both plate-tectonic and aulacogen models for the Damara, the initial stages involve rifting of the pre-Damara crust. In the aulacogen model the serpentinites remain passive from the graben to the compressional phase. During the compressional phase the serpentinites might be emplaced along planes parallel to dS_2 .

In the plate-tectonic model the serpentinites remain passive in the southern continental block until this is subducted during closure of the Damara ocean. Then the serpentinites move, for reasons given in Section 6.2.3, and are re-emplaced along planes parallel to dS_2 .

As is explained in Sections 3 and 4 the earliest fabric contained by the talc and chlorite schists is of Damara age and can therefore not represent a pre-Damara deformational event. It is noted that pre-Damara country rocks adjacent to serpentinites do contain pre-Damara fabrics. The talc is believed to have formed by the reaction:



Consequently conditions during the pre-Damara cannot have exceeded curve (b) in Figure 4.2. The amphiboles developed after Damara deformation so conditions can also not have exceeded curve (c) in the figure. As both the plate-tectonic and aulacogen models invoke rifting prior to the Damara, the maintenance of PT conditions below curve (b) seems unlikely. During rifting, heat flow and hence the geothermal gradient rise as a result of heat transfer, first due to degassing and later due to movement of melts (Bailey 1974). Estimates of the geothermal gradient in rifted areas vary from 30°C/km (Holmes 1965) to 40°C/km (Von Henzer, quoted by Bailey 1974). Hence, the serpentinites

REFERENCES

- ARCULUS, R.J. and SMITH, D. 1977. Dense inclusions in the Sullivan Buttes Latite, Chino Valley, Yavapai country, Arizona. *In*: Extended Abstracts, 2nd Int. Kimberlite Conference, Bishop's Lodge, Santa Fe, New Mexico.
- ARCULUS, R.J., DUNCAN, M.A., LOFGREN, G.E. and RHODES, J.M. 1977. Iherzolite inclusions and megacrysts from the Geronimo Volcanic Field, San Bernardino Valley, southeastern Arizona. *In*: Extended Abstracts, 2nd Int. Kimberlite Conference, Bishop's Lodge, Santa Fe, New Mexico.
- ARNDT, N.T. 1977. Thick, layered peridotite-gabbro lava flows in Munro Township, Ontario. *Can. J. Earth Sci.*, 14, p. 2 620-2 637.
- ASISH, R.B. and MURTHY, V.R. 1977. Trace elements and Sr-isotopic geochemistry of the constituent minerals in ultramafic xenoliths from San Quentin, Baja California. *In*: Extended Abstracts, 2nd Int. Kimberlite Conference, Bishop's Lodge, Santa Fe, New Mexico.
- While the possibility exists that the serpentinites were present in the pre-Damara basement and were then re-emplaced during the Damara deformation in a plate-tectonic or aulacogen model, this sequence of events requires the following remarkable number of coincidences:
- An ocean formed exactly in the same place as the proposed Damara ocean.
 - Continental collision took place north of the later Damara-Rietfontein rift (Fig. 6.1).
 - The serpentinites escaped any obvious pre-Damara metamorphism or deformation.
 - The pre-Damara subducting plate dipped northwards.
- If the plate had dipped southwards the serpentinites in the pre-Damara would have been tectonically emplaced along southward-dipping thrust planes. Then had these been subducted during the Damara the likelihood of southward-dipping serpentinites being intersected and brought up along northward-dipping thrusts seems remote. What little evidence there is for a pre-Damara plate-tectonic model, namely the calc-alkali volcanism and the Gamsberg Granite (Watters 1974), suggests that the plate would have subducted southwards.

6.3 SUMMARY

With reference to the three major points under consideration, it is concluded that the serpentinites as well as the talc schists, chlorite schists and the amphibole- or carbonate-bearing serpentinites were derived from harzburgite containing lenses of spinel harzburgite and Iherzolite; that serpentinites from all four types of field occurrences were derived from Alpine material which was depleted to varying degrees and that the serpentinites were emplaced during Damara deformation. Furthermore their chemically depleted nature and the low temperature of original serpentinitisation favour a plate-tectonic model for the Damara Mobile Belt.

- AUMENTO, F. 1970. Serpentine mineralogy of ultrabasic intrusions in Canada and on the Mid-Atlantic Ridge. *Pap. geol. Surv. Can.*, 69-53, 51 p.
- AVÉ LALLEMANT, H.G. 1969. Structural and petrofabric analysis of an 'alpine-type' peridotite: the Iherzolite of the French Pyrenees. *Leid. geol. Meded.*, 42, p. 1-57.
- BAILEY, D.K. 1974. Origin of alkaline magmas as a result of anatexis. *In*: Soronsen, H., Ed., *The alkaline rocks*, Wiley, London, p. 436-442.
- BARNES, I. and O'NEIL, I. 1969. The relationship between fluids in some fresh Alpine-type ultramafics and possible modern serpentinization, Western United States. *Bull. geol. Soc. Am.*, 80, p. 1 947-1 960.
- BARNES, S.J. 1977. Serpentinities in central South West Africa. *Rep. geol. Surv. S. Afr.*, Windhoek (unpubl.).
- BARRETT, T.J. and SPOONER, E.T.C. 1977. Ophiolitic breccias associated with allochthonous oceanic crustal rocks in the eastern Ligurian Apennines, Italy - a comparison with observations from rifted oceanic ridges. *Earth Planet. Sci. Lett.*, 35, p. 79-91.
- BECCALUVA, L., OHNENSTETTER, D., OHNENSTETTER, M. and VENTURELLI, G. 1977. The trace element geochemistry of Corsican ophiolites. *Contrib. Mineral. Petrol.*, 64, p. 11-31.
- BICKLE, M.J. and COWARD, M.P. 1977. A major thrust in the southern Damaran belt, Namibia. *A. Rep. res. Inst. Afr. geol.*, Univ. Leeds, 20, p. 8-13.
- BENCE, A.E. and ALBEE, A.L. 1968. Empirical correction factors for the electron microanalysis of silicates and oxides. *J. Geol.*, 76, p. 382-403.
- BINNS, R.A., GROVES, D.I. and GUNTHORPE, R.J. 1975. Nickel sulphides in Archaean ultramafic rocks of western Australia. *In*: *Correlation of the Precambrian*, Int. geol. Congress Symposium, Moscow.
- BLAINE, J.L. 1977. Tectonic evolution of the Waldau Ridge Structure and the Okahandja Lineament in part of the central Damara Orogen, west of Okahandja, South West Africa. *Bull. Precambrian Res. Unit, Univ. Cape Town*, 21, 99 p.
- BLOOMER, A.G. and NIXON, P.H. 1973. The geology of Letseng-la-terae kimberlite pipes. *In*: *Lesotho Kimberlites*, Lesotho Natn. Dev. Corp., Maseru, p. 20-36.
- BONATTI, E. 1976. Serpentinite protrusions in the oceanic crust: *Earth Planet. Sci. Lett.*, 32, p. 107-113.
- BONATTI, E., HORNNOREZ, J. and FERRARA, G. 1971. Peridotite-gabbro-basalt complex from the equatorial Mid-Atlantic Ridge. *Phil. Trans. R. Soc., Ser. A*, 268, p. 385-402.
- BOWES, D.R., SKINNER, W.R. and WRIGHT, A.E. 1969. petrochemical comparison of the Bushveld Igneous Complex with some other mafic complexes: *In*: Visser, D.J.L. and Von Gruenewaldt, G., Eds, *Symposium on the Bushveld Igneous Complex and other layered intrusions*, Spec. publ. geol. Soc. S. Afr., 1, p. 425-440.
- BRICKER, O.P., NESBITT, H.W. and GUNTER, W.D. 1973. The stability of talc. *Am. Miner.*, 58, p. 64-72.
- BURK, C.A. 1964. A study of serpentinite. *Publ. Natn. Res. Corom., Natn. Acad. Sci., U.S.A.*, 1 188.
- CANN, J.A. 1971. Petrology of basement rocks from Palmer Ridge, NE Atlantic. *Phil. Trans. R. Soc., Ser. A*, 268, p. 605-617.
- CHEKUNOV, A.V. 1967. Mechanism responsible for structures of the aulacogen type (taking the Dnieper-Donets basin as an example). *Geotectonics*, No. 3, p. 137-144.
- CHIDESTER, A.H. 1962. Petrology and geochemistry of selected talc-bearing ultramafic rocks and adjacent country rocks in north-central Vermont. *Prof. Pap. U.S. geol. Surv.*, 345, 207 p.
- CLIFFORD, T.N. 1967. The Damaran episode in the upper Proterozoic-lower Paleozoic structural history of Southern Africa. *Spec. Pap. geol. Soc. Am.*, 92, 100 p.
- COLEMAN, R.G. 1966. New Zealand serpentinites and associated metasomatic rocks. *Bull. N.Z. geol. Surv.*, 76.
- _____ 1967. Low-temperature reaction zones and Alpine ultramafic rocks of California, Oregon and Washington. *Bull. U.S. geol. Surv.*, 1 247, 49 p.
- _____ 1971. Petrologic and geophysical nature of serpentinites. *Bull. geol. Soc. Am.*, 82, p. 897-918.
- _____ 1971a. Plate tectonic emplacement of upper mantle peridotites along continental edges. *J. geophys. Res.*, 76, p. 1 212-1 222.
- COLEMAN, R.G. and KEITH, T.E. 1971. A chemical study of serpentinization-Burro Mountain, California. *J. Petrology*, 12, p. 311-328.
- DAVIES, J.C. 1973. *Statistics and data analysis in geology*. Wiley, New York.
- DEER, W.A., HOWIE, R.A. and ZUSSMANN, J. 1974. *An introduction to the rock-forming minerals*. Longmans, London

- DE VILLIERS, J.S. 1969. The structure and petrology of the mafic rocks of the Bushveld Complex south of Potgietersrus: *In*: Visser, D.J.L. and Von Gruenewaldt, G., Eds, Symposium of the Bushveld Igneous Complex and other layered intrusions, Spec. Publ. geol. Soc. S. Afr., 1, p. 23-35.
- DE WAAL, S.A. 1971. South African nickeliferous. Serpentinities. *Miner. Sci. Engng*, 3(2), p. 32-45.
- DEWEY, J.F. 1977. Suture zone complexities: a review. *Tectonophysics*, 40, p. 53-67.
- DEWEY, J.F. and BIRD, J.M. 1971. Origin and emplacement of the ophiolite suite: Appalachian ophiolites in Newfoundland. *J. geophys. Res.*, 76, p. 3 179-3 206.
- DE WIT, M.J., DUTCH, S., KLIGFIELD, R., RICHARDSON, A. and STERN, C. 1977. Deformation, serpentinization and emplacement of a dunitic complex, Gibbs Island, South Shetland Islands: possible fracture zone tectonics. *J. Geol.*, 85, p. 745-762.
- DIXON, W.J. 1975. Biomedical computer programs: Univ. California Press, Berkeley.
- DOLENKO, G.N. 1970. Paleozoic stage of the Dnieper-Donets trough. *Geotectonics*, No. 1, p. 27-30.
- ENGEL, C.G. and FISHER, R.L. 1969. Iherzolite, anorthosite, gabbro, and basalt, dredged from the mid-Indian ridge. *Science*, 166, p. 1 136-1 141.
- EVANS, B.W. and TROMMSDORFF, V. 1970. Regional metamorphism of ultramafic rocks in the Central Alps: parageneses in the system CaO-MgO-SiO₂-H₂O. *Schweiz. miner. petrogr. Mitt.*, 50, p. 481-492.
- EVANS, B.W., JOHANNES, W., OTERDOOM, H. and TROMMSDORFF, V. 1976. Stability of chrysotile and antigorite in the serpentinite multisystem. *Schweiz. miner. petrogr. Mitt.*, 56, p. 79-93.
- FERRY, J.M. and SPEAR, F.S. 1977. Experimental calibration of the partitioning of Fe and Mg between biotite and garnet. *Yb. Carnegie Instn, Washington*, 76, p. 579-581.
- FESQ, H.W., KABLE, E.J.D. and GURNEY, J.J. 1976. The geochemistry of some selected South African kimberlites and associated heavy minerals. *Rep. Natn. Inst. Metall., Johannesburg*, 1 703, 33 p.
- FINDLAY, D.C. 1969. Origin of the Tulameen ultramafic-gabbro complex, southern British Columbia. *Can. J. Earth Sci.*, 6, p. 399-426.
- FLEUTY, M.J. 1964. The description of folds. *Proc. Geol. Ass.*, 75, p. 461-492.
- FOMIN, A.B. and KOZAK, S.A. 1971. Distribution of Cr, Co, and Ni in ultramafic rocks of the middle. Bug region. *Geochem. Int.*, 8, p. 878-884.
- GOGINENI, S.V., MELTON, C.E. and GIARDINI, A.A. 1978. Some petrological aspects of the prairie Creek diamond-bearing kimberlite diatreme, Arkansas. *Contrib. Mineral. Petrol.*, 66, p. 251-261.
- GOLDING, H.G. 1971. Local and regional trends of serpentinisation and metaserpentinisation in the Coolac-Goobarragandra ultramafic mass, New South Wales. *Spec. Publ. geol. Soc. Aust.*, 3, p. 321-329.
- GORMAN, B.E., PEARCE, T.N. and BIRKETT, T.C. 1978. On the structure of Archaean greenstone belts. *Precambrian Res.*, 6, p. 23-41.
- GREEN, D.H. 1964. The petrogenesis of the high temperature peridotite intrusion in the Lizard area, Cornwall. *J. Petrology*, 5, p. 134-189.
- GULLACAR, O. F. and DELALOYE, M. 1976. Geochemistry of nickel, cobalt and copper in alpine-type ultramafic rocks. *Chem. Geol.*, 17, p. 269-280.
- GURNEY, J.J., JACOB, W.R. and DAWSON, J.B. 1977. Megacrysts from the Monastery Mines. *In*: Extended Abstracts, 2nd Int. Kimberlite Conference, Bishop's Lodge, Santa Fe, Mexico.
- GURNEY, J.J., LAWLESS, P.J. and DAWSON, J.B. 1977a. peridotites and garnet olivine websterites at Bultfontein mine. *In*: Extended Abstracts, 2nd Int. Kimberlite Conference, Bishop's Lodge, Santa Fe, New Mexico.
- HÄLBICH, I.W. 1970. The geology of the western Windhoek and Rehoboth districts. Ph.D. thesis, Univ. Stellenbosch (unpubl.).
- HAM, W.E. and WILSON, J. L. 1967. Paleozoic epeirogeny and orogeny in the central United States. *Am. J. Sci.*, 265, p. 332-407.
- HANCOCK, W., RAMSDEN, D.R., TAYLOR, G.F. and WILMSHURST, J.R. 1971. Some ultramafic rocks of the Spargoville area, Western Australia. *Spec. publ. geol. Soc. Aust.*, 3, p. 269-280.
- HARKER, A. 1970. *Metamorphism*. Methuen, London.
- HARTNADY, C. in press. The structural geology of the Naukluft Nappe Complex, S.W.A. and its relationship to the Damara orogenic belt. *Bull. Precambrian Res. Unit, Univ. Cape Town*, 25.
- HATTON, C. and GURNEY, J.J. 1977. Igneous fractionation trends in Roberts Victor eclogites. *In*: Extended Abstracts, 2nd Int. Kimberlite Conference, Bishop's Lodge, Santa Fe, New Mexico.

- HEMLEY, J.J., MONTOYA, J.W., SHAW, D.R. and LUCE, R.W. 1977. Mineral equilibria in the MgO-SiO₂-H₂O system: II Talc-antigorite-forsterite-anthophyllite-enstatite stability relations and some geological implications in the system. *Am. J. Sci.*, 277, p. 353-383.
- HIMMELBERG, G.R. and COLEMAN, R.G. 1968. Chemistry of primary minerals and rocks from Red Mountain-Del Puerto ultramafic mass, California. *Prof. Pap. U.S. geol. Surv.*, 600C, p. C18-C26.
- HOFFER, E. 1978. On the "late" formation of paragonite and its breakdown in pelitic rocks of the southern Damara Orogen (Namibia). *Contrib. Mineral. Petrol.*, 67, p. 209-219.
- HOFFER, E. and PUHAN, D. 1975. Isoreaktionsgrade in den Metapeliten des Damara Orogens. *Bericht des Sonderforschungsbereiches, Univ. Gottingen*, 48, p. 111-151.
- HOFFMAN, P. 1974. Aulacogens and their generic relation to geosynclines, with a Proterozoic example from the Great Slave Lake, Canada. *In: Dott, H.R. and Shaver, Ed., Modern and ancient geosynclinal sedimentation, Spec. Publ. Soc. Econ. Paleont. Miner.*, 19.
- HOLMES, A. 1965. Principles of physical geology. Nelson, London.
- HOSCHEK, G. 1969. The stability of staurolite and chloritoid and their significance in the metamorphism of pelitic rocks. *Contrib. Mineral. Petrol.*, 22, p. 208-232.
- IISHI, K. and SAITO, M. 1973. Synthesis of antigorite. *Am. Miner.*, 58, p. 915-919.
- IRVINE, T.N. 1974. Petrology of the Duke Island ultramafic complex, southeastern Alaska. *Mem. geol. Soc. Am.*, 138.
- IRVING, A.J. 1977. Mantle pyroxenitic "liquids" and cumulates: geochemistry of complex xenoliths from San Carlos, Kilbournes Hole and eastern Australia. *In: Extended Abstracts, 2nd Int. Kimberlite Conference, Bishop's Lodge, Santa Fe, New Mexico.*
- JAHNS, R.H. 1967. Serpentinities of the Roxbury district, Vermont. *In: Wyllie, P.J., Ed., Ultramafic and related rocks, Wiley, New York*, p. 137-160.
- JOHANNES, W. 1969. An experimental investigation of the system MgO-SiO₂-H₂O-CO₂. *Am. J. Sci.*, 267, p. 1083-1104.
- KASCH, K.W. 1978. Recognition of a major shear zone in the southern Damara belt, SWA/Namibia. *Trans. geol. Soc. S. Afr.*, 81, p. 205-209.
- KLEMM, D.D. and LAMMERER, B., 1974. A basic-to-ultramafic layered extrusion in east Elba. *Chem. Geol.*, 13, p. 23-38.
- KOGARKO, L.N. 1973. The Ni/Co ratio as an indicator of the mantle origin of magmas. *Geochem. Int.*, 10, p. 1 081-1 086.
- KORNPROBST, J. 1969. Le massif ultrabasique des Beni Bouchera (Rif Interne, Maroc): Etude des péridotites de haute température, et haute pression des pyroxénolite a grenat ou sans grenat qui leur sont associées. *Contrib. Mineral., Petrol.*, 23, p. 283-322.
- LAWLESS, P.J., GURNEY, J.J. and DAWSON, J.B. 1977. Polymictic peridotites from the Bultfontein and De Beers Mines, Kimberley, South Africa. *In: Extended Abstracts, 2nd Int. Kimberlite Conference, Bishop's Lodge, Santa Fe, New Mexico.*
- LEBEDINSKIY, V.I. 1967. Magmatic formations in the graben-shaped Pripjat-DnieperDonets downwarp. *Dokl. Acad. Sci. U.S.S.R., Earth Sci., Sect. V*, 174, p. 52-59.
- LEVEY, B.D. and HERMES, O.D. 1977. Mantle xenoliths from southeastern New England. *In: Extended Abstracts, 2nd Int. Kimberlite Conference, Bishop's Lodge, Santa Fe, New Mexico.*
- LEWIS, R. and MEYER, H. 1977. Diamond-bearing kimberlite of prairie Creek, Murfreesboro, Arkansas. *In: Extended Abstracts, 2nd Int. Kimberlite Conference, Bishop's Lodge, Santa Fe, New Mexico.*
- LIEBENBERG, C.J. 1960. Trace elements of the rocks of the Bushveld Igneous Complex. *Publ. Univ. Pretoria, NNRS* 12 and 13.
- LONEY, R. A., HIMMELBERG, G.R. and COLEMAN, R.G. 1971. Structure and petrology of the alpine-type peridotite at Burro Mountain, California, U.S.A.. *J. Petrology*, 12, p. 245-309.
- LOUBET, M., SHIMIZU, N. and ALLEGRE, C.J. 1975. Rare earth elements in Alpine peridotites. *Contrib. Mineral. Petrol.*, 53, p. 1-12.
- LYASHKEVICH, Z.M. 1974. Volcanic rocks of the Dnieper-Donets basin, the formations of an old rift zone. *Dokl. Acad. Sci. U.S.S.R., Earth Sci., Sect. V*, 214, p. 99-102.
- MACLEAN, W.H. and SIMAZAKI, H. 1976. The partition of Co, Ni, Cu and Zn between sulfide and silicate liquids. *Econ. Geol.*, 71, p. 1 049-1 057.
- MCCALL, G.J.H. and LEISHMAN, J. 1971. Clues to the origin of Archaean eugeosynclinal peridotites and the nature of serpentinisation. *Spec. publ. geol. Soc. Aust.*, 3, p. 281-299.
- MARTIN, H. 1965. The Precambrian geology of South West Africa and Namaqualand. *Precambrian Res. Unit, Univ. Cape Town*, 159 p.

- MARTIN, H. and PORADA, H. 1977. The intracratonic branch of the Damara Orogen in S.W.A. *Precambrian Res.*, 5, p. 311-357.
- MEANS, W.D. 1976. *Stress and strain*. Springer-Verlag, New York.
- MELSON, W.G. and THOMPSON, G. 1971. Petrology of a transform fault zone. *Phil. Trans. R. Soc., Ser. A*, 268, p. 423-441.
- MELSON, W.G., HART, S.R. and THOMPSON, G. 1972. St Paul's Rocks, equatorial Atlantic; petrogenesis, radiometric ages and implications on sea-floor spreading. *Mem. geol. Soc. Am.*, 132, p. 241-272.
- MENZIES, M. 1975. Rifting of a Tethyan continent-rare earth evidence of an accreting plate margin. *Earth Planet. Sci. Lett.*, 28, p. 427-438.
- _____ 1976. Rare earth geochemistry of fused ophiolitic and alpine Iherzolites, I Othris, Lanzo and Troodos. *Geochim. Cosmochim. Acta*, 40, p. 645-656.
- MENZIES, M., BLANCHARD, D., BRANNON, J. and KOROTEV, R. 1977. Rare earth geochemistry of fused ophiolitic and alpine Iherzolites II, Beni Bouchera, Ronda and Lanzo. *Contrib. Mineral. Petrol.*, 64, p. 53-74.
- MERRILL, R.B., BICKFORD, M.E. and IRVING, A.J. 1977. The Hills Pond peridotite, Woodson Country Karoo, a richterite-bearing Cretaceous intrusive with kimberlitic affinities: *In*: Extended Abstracts, 2nd Int. Kimberlite Conference, Bishop's Lodge, Santa Fe, New Mexico.
- MIYASHIRO, A. 1973. *Metamorphism and metamorphic belts*. Allen and Unwin, London, 492 p.
- MIZAR, Z. 1973. Precambrian ultramafic rocks south of Sermilik Frederickshab District, S.W. Greenland. *Meddr Gronland*, 196, Gronland Geolosiske Unders., 107.
- MONTIGNY, R. 1973. Trace element geochemistry and genesis of the Pindos ophiolite suite. *Geochim. Cosmochim. Acta*, 37, p. 2 135-2 141.
- MOODY, J.B. 1976. Serpentinization: a review. *Lithos*, 9, p. 125-138.
- MOORES, E.M. 1969. Petrology and structure of the Vourinos Ophiolite Complex of northern Greece. *Spec. Pap. geol. Soc. Am.*, 118, 74 p.
- _____ 1973. Geotectonic significance of ultramafic rocks. *Earth Sci. Rev.*, 9, p. 241-258.
- MOORES, E.M. and MACGREGOR, I.D. 1972. Types of alpine ultramafic rocks and their implications for fossil plate interactions. *Mem. geol. Soc. Am.*, 132, p. 209-223.
- MOORES, E.M. and VINE, J.F. 1971. The Troodos Massif, Cyprus, and other ophiolites as oceanic crust. *Phil. Trans. R. Soc., Ser. A*, 268, p. 385-405.
- NALDRETT, A.J. 1973. Nickel sulphide deposits-their classification and genesis, with special emphasis on deposits of volcanic association. *Trans. Can. Inst. Min. Metall.*, 76, p. 183-201.
- NESBITT, H.W. and BRICKER, O.P. 1978. Low temperature alteration processes affecting ultramafic bodies. *Geochim. Cosmochim. Acta*, 42, p. 403-409.
- NESBITT, R. W. and SUN, SHEN-SU 1976. Geochemistry of Archaean spinifex-textured peridotites and magnesian and low-magnesian tholeiites. *Earth Planet. Sci. Lett.*, 31, p. 433-453.
- NESBITT, E.G., BICKLE, M.J. and MARTIN, A. 1977. The mafic and ultramafic lavas of the Belingwe greenstone belt, Rhodesia. *J. Petrology*, 18, p. 521-566.
- NIXON, P.H. 1973. Lesotho Kimberlites. *Lesotho Natn. Dev. Corp., Maseru*.
- NORRISH, K. and HUTTON, J.T. 1969. An accurate X-ray spectrographic method for the analysis of a wide range of geological samples. *Geochim. Cosmochim. Acta*, 33, p. 431-453.
- NWACHUKWU, S.D. 1972. The tectonic evolution of the southern portion of the Benue Trough, Nigeria. *Geol. Mag.*, 109, p. 411-419.
- O'HARA, M.J., SAUNDERS, M.J. and MERCY, E.L.P. 1975. Garnet-peridotite, primary ultrabasic magma and eclogite: interpretation of the upper mantle processes in kimberlite. *In*: *Physics and Chemistry of the Earth*, Ahrens *et al.* Eds, Pergamon Press, Oxford, 9, p. 571-604.
- OLADE, M.A.D. and MORTON, R.D. 1972. Observations on the Proterozoic Seton Formation, East Arm of Great Slave Lake, North Western Territories. *Can. J. Earth Sci.*, 9, p. 1 110-1 123.
- PAGE, N.J. 1968. Chemical differences among the serpentine "polymorphs". *Am. Miner.*, 53, p. 201-215.
- _____ 1976. Serpentinization and alteration in an olivine cumulate from the Stillwater complex, southwestern Montana. *Contrib. Mineral. Petrol.*, 54, p. 127-137.
- PAMIĆ, J. and MAJER, V. 1977. Ultramafic rocks of the Dinaride central ophiolite zone in Yugoslavia. *J. Geol.*, 85, p. 553-569.
- PEARCE, J.A. 1977. Statistical analysis of major element patterns in basalts. *J. Petrology*, 17, p. 15-43.

- PEARCE, J.A. and CANN, J.R. 1973. Tectonic setting of basic volcanic rocks determined-using trace element analyses. *Earth Planet. Sci. Lett.*, 19, p. 290-300.
- PINUS, G.V. 1965. Some problems of geochemistry of Cambrian alpine-type ultrabasites in the southern part of Siberia. *Geochem. Int.*, 2, p. 1 057-1 065.
- PORADA, H. and WITTIG, R. 1975. Zur Tektonik des slidlichen Damarabelts. Bericht des Sonderforschungsbereiches, Univ. Göttingen, 48, p. 51-70.
- PRESS, F. and SIEVER, R. 1974. *Earth*. Freeman, San Francisco.
- RALEIGH, C.B. and PATERSON, M.S. 1965. Experimental deformation of serpentinite and its tectonic implications. *J. geophys. Res.*, 70, p. 3 965-3 985.
- RAWLINSON, P. and DAWSON, J.B. 1977. A quench orthopyroxene-ilmenite xenolith from kimberlite-evidence for Ti-rich liquid in the upper mantle. *In: Extended Abstracts, 2nd Int. Kimberlite Conference, Bishop's Lodge, Santa Fe, New Mexico.*
- RHODES, J.M. and DAWSON, J.B. 1975. Major and trace element chemistry of peridotite inclusions from the Lashaine volcano, Tanzania. *In: Physics and Chemistry of the Earth, Ahrens et al. Eds, Pergamon Press, Oxford, 9, p. 545-557.*
- RICHARDSON, S.W., GILBERT, M.C. and BELL, P.M. 1969. Experimental determination of kyanite, andalusite and andalusite-sillimanite equilibrium the aluminium-silicate triple point. *Am. J. Sci.*, 267, p. 259-272 .
- RINGWOOD, A.E. 1977. Composition and origin of the earth. *Publ. Res. School Earth Sci., Aust. Natn. Univ., Canberra, 1 299.*
- ROD, E. 1974. Geology of eastern Papua: Discussion. *Bull. geol. Soc. Am.*, 85, p. 653-658.
- ROSS, E.S., FOSTER, M.D. and MYERS, A.T. 1954. Origin of dunites and of olivine-rich inclusions in basaltic rocks. *Am. Miner.*, 39, p. 693-737.
- SAGGERSON, E.P. and LOGAN, C.I. 1969. Distribution controls of layered and differentiated mafic intrusions in the Lebombo volcanic subprovince. *In: Visser, D.J.L. and Von Gruenewaldt, A., Eds, Symposium on the Bushveld Igneous Complex and other layered intrusions, Spec. publ. geol. Soc. S. Afr.*, 1, p. 721-733.
- SAWYER, E.W. 1978. Structure and metamorphic geology of the Damara in an area southeast of Walvis Bay. M.Sc. thesis, Univ. Cape Town (unpubl.).
- SHIMIZU, N. and ALLEGRE, C. J. 1977. Geochemistry of transition elements in garnet lherzolite nodules in kimberlites. *In: Extended Abstracts, 2nd Int. Kimberlite Conference, Bishop's Lodge, Santa Fe, New Mexico.*
- SOBOLEV, N.D. 1977. Deep-seated inclusions in kimberlites and the problem of the composition of the mantle. Edward Brothers.
- SPRY, A. 1969. *Metamorphic textures*. Pergamon, Oxford.
- STAUDIGEL, H. and SCHREYER, W. 1977. The upper thermal stability of clinocllore $Mg_5Al(AlSi_3O_{10})(OH)_8$ at 10-35 kb P_{H_2O} . *Contrib. Mineral. Petrol.*, 61, p. 187-198.
- TILL, R. 1974. *Statistical methods for the earth scientist*. MacMillan, London, 154 p.
- TRACY, R.J. and ROBINSON, P. 1977. Petrology of ultramafic xenolith suite from Tahiti and reactions with enclosing basalt. *In: Extended Abstracts, 2nd Int. Kimberlite Conference, Bishop's Lodge, Santa Fe, New Mexico.*
- TROMMSDORFF, V. and EVANS, B.W. 1974. Alpine metamorphism of peridotitic rocks. *Schweiz. miner. petrogr. Mitt.*, 54, p. 333-352.
- _____ 1977. Antigorite-ophicarbonates: phase relations in a portion of the system $CaO-MgO-SiO_2-H_2O-CO_2$. *Contrib. Mineral. Petrol.*, 60, p. 39-56.
- _____ 1977a. Antigorite-ophicarbonates: contact metamorphism in Valmalenco, Italy. *Contrib. Mineral. Petrol.*, 62, p. 301-312.
- TURNER, F.J. and WEISS, L.E. 1963. *Structural analysis of metamorphic tectonites*. McGraw-Hill, New York, 545 p.
- VAN DER KAADEN, G. 1969. Ghromite-bearing ultramafic and related gabbroic rocks and their relation to ophiolitic extrusive basic rocks and diabases in Turkey. *In: Visser, D.J.L. and Von Gruenewaldt, G., Eds, Symposium on the Bushveld Igneous Complex and other layered intrusions, Spec. publ. geol. Soc. S. Afr.*, 1, p. 551-531.
- VETTER, U.R. and MEISSNER, R.O. 1977. Creep in geodynamic processes. *Tectonophysics*, 42, p. 37-54.
- VILJOEN, R.P. and VILJOEN, M.J. 1969. The effects of metamorphism and serpentinization on the Barberton Region. *In: Upper Mantle Project, Spec. Publ., geol. Soc. S. Afr.*, 2, p. 29-53.
- VILLAUME, J.F. and ROSE, A.W. 1977. The geochemistry of some Archaean ultramafic lavas. *Chem. Geol.*, 19, p. 43-60.

- WAGER, L.R. and BROWN, G.M. 1967. Layered igneous rocks: Oliver and Boyd, Edinburgh.
- WASS, S.Y. 1977. Evidence for fractional crystallization in the mantle of late stage kimberlitic liquids. *In*: Extended Abstracts, 2nd Int. Kimberlite Conference, Bishop's Lodge, Santa Fe, New Mexico.
- WATTERS, B.R.L. 1974. Stratigraphy, igneous petrology and evolution of the Sinclair Group in southern South West Africa. *Bull. Precambrian Res. Unit, Univ. Cape Town*, 16, 235 p.
- WEDEPOHL, K.H. (Ed) 1970. *Handbook of geochemistry*. 11-1 to 11-4, Springer, Berlin.
- WENNER, D.B. and TAYLOR, Jr., H.P. 1971. Temperatures of serpentinization of ultramafic rocks based on O18/O16 fractionation between coexisting serpentine and magnetite. *Contrib. Mineral. Petrol.*, 32, p. 165-185.
- WICKS, F.J. and WHITTAKER, E.J.W. 1977. Serpentinite textures and serpentinization. *Can. Mineralogist*, 15, p. 459.
- WICKS, F.J., WHITTAKER, E.J.W. and ZUSSMAN, J. 1977. An idealized model for serpentine textures after olivine. *Can. Mineralogist*, 15, p. 445-458.
- WILKINSON, J.F.G. and BINNS, R.A. 1977. Relatively iron-rich Iherzolite xenoliths of the Cr-diopside suite: a guide to the primary nature of anorogenic tholeiitic andesite magmas. *Contrib. Miner. Petrol.*, 65, p. 199-212.
- WILLIAMS, D.A.C. 1971. Determination of primary mineralogy and textures in ultramafic rocks from Mt Monger, Western Australia. *Spec. Publ. geol. Soc. Aust.*, 3, p. 259-268.
- WILLIS, J.P., FORTUIN, H.H.G. and EAGLE, G.A. 1971. A preliminary report on the geochemistry of recent sediments in Saldanha Bay and Langebaan lagoon. *Trans. R. Soc. S. Afr.*, 42, p. 497-509.
- WINKLER, H.G.F. 1974. *Petrogenesis of metamorphic rocks*. 3rd Edn, Springer, New York, 320 p.
- WORST, B.G. 1960. Geology of the Great Dyke, Southern Rhodesia. *Bull. geol. Surv. Sth. Rhod.*, 47, 234 p.
- WRIGHT, J.B. 1968. South Atlantic continental drift and the Benue Trough. *Tectonophysics*, 6, p. 301-310.
- YEFIMOV, A.A. and IVANOVA, L.P. 1963. Behaviour of chromium, nickel and cobalt during the formation of the Kytlym platiniferous massif. *Geochem.*, 11, p. 1 076-1 085.

APPENDIX I - SUMMARY OF THE CHARACTERISTICS OF THE SERPENTINITE BODIES INVESTIGATED

Location					
Longitude (°E)	Latitude (°S)	Farm	Size of body (m)	Shape	Orien- tation of long axis
23°19'	15°45'	Schlesien 483	500 x 300	3 Lenses	040°
23°18'	15°57'	Schlesien 483	200 x 50	Lens	040°
22°24'	17°11'	Von Francois-Ost 60	2 200 x 100	7 Lenses	055°
22°47'	17°14'	Gocheganas 26	500 x 300	Lens	060°
22°50'	17°13'	Gocheganas 26	200 x 200	Round	NA
22°27'	17°20'	Neudamm 63	400 x 200	Lens	020°
22°44'	17°17'	Unkenfels 73	2 000 x 200	6 Lenses	040°
22°43,5'	17°18'	Unkenfels 73	300 x 50	2 Lenses	040°
22°42,5'	17°25,5'	Humanskuppe 75	40 x 30	2 Round bodies	020°
22°44,5'	17°25,5'	Brack 83	50 x 20		320°
22°45'	17°25,75'	Brack 83	200 x 100	Lens	090°
22°44,5'	17°26'	Brack 83 Waldburg 82	3 000 x 400	Lens	030°
22°44'	17°27'	Waldburg 82	300 x 100	Lens	010°
22°33'	17°27'	Detmont 78	50 x 40	Round	070°
22°52'	17°18'	Binsenheim 85	700 x 500	Round	010°
22°48'	17°22'	Binsenheim 85	200 x 50	Lens	020°
22°50'	17°23'	Binsenheim 85	2 000 x 1 200	Round	040°
22°49'	17°23'	Binsenheim 85	100 x 50	Lens	050°
22°46'	17°23'	Binsenheim 85	90 x 80	2 Round	030°
22°48'	17°23'	Binsenheim 85	100 x 50	Lens	040°
22°52'	17°25'	Rietfontein 85	50 x 20	Lens	040°
22°49'	17°26'	Elisenhöhe 88	3 500 x 500	5 Lenses	040°
22°48'	17°28'	Elisenhöhe 88	10 x 10	Round	NA
22°51'	17°38'	Coas 92	500 x 50	5 Lenses	090°
22°13'	17°42'	Otjihaenena 196	750 x 350	Lens	060°
22°07'	17°48'	Okahau 185	700 x 200	2 Lenses	070°
22°03'	17°54'	Omieve 79	3 000 x 2 000	Round	050°
22°08'	17°56'	Amerongen 181	3 000 x 1 500	Lens	030°
22°07'	17°59'	Otjiaha 130	750 x 500	Round	030°
22°06'	18°1'	Otjiaha 130 Kanonschoot 131	7 000 x 75	6 Lenses	030°
22°06'	18°06'	Osombahe North 127	50 x 50	Round	NA
22°07'	18°07'	Osombahe North 127	50 x 50	Round	NA
21°49'	17°57'	Otjere 164	200 x 100	Lens	090°
21°47'	17°48'	Otjere 164	100 x 100	Round	NA
21°44'	18°13'	Talana 199	500 x 400	Round	

FoS = Forsterite serpentinite
HobS= Hobnail serpentinite
TaS = Talcose serpentinite
Cas = Carbonate serpentinite

AcFel = Actinolite fels
TaSc = Talc schist
TaAmSc= Talc-amphibole schist
ChlSc = Chlorite-amphibole schist

Approximate percentage of ultramafic rocks present												Type of country rocks						Country rocks	
												Pre-Damara			Damara			Metasomatised?	
FoS	HobS	TaS	CaS	Ac Fel	Ta Sc	TaAm Sc	Chl Sc	ChAm	An	Hb	QF Sc	Gn	Amp	Mic Sc	QF Sc	Bi Sc	Amp	EpAmp	EpQF
	95				3		1		1						50	50		NOT	
					50	20	30									100		NOT	
					40	10	50									75	25	?	
			100											100				?	
					25	75								100				?	
					25		50	5		20						100		x	
		10			25		25	40			50	30	20					?	
		10			75			15						100				?	
						50		50						100				?	
					70		25				50			50				?	
					70		25				50			50				?	
	10	50			10		25			5	20	70	10					x	
					50		50				25	75						?	
				15		50		35				95	5					?	
	20	50			20	4	5			1	25	75						x	
					25	70				5		100							
10	50	10	5	1	10	1	7	3		3	20	40	10	30				x	x
		10			10	10	40	10		10	30	50	20					x	x
					10	50	40				100							?	
			25	25	25	25					100							?	
			30	20	20		25	5			100							?	
	20	38	20		10		10		1	1	20	29	1		50			?	x
					75		25				50				50			x	x
	10	10			40		40				50				50			x	
20	50	10	7		5				1	2					10	85	5	x	x
	10			50			40									100		?	
	74	5	1		9	1	10									100		?	
	68	5	5		10		10		1	1					90		10	x	
	30				35		35								100			?	
	30				35		35								100			?	
	10				45		45											?	
	10				45		45											?	
	80				10		10											?	
											100							?	
	80				10		10					100				100		?	

An = Ankerite/dolomite/siderite
Hb = Hornblendite
QFSc = Quartzo-feldspathic schist
Gn = Gneiss
Amp = Amphibolite

MicSc = Mica schist
BiSc = Biotite schist
EpAmp = Epidote amphibolite
EpQF = Epidotised quartzo-feldspathic rocks

APPENDIX II - PETROGRAPHIC DESCRIPTIONS

1. PRE-DAMARA COUNTRY ROCKS

1.1 GNEISS AND EPIDOTISED GNEISS

The descriptions are based on slides made from rocks taken on a traverse across the country rocks to the contact with the serpentinite at Gauchab. Numbers in brackets represent percentages of the component minerals.

GB 78-240 m from the contact the minerals are: plagioclase of composition An_{35} (40), quartz (30), K feldspar (20), biotite (5), muscovite (4) and spinel (1). The texture is granoblastic polygonal. The felsic minerals are equigranular.

GB 90-180 m from the contact a stronger fabric is developed in the gneiss. The minerals are: quartz (40), An_{30} (30), muscovite (10), microcline (10), biotite (7), magnetite (2) and zoisite (1). The texture is poorly lepidoblastic as outlined by biotite. The muscovite is intergrown with the biotite. The felsic material appears to be granoblastic.

GB 91-60 m from the contact, the gneiss is practically a schist, comprising perthite (25), quartz (20), muscovite (20), microcline (14), biotite (13), epidote (5) and magnetite (3). The texture is lepidoblastic, outlined by biotite, mineral layering and the long axes of feldspar porphyroblasts.

GB 93-10 m from the contact, chlorite and amphiboles have developed in the rock which consists of quartz (20), biotite (20), plagioclase (20), epidote (15), hornblende (10), garnet (8), chlorite (5), magnetite (1) and apatite (1). The texture is lepidoblastic as outlined by biotite, mineral layering and the long axes of the feldspar porphyroblasts. This rock type has been named epidotised gneiss.

1.2 AMPHIBOLITE, EPIDOTE AMPHIBOLITE AND CHLORITE AMPHIBOLITE

300 m from the contact, the country rock is an amphibolite composed of actinolite, oligoclase, quartz and chlorite. The fabric is poorly lepidoblastic and is outlined by the long axes of actinolite and by mineral layering.

10 m from the main body of serpentinite, amphibolite containing epidote is present. It consists of hornblende, actinolite, epidote, oligoclase and magnetite. The fabric is poorly lepidoblastic, outlined by alternating layers of amphibole and epidote plus oligoclase.

5 m from the contact between the chlorite schist of the ultramafic body and the country rock, epidote amphibolite consisting of hornblende, epidote, labradorite, sphene and chlorite is developed. The texture is poorly lepidoblastic and is outlined by mineral layering. Epidote makes up 40 per cent of the rock.

At the edge of the Gauchab and Elisenhöhe serpentinites, chlorite amphibolite is present. This rock type is believed to be an altered amphibolite.

1.3 MICA SCHIST, EPIDOTE-MICA SCHIST AND CHLORITE-MICA SCHIST

240 m from the contacts at Gauchab and Elisenhöhe, mica schist composed of biotite (30), andesine (25), muscovite (20), quartz (19), opaques (5) and apatite is developed. The texture is poorly lepidoblastic, outlined by mineral layering. The biotite forms 4-mm poikiloblasts enclosing quartz, plagioclase, apatite and opaque minerals. The biotite has straight grain boundaries with muscovite and opaques but with quartz and plagioclase the margins are cusped. Muscovite also forms 4-mm poikiloblasts and is usually closely associated with biotite. Opaques are present within the poikiloblasts. The muscovite has straight grain boundaries with the other minerals. The andesine is poikiloblastic, containing muscovite and biotite. The andesine, partly altered to sericite, has straight grain boundaries with all minerals. Closely associated with the andesine is xenoblastic quartz which may contain apatite.

50 m from the contact, epidote is developed and the rock contains biotite (30), quartz (20), muscovite (20), oligoclase (20), epidote (5) and opaques (5). The texture is strongly lepidoblastic.

At the contact, chlorite is developed in the mica schist which consists of chlorite (40), quartz (20), oligoclase (15), biotite (10), muscovite (5), epidote (5) and opaques (5).

2. DAMARA COUNTRY ROCKS

2.1 METACONGLOMERATE AND EPIDOTISED METACONGLOMERATE

The Nosib conglomerate on the farm Elisenhöhe appears to have been modified in the vicinity of the serpentinite. Some 100 m east of the body it has an arkosic matrix and contains subangular pebbles of gneiss, mica schist and minor amphibolite.

Thin sections reveal the matrix minerals to be quartz, orthoclase, microcline, perthite, muscovite, biotite and opaques. Lithic fragments may also be present. The texture is granoblastic. The quartz grains measure 0,15 mm and have straight boundaries. The orthoclase and microcline form xenoblastic grains 0,2 mm in size with lobate boundaries. Perthite forms xenoblastic grains 0,3 mm in size with lobate grain boundaries and contains numerous inclusions, with high relief, that are too small to identify. Biotite and muscovite laths are 0,07 mm long. Opaques occur scattered through the slide as xenoblastic grains with straight boundaries.

At 10 m from the contact, the conglomerate matrix is dark green and contains pebbles of epidotised gneiss, epidote amphibolite and chlorite-amphibole schist. The matrix is composed of actinolite, epidote, plagioclase, orthoclase, quartz, opaques and sphene.

The texture is nematoblastic and is outlined by actinolite needles 2 mm long in between remnants of pebbles. Actinolite also occurs in clusters, approximately 5 mm in size, in which the crystals have a different optical orientation to the needles in the matrix. Epidote forms small xenoblastic grains which occur as veins in the gneiss pebbles and throughout the chlorite-amphibole schist pebbles. Epidote forms lobate grain boundaries. Oligoclase forms 2-mm xenoblastic grains. The grain boundaries are sutured, suggesting recrystallisation. The twin lamellae are deformed and the oligoclase has undulose extinction. Exsolution of new untwinned plagioclase associated with epidote is apparent. Orthoclase occurs in pebble fragments of the gneiss and quartz occurs as small xenoblastic grains with epidote. Opaques and sphene are intergrown and are usually associated with actinolite. They form xenoblastic grains with lobate boundaries.

2.2 BIOTITE SCHIST, EPIDOTISED BIOTITE SCHIST AND CHLORITE-BIOTITE SCHIST

10 m from the serpentinite-country rock contact at Okahau, the biotite schist consists of quartz (28), biotite (20), muscovite (20), An₄₅ (10), orthoclase (10), garnet (5), kyanite (2), opaques (3), spinel (1) and staurolite (1).

The lepidoblastic texture is outlined by muscovite which is crenulated by S₃. Biotite grows mimetically as laths on dS₂ planes. Quartz and feldspar form a granoblastic polygonal texture except where quartz has formed porphyroblasts. The garnet is idioblastic and poikiloblastic and contains muscovite, quartz and feldspar. Kyanite forms laths in the muscovite. Opaques grow along dS₂ planes and are lath shaped. Spinel forms idioblastic grains throughout. Staurolite forms small subidioblastic grains intergrown with quartz and muscovite.

In slides from rock collected along the contact, the mineralogy and mineral relationships remain the same except that up to 5 per cent of epidote is present and chlorite replaces biotite. The epidote forms small round grains in association with plagioclase.

2.3 AMPHIBOLITE AND EPIDOTE AMPHIBOLITE

At Otjihaenena and Talana, amphibolite is present in the mica schist. The amphibolite 3 m from the contact consists of hornblende, plagioclase, opaques, garnet, chlorite and epidote. Epidote makes up less than 5 per cent of the rock.

The felsic material is granoblastic polygonal. The feldspars are 0,07 mm in size. The hornblende forms laths 0,17 mm long. The opaques are poikiloblastic and contain feldspar. The poikiloblasts are 0,5 mm in size with straight grain boundaries. Garnet occurs as subidioblastic poikiloblasts partly altered to chlorite. Epidote occurs as small round grains throughout the rock.

The amphibolite 1 m from the contact consists of epidote, oligoclase, biotite, hornblende and opaques. The mineral relationships remain the same as those described. Epidote can clearly be seen replacing plagioclase.

3. ULTRAMAFIC ROCKS

3.1 OLIVINE SERPENTINITE

The terminology used to describe textures here is after Wicks and Whittaker (1977).

The rock consists of a non-pseudomorphic fine-grained groundmass containing antigorite laths, antigorite pseudomorphs and forsterite (Fogo). The non-pseudomorphic fine-grained groundmass of antigorite contains dust-like magnetite particles. The texture is interlocking. Around the edge of forsterite a mesh-textured C-antigorite is developed. In the fine-grained material there are laths 0,7 mm long with an hourglass texture. The antigorite pseudomorphs contain optically aligned grains which produce a curtain texture. The pseudomorphs contain both C- and A-antigorite. Antigorite may form veinlets in which the small laths have grown both parallel and perpendicular to the walls. Forsterite forms polygonal grains, 0,06 mm in diameter, some of which are in optical continuity. Opaques occur as xenoblasts 0,35 mm in size and as a fine dust in the pseudomorphic material.

3.2 HOBNAIL SERPENTINITE

The hobnail serpentinite consists essentially of antigorite and magnetite although chlorite, carbonate and quartz are present in a few specimens. It has a fine-grained non-pseudomorphic matrix with interpenetrating and interlocking grains. Pseudomorphs 2 mm in size consist of A and C-antigorite, magnetite and occasionally carbonates. The veinlets, containing non-asbestose A-antigorite laths 0,125 mm in size, cut across the matrix.

The three different forms produce the hobnail weathering surface. The pseudomorphs weather light brown and more rapidly than the matrix, hence forming a negative surface. The matrix weathers a deep brown and more rapidly than the veins thus forming a neutral surface. The veins form pale-brown ridges.

The antigorite in the veins has a comb structure with sutured grain boundaries and undulose extinction. The texture in the pseudomorphs varies considerably. There may be an inner core of curtain-textured A- and C-antigorite surrounded by a coarse-grained mesh-structured antigorite. In some cases only the core or rim of the pseudomorphs is developed. Occasionally, the magnetite dust appears to follow pyroxene cleavages in the pseudomorphs. In rare instances clay is developed in the pseudomorphs. Magnetite occurs as a fine dust along lines in the curtain-textured pseudomorphs and as large xenoblastic grains in the antigorite mesh.

In weathered specimens, veinlets of chalcedony and quartz or carbonate are present. The quartz in these veinlets exhibits growth lines.

3.3 TALCOSE SERPENTINITE

This rock consists of talc, antigorite and magnetite. Ankerite and actinolite are present in some specimens. A- and C-antigorite pseudomorphs are surrounded by a matrix of non-pseudomorphic C-antigorite, talc and magnetite. veinlets of non-asbestose C-antigorite traverse the matrix.

Magnetite occurs as a fine dust surrounding pseudomorphs and along cleavage traces. The grains are subidioblastic and have straight boundaries. Magnetite also occurs as idioblastic cubes 0,1 mm in size in the pseudomorphs. Talc occurs as laths and xenoblastic grains in the matrix. Normally grain boundaries are straight, however, in some thin sections the talc exhibits a decussate growth with cusped grain boundaries. Ankerite forms 0,5-mm subidioblastic grains and contains numerous inclusions of talc, magnetite and antigorite. The ankerite is rimmed by iron staining. Actinolite forms subidioblastic needles 0,1 mm in size. Occasionally it is pseudomorphous after pyroxene.

3.4 CARBONATE SERPENTINITE

Carbonate serpentinite consists of either ankerite or dolomite plus antigorite and magnetite. The texture is made up of A- and C-antigorite pseudomorphs with curtain textures surrounded by a non-pseudomorphic matrix of C-antigorite with interlocking and interpenetrating textures. Long needles of antigorite with hourglass texture are also present. These needles penetrate large xenoblastic grains of carbonate which are filled with minute inclusions. Magnetite forms subidioblastic grains in the matrix or small cubes associated with ankerite.

3.5 TALC SCHIST

The talc schist consists of talc and magnetite, together with chlorite and carbonate in some specimens. Its lepidoblastic texture is outlined by the long axes of pod-shaped talc aggregates and by iron staining. The long axes of the talc laths within the pods commonly make an angle of 30° with the main schistosity. Magnetite forms dust-like particles along the main schistosity and also occurs as 1-mm cubes growing across it. Small grains of chlorite and carbonate may be present in the pod-shaped aggregates.

3.6 TALC-AMPHIBOLE SCHIST

The talc-amphibole schist consists of talc, either actinolite or anthophyllite, and magnetite. Chlorite is present in some specimens.

The texture is lepidoblastic, outlined by the long axes of pod-shaped talc aggregates. The talc forms either as subidioblastic laths in the pods or large xenoblastic flakes in a matrix around the pods. The actinolite needles in the pods appear to have been altered to talc and chlorite. There are aggregates of anthophyllite needles in the talc matrix.

Chlorite which forms as large flakes in the matrix is not found in contact with the amphibole. Idioblastic magnetite cubes disrupt the schistosity.

3.7 CHLORITE SCHISTS

In hand specimen the schist is usually dark green with a silvery sheen on foliation surfaces. It is strongly schistose and consists almost solely of clinocllore and magnetite, although idocrase may be a minor component. The texture is poorly lepidoblastic.

Along cleavage planes there is iron staining. The texture resembles that of the hobnail serpentinite, suggesting that the parent rock was similar in both cases or that the chlorite has replaced the serpentinite. The chlorite forms a matrix of interlocking laths with sutured and straight boundaries, in which are pseudomorphs of chlorite with curtain texture. Magnetite forms dust-like particles along the main schistosity and occurs as small cubes with a random distribution. These cubes may coalesce to form large aggregates.

3.8 ACTINOLITE FELS

The actinolite fels consists of actinolite, talc and chlorite with quartz as a minor component. Needles of actinolite, as much as 30 mm long, with a radiating acicular structure lie in a groundmass of talc and chlorite. There are subidioblastic laths of talc in the groundmass and also penetrating into cracks in the actinolite. The chlorite forms as large xenoblastic grains in the groundmass and the quartz occurs as polygonal grains in the talc.

3.9 HORNBLENDITE DYKES

The hornblendite 'dykes' consist of hornblende, epidote, sphene and magnetite with minor amounts of plagioclase, chlorite, augite and quartz. The texture is blastophitic, outlined by hornblende and epidote. Hornblende occurs as subidioblastic poikiloblasts which contain all the other minerals. Epidote forms a fine-grained groundmass with a granoblastic polygonal texture. Sphene occurs as a fine-grained aggregate within the hornblende or at the margins of the hornblende crystals. Magnetite forms cubes which coalesce into xenoblastic aggregates containing epidote and hornblende. Plagioclase is intergrown with epidote, as is the quartz. Chlorite appears to be replacing the hornblende.

APPENDIX III - MICROPROBE ANALYSES. THE RESULTS OF 27 ANALYSES OF GARNET AND MICA SAMPLES, MADE USING A JEOL JXA 50 ELECTRON-PROBE MICRO-ANALYSER

Garnet analyses

	AM105A	AM105B	AM107A	AM107C	AM107B	AM107D	AM107E	AM107F	AM107G	OU1A	OU1B	OU1C	OU1D	OU1E
SiO ₂	37,22	37,91	37,46	37,57	37,86	38,20	37,37	37,07	37,45	37,44	36,94	37,36	37,51	37,18
Al ₂ O ₃	22,82	21,77	21,38	21,36	21,32	20,61	21,70	21,27	22,17	21,53	22,40	21,96	21,83	22,37
TiO ₂	0,12	0,05	0,14	0,12	0,14	0,11	0,11	0,13	0,13	0,10	0,14	0,10	0,17	0,10
MgO	3,62	4,19	3,85	3,76	3,71	3,91	4,15	3,97	4,21	3,79	3,45	3,50	3,73	3,63
FeO	31,39	32,01	29,35	29,55	29,71	29,54	30,35	28,67	30,65	29,49	29,97	29,86	29,01	29,98
MnO	0,74	0,59	2,07	3,31	3,16	3,49	3,20	2,62	2,79	2,87	3,35	3,30	2,15	2,13
Cr ₂ O ₃	0,13	0,04	0,11	0,10	0,10	0,07	0,05	0,11	0,12	0,09	0,05	0,11	0,09	0,17
CaO	4,07	4,30	4,10	3,72	4,58	3,46	3,50	4,28	3,85	3,79	3,98	4,25	5,12	4,27
Na ₂ O	-	-	-	-	-	-	-	-	-	0,05	0,05	-	0,06	-
K ₂ O	-	-	-	-	-	-	-	-	-	0,06	0,04	-	0,04	-
TOTALS	100,11	100,86	98,46	99,49	100,58	99,39	100,43	98,12	101,37	99,21	100,37	100,44	99,71	99,83

Atomic proportions - 12 oxygens

Si	2,943	2,982	3,001	2,992	2,995	3,050	2,963	2,983	2,934	2,990	2,930	2,958	2,972	2,952
Al	2,127	2,018	2,018	2,004	1,988	1,941	2,028	2,017	2,047	2,027	2,094	2,049	2,039	2,093
Ti	0,007	0,003	0,007	0,006	0,008	0,008	0,007	0,008	0,007	0,006	0,008	0,006	0,009	0,006
Mg	0,429	0,491	0,461	0,447	0,437	0,466	0,489	0,476	0,491	0,451	0,408	0,413	0,441	0,430
Fe	2,078	2,106	1,968	1,974	1,965	1,974	2,011	1,930	2,009	1,970	1,988	1,977	1,923	1,991
Mn	0,051	0,039	0,141	0,224	0,212	0,237	0,214	0,180	0,185	0,194	0,225	0,222	0,144	0,143
Cr	0,007	0,003	0,006	0,005	0,006	0,006	0,003	0,006	0,007	0,006	0,003	0,007	0,006	0,016
Ca	0,345	0,362	0,353	0,319	0,388	0,297	0,296	0,369	0,323	0,324	0,338	0,361	0,440	0,363
Na	-	-	-	-	-	-	-	-	-	0,007	0,008	-	0,011	-
K	-	-	-	-	-	-	-	-	-	0,006	0,004	-	0,004	-
TOTALS	7,987	8,004	7,955	7,971	7,999	7,979	8,011	7,969	8,003	7,981	8,006	7,993	7,989	7,994

Biotite analyses

	AM105A	AM105B	AM107A	AM107B	AM107C	AM107D	AM107E	OU1A	OU1B	OU1C	OU1D	OU1E	AM105A*
SiO ₂	35,48	36,98	36,42	35,79	36,96	35,61	35,18	36,30	36,62	36,04	36,49	34,90	46,53
Al ₂ O ₃	18,40	18,09	17,58	17,71	17,48	17,61	17,08	19,43	17,59	18,68	18,18	19,36	35,00
TiO ₂	1,33	1,36	1,57	1,55	1,84	1,72	1,62	1,53	1,08	1,56	1,24	1,07	0,59
MgO	12,42	13,11	12,45	12,93	12,10	12,45	12,79	12,07	12,31	12,53	11,68	12,57	0,75
FeO	16,70	16,20	16,43	16,46	16,97	17,06	16,99	16,41	16,98	17,04	15,76	17,37	2,24
MnO	0,09	0,09	0,16	0,13	0,13	0,09	0,23	0,16	0,18	0,14	0,16	0,14	-
Cr ₂ O ₃	0,09	-	0,12	0,09	0,11	0,10	0,13	0,19	0,13	0,16	0,12	0,17	-
CaO	0,05	0,05	0,06	0,05	0,05	0,07	0,03	0,06	0,04	0,06	0,05	0,05	0,05
Na ₂ O	2,05	0,29	0,25	0,27	0,23	0,17	0,24	0,24	0,25	0,31	0,32	0,30	1,32
K ₂ O	8,92	9,73	9,43	10,02	9,93	9,20	10,05	9,16	9,35	9,75	9,73	10,17	9,36
TOTALS	95,53	95,90	94,47	95,00	95,80	94,08	94,34	95,55	94,53	96,27	93,73	96,10	95,84

Atomic proportions - 22 oxygens

Si	5,417	5,509	5,819	5,424	5,544	5,438	5,402	5,408	5,546	5,378	5,524	5,254	6,163
Al	3,311	3,176	3,140	3,163	3,090	3,169	3,091	3,412	3,139	3,285	3,260	3,439	5,463
Ti	0,153	0,152	0,179	0,177	0,208	0,198	0,187	0,172	0,123	0,176	0,142	0,124	0,059
Mg	2,826	2,911	2,812	2,920	2,705	2,834	2,917	2,681	2,779	2,786	2,648	2,818	0,148
Fe	2,132	2,081	2,082	2,086	2,129	2,179	2,181	2,044	2,151	2,126	2,005	2,188	0,248
Mn	0,012	0,011	0,021	0,017	0,017	0,012	0,030	0,020	0,024	0,018	0,021	0,018	-
Cr	0,011	-	0,014	0,011	0,013	0,012	0,016	0,022	0,016	0,019	0,015	0,023	-
Ca	0,008	0,008	0,010	0,008	0,008	0,012	0,005	0,009	0,007	0,010	0,007	0,008	0,007
Na	0,607	0,084	0,073	0,079	0,067	0,050	0,071	0,070	0,073	0,090	0,095	0,087	0,339
K	1,737	1,849	1,823	1,937	1,900	1,792	1,968	1,741	1,807	1,857	1,888	1,956	1,581
TOTALS	16,214	15,781	15,973	15,822	15,681	15,696	15,868	15,579	15,665	15,745	15,605	15,915	14,008

* Muscovite

Analyst: R.C. Wallace, Geological Survey, Pretoria